Aalborg Universitet

Using building simulation to evaluate thermal comfort

Vorre, Mette Havgaard

Publication date:
2015

Document Version
Publisher's PDF, also known as Version of record

[Link to publication from Aalborg University](#)

USING BUILDING SIMULATIONS TO EVALUATE THERMAL COMFORT

BY
METTE HAVGAARD VORRE

DISSERTATION SUBMITTED 2015

AALBORG UNIVERSITY
DENMARK

.

USING BUILDING SIMULATIONS TO EVALUATE THERMAL COMFORT

by

Mette Havgaard Vorre

Dissertation submitted 25. October 2015

CV

Mette Havgaard Vorre holds a Master Degree in Indoor Environmental Engineering and Energy Economics from Aalborg University 2002.

Since graduating Mette has worked at WindowMaster A/S with dimensioning of natural ventilation in several buildings in Denmark and the rest of Europe, and at the Institute of Product Development as a consultant in refrigeration and energy technologies for e.g. Danfoss and the Technological Institute of Denmark on developments and research project, before starting the PhD-stdudy.

Mette now works as a consulting engineer at Niras A/S.

ENGLISH SUMMARY

More than 40 years ago Povl Ole Fanger presented his doctor dissertation on thermal comfort. The discoveries of Fanger are still the foundation of thermal comfort evaluations in several standards and norms all over the world. Alternative methods have been suggested, but Fanger's research still gives the most detailed view on how to create good thermal indoor environment. A knowledge that is essential in order to secure and optimise thermal comfort for building occupants.

This Ph.D. study presents a tool for simulation and evaluation of thermal comfort based on building energy simulations. The gap of missing input parameters for thermal comfort calculations has been closed with calculation methods for clothing level, air velocities and thermal radiant exchange.

Simulation of thermal comfort is not and will never be exact predictions, a fact that is important to communicate to decision makers; the tool therefor presents the results with clear visualisation of uncertainties.

DANSK RESUME

Det er over 40 år siden Povl Ole Fanger præsenterede sin doktorafhandling om termisk komfort. Fangers opdagelser er i dag grundlaget for vurdering af termisk komfort i en lang række standarder og normer over hele verden. Alternative metoder er blevet opstillet, men det er stadig Fangers forskning, der giver det mest detaljerede indblik i, hvad der skaber et godt termisk indeklima. En viden, der er nødvendig, for at sikre og optimere den termiske komfort for brugerne af en bygning.

Med denne ph.d. afhandling præsenteres et værktøj til simulering og evaluering af termisk komfort baseret på bygningsenergisimuleringer. Kløften af manglende input data er blevet lukket med metoder til beregning af beklædningsniveau, lufthastigheder og strålingspåvirkninger.

Simulering af termisk komfort er ikke og bliver aldrig en eksakt forudsigelse, hvilket er væsentligt at kunne formidle til beslutningstagere, derfor præsenteres resultatet af simuleringerne på en måde hvor betydningen af usikkerheder og variationer fremgår tydeligt.

PREFACE

This thesis sums up the work carried out during my PhD study. The basic idea behind the study is optimising thermal comfort in buildings through improved simulations for thermal comfort evaluation.

The thesis compiles the five articles written in connection with the study.

The first article to be presented is a review of the aspects of thermal comfort simulation. Then three articles are presented, each focusing on researching and improving simulations of an indoor thermal parameter. The last article to be presented explores the handling of uncertainties in simulations and how to present simulation results with respect to the underlying uncertainties. The connection between the articles is illustrated below.

The articles in the thesis are exact replicas of the published, presented and submitted articles when it comes to structure, wording and figures. The only things changed compared with the original articles are:

- The layout of the articles has been changed to get a uniform layout of the entire thesis
- Nomenclature has been unified to ease reading of the thesis
- Acknowledgements have been removed from the articles to gain better flow in the thesis
- References have been moved to a complete reference list at the end of the thesis
- Figures, tables and equations are numbered continuously through the thesis
- An error in a table has been corrected. A note about it is placed in the table caption

The thesis is based on the following five articles:

"A review of thermal comfort models and their implementation in building simulation tools"
Vorre, M. H, Jensen, R.L.
Submitted to Building simulation

"Does variation in clothing make us more thermally comfortable?"
Vorre, M. H, Jensen, R.L.
Indoor Air 2014 Conference in Hong Kong

"Draught risk index tool for building energy simulations"
Vorre, M. H, Jensen, R.L, Nielsen, P.V.
World Sustainable Building 2014 Conference in Barcelona

"Radiation exchange between persons and surfaces for building energy simulations"
Vorre, M. H, Jensen, R.L, Dréau, J. L.
Energy and Buildings, Volume 101, 15 August 2015

"Using building simulation to evaluate global and local thermal comfort according to ISO 7730"
Vorre, M. H, Jensen, R.L, Jønsson, K.T.
Submitted to Journal of Building Performance Simulation

.

ACKNOWLEDGEMENTS

Jeg skylder en stor tak til Rasmus Lund Jensen for hans tålmodighed og vedholdenhed. For at række hånden ud før jeg selv blev klar over jeg var ved at falde og for at holde fast til jeg var helt oppe at stå igen. For at tro på projektet og bakke op da jeg valgte at fortsætte, og for en helt igennem uvurderlig støtte i at komme igennem med projektet og kunne indlevere denne afhandling. Det var ikke sket uden ham!

Tak til Ásta Logadóttir a.k.a. Gregory Clark Flame. Uden dig havde jeg nok givet op, da det hele var noget -biiip-. Du gav mig noget at komme tilbage til og var en kæmpe støtte. Fra den dag jeg satte mig ved skrivebordet i vores lille fælleskontor i Hørsholm, har vi haft det sjovt sammen. Vi har hjulpet og støttet hinanden, og fundet det sjove i det groteske. Jeg savner allerede kaptajnen i Rungsted og bøssesaunaen i Istedgade!

Tak til Lone Hedegaard Mortensen for flere hundred kilometers gåture i frokostpauserne inde på Sydhavnen, hvor både arbejde, privatliv og verdenssituationen er blevet vendt og drejet. Det har givet en masse ny energi og overblik til eftermiddagstimerne!

Tak til Søren Aggerholm for at have givet mig muligheden for at lave en phd og for at holde fast i hvad der var bedst for mig. Det har betydet alverden!

Tak til Kjeld Johnsen for at pirre min nysgerrighed for SBi og få mig i gang med phd-projektet.

Tak til Karin, Jakob, Anne og alle andre på SBi for en masse skønne timer sammen med gode diskussioner og en masse grin. Tak til Solveig for hjælp til at få det engelske sprog til at flyde lettere.

Og sidst, men absolut ikke mindst, tak til min familie for støtte og opbakning. Tak til Anders for altid at stå ved min side og for i perioder at have taget sig af alt bøvlet derhjemme. Tak til Lærke og Malthe for konstant at minde mig om, hvad der faktisk er det vigtigste i livet. Tak til min mor og far for at have givet en ordentlig tørn med hus og børn, når jeg har haft brug for at begrave mig i arbejdet. Tak til min søster for at lytte, give kram og hygge med ungerne, når der var brug for det. Tak til hele min svigerfamilie for opbakning til projektet og tak til en frygtelig masse dejlige venner, der har givet mig en masse støtte og tro på at det kunne lade sig gøre. - Jeg glæder mig til at have mere tid med jer alle!

TABLE OF CONTENTS

.

NOMENCLATUR

$A_{i,\,eff}$	effective radiation area of object i	m^2
A_i	area of object i	m^2
α	azimuth angle measured from the persons sight direction	°
a_0	geometrical inlet area of opening	m^2
A_{person}	effective radiation area of a person	m^2
$A_{projected}$	a person's projected area	m^2
Ar	Archimedes number	-
A_{sphere}	area of sphere	m^2
β	altitude	°
C	clothing insulation	Clo
DR	draught rate	-
ε	emissivity	-
$F_{i \rightarrow j}$	view factor or angle factor from object i to object j (how big an area does object j cover compared with the whole area that object i radiates to)	-
$f_{projected}$	projected area factor	-
γ	angle	°
h_0	geometrical inlet height of opening	m
H	height	m
K_a	inlet constant for a 3D jet	-
K_p	inlet constant for a plane jet	-

K_{sa}	room constant for a 3D jet	-
K_{sp}	room constant for a plane jet	-
M	metabolic activity	met
μ	mean	~
P	productivity relative to maximum value	-
PD	Percentage Dissatisfied	-
PMV	Predicted Mean Vote	-
PPD	Predicted Percentage Dissatisfied	-
$q_{i \rightarrow j}$	heat flow by radiation from object i to object j	W
R	correlation koefficient	-
r	radius	m
rh	relative humidity	-
σ	standard deviation	~
σ_s	the Stefan-Boltzmann constant	$W/m^2 K^4$
t_{air}	air temperature	°C
t_{comf}	optimum comfort temperature inside	°C
T_i	the surface temperature of object i	K
t_i	optimum operative temperature indoor	°C
t_{in}	indoor temperature	°C
$t_{mean,out}$	mean outdoor temperature for a time period	°C
T_{mr}	mean radiant temperature	K
t_{mr}	mean radiant temperature	°C

$t_{air,oc}$	air temperature in the occupied zone	°C
t_{op}	operative temperature	°C
t_{out}	outside temperature	°C
$t_{out,6AM}$	outside temperature at 6 AM	°C
$\Delta T_{radiant}$	radiant asymmetry	K
t_{rm}	outside running mean temperature	°C
tsv	thermal sensation vote on a scale from -3 to 3	-
t_{window}	surface temperature of window	°C
u	air velocity	m/s
u_0	inlet air velocity	m/s
u_x	air velocity in the center of the jet in the distance x from the inlet	m/s
x	distance	m
x_0	distance to the virtual origin of the flow at the opening	m
x_s	penetration length	m
y	vertical displacement of flow	m

THE STEPS FOR BETTER THERMAL COMFORT SIMULATIONS

In order improve simulation of thermal comfort and thereby hopefully optimise thermal comfort in future buildings, the following steps were set up:

1. Explore the state of the art in simulation of thermal comfort:
    a. The methods for calculating thermal comfort
    b. The capabilities of current building simulation tools
    c. The research in calculation of the input parameters required for calculating thermal comfort
    d. How to handle uncertainties on input parameters in simulations
2. Select which parameters to focus on, in order to improve simulation of thermal comfort
3. Research the selected parameters one at a time and develop methods for simulation
4. Gather the findings in an application that can calculate thermal comfort and take uncertainties and variations into account

The first article is presented on the next page and covers steps 1 and 2.

The second, third and fourth articles each cover the research of one parameter.

The fifth article describes the handling of uncertaianties and presents a final application.

First article:

A REVIEW ON THERMAL COMFORT MODELS AND THEIR IMPLEMENTATION IN BUILDING SIMULATION

Mette H VORRE[1,*], Rasmus L JENSEN[2]

[1]Energy and Environment, Danish Building Research Institute, Aalborg University, Copenhagen, Denmark
[2]Department of Civil Engineering, Aalborg University, Aalborg, Denmark

[*] *Corresponding author: Mette Havgaard Vorre*

ABSTRACT

Thermal comfort in a building is inevitably connected with the building's energy consumption. An optimisation of either one will affect the other and a combined optimisation process is, therefore, the ideal way to ensure that expectations to both the energy performance and the thermal comfort of the occupants are met. This literature review investigates the possibilities of basing thermal comfort simulations on building energy simulation tools. Firstly methods for the evaluation of thermal comfort are explored, secondly the capabilities of thermal comfort simulation in current building simulation tools are investigated and thirdly the possibilities of calculating the needed input parameters for thermal comfort calculations are explored. For design optimisation, Fanger's local thermal discomfort measures give the most useful information, while for compliance check of a design both Fanger's global thermal comfort and de Dear's adaptive thermal comfort are very adequate. None of the investigated building simulation tools can simulate local thermal discomfort, some can partly simulate global thermal comfort and several can simulate adaptive thermal comfort. Finally it appears promising to develop calculation methods based on existing research for the needed input parameters in order to simulate local thermal discomfort and global thermal comfort.

KEYWORDS

Mean radiant temperature, air velocity, PMV, long-term thermal comfort model, clothing, uncertainty

INTRODUCTION

Wishes for better comfort drove man to develop buildings. The basic needs were fulfilled centuries ago, and buildings today are much more than just shelters against the outdoor environment. Yet occupants' satisfaction with the thermal environment can still not be taken for granted. Brand new buildings experience problems with draught, warm / cold thermal radiation, overheating in summer and low temperatures in winter.

One way to ensure indoor thermal comfort is through large plants for heating and cooling, the way it has been done for decades, but also a way which has led to massive energy consumption.

Another way is to improve simulation of thermal comfort in order to foresee the problems, and then optimise the building design for high thermal comfort and low energy consumption. Building energy simulation tools are already used in the optimisation of the building's energy efficiency. By expanding the tools' capabilities in the simulation of thermal comfort, the energy efficiency and thermal comfort can be optimised in parallel. Through an overview of the thermal comfort in the building over a longer period, is it possible to point out areas and periods of interest for further analysis in order to optimise the building design for better thermal comfort.

This paper explores the possibilities of expanding building energy simulation tools for better thermal comfort simulations. The main section headings of the paper are listed below.

- Background
- Measures of thermal comfort
- Building energy simulation tools and thermal comfort
- Radiant impact
- Air velocities
- Personal factors: Clothing and activity level
- Dealing with uncertainties
- Conclusion

First the background for the need of improved simulations of thermal comfort is presented, followed by assessment of methods for evaluation of thermal comfort and the capabilities of thermal comfort simulation in existing building simulation tools.

Then calculation methods for the needed input parameters are explored together with a short overview of possibilities for handling input parameters' uncertainties in the simulations. Finally a conclusion is made on the possibilities of expanding building energy simulations with better thermal comfort simulations.

BACKGROUND

The need for better thermal comfort simulations is founded on at least three main causes:

- Demands to energy efficiency
- Rapid development in building technologies
- Occupants' rising expectations to thermal comfort.

Since the energy crisis in the 1970s, northern European countries have focused on energy optimisation of buildings. This has led to passive houses, zero-energy buildings and to legislation on the energy efficiency and insulation requirements for buildings.

Researchers from Aalborg University monitored the indoor environment in eight new, passive houses in Denmark after the occupants moved into their new homes (Brunsgaard et al. 2012). The researchers found that some of the houses both overheated in summer and had insufficient heating capacity in winter. Something in the design had simply failed.

EARLIER EXPERIENCE WAS ENOUGH

Some decades ago, experience was the key word. Buildings in Denmark were made of brick with windows covering a minor part of the façade and inside rooms were relatively small compared with today's standard. The exterior walls and windows were poorly insulated and created draught and radiant asymmetry in the room. The same scenario of thermal comfort issues applied for most rooms and therefor the same solutions could be applied.

Nowadays new building techniques make it possible to build large glassed façades, with rooms stretching over the entire floor plan and with atriums in the middle. Air changes can be handled by automatically controlled windows, where openings are adjusted according to inside and outside climate. Thermal comfort can vary greatly in a room, over time and between buildings, making it harder to predict thermal comfort based solely on experience and thereby harder to foresee consequences of building energy optimisation on experienced thermal comfort.

BUILDING ENERGY SIMULATIONS

In the design process of buildings, simulations are performed in building energy simulation tools like EnergyPlus (Crawley et al. 2000)or ESP-r (Hand 2006) to optimise a building energy wise. Most tools utilise internal air temperature as control parameter for their heating and cooling systems, which to some extent is also how systems are controlled in real life, but some are also able to control according to operative temperature or predicted mean vote (PMV). The calculations of these parameters in the programs are described in more detail later in this article.

To ensure acceptable thermal comfort, while optimising energy consumption, boundaries are set for internal temperatures; for example the maximum number of hours above or below certain temperature limits. In a design process, the simulated number of hours when the operative temperature is outside these limits are counted and used for assessing thermal comfort, even though more parameters affect the thermal comfort of the occupants, e.g. air movements, clothing level and the weather outside.

THERMAL COMFORT AND ENERGY CONSUMPTION

Thermal comfort is essential for the energy optimisation of a building, because poor thermal comfort can increase energy consumption. Some occupants will simply put on a sweater when it is cold, or wear short sleeves when it is warm. Others choose to adjust the settings of heating and cooling systems. Interventions could also be to block inlet openings or put up small air conditioning devices. All these interventions are caused by dissatisfactory thermal environment and they can affect the energy consumption of a building.

A way to improve thermal comfort in buildings is through better measures for thermal comfort in building energy simulation tools, which would also lead to more robust building energy simulations. Furthermore early knowledge on thermal comfort problems makes it both easier and cheaper to change an inopportune building design.

The objective of this paper is a) to find a measure of thermal comfort that is suitable for optimisations in parallel with building energy optimisations, b) to investigate features of existing building energy simulation tools for thermal comfort evaluation and c) to explore the possibilities for simulating the input parameters needed for calculating thermal comfort based on building energy simulation tools.

MEASURES OF THERMAL COMFORT

To predict how occupants will perceive thermal comfort, researchers have described the connection between a number of objective parameters and occupant's satisfaction with the thermal environment.

In Europe the indoor environment standard EN 15 251 (CEN 2007) is used for assessing thermal comfort and in the US ASHRAE 55 (ASHRAE 2010) is used. Both describe how thermal comfort can be assessed either using the equations for global thermal comfort and local thermal discomfort or the equation for adaptive thermal comfort. A third method relates thermal environment to productivity of the occupants, which is interesting because the price of obtaining a desired thermal environment can then be compared with the earnings through workers' higher performance.

In the next sections, the three methods for evaluating thermal comfort are explored in relation to optimisation through simulation of thermal comfort based on building energy simulations.

GLOBAL THERMAL COMFORT AND LOCAL THERMAL DISCOMFORT

The concepts of global thermal comfort and local thermal discomfort are both based on research by P.O. Fanger. The equations are based on studies in climate chambers under strictly controlled climate conditions, activity levels and clothing levels, and the equations therefore only apply to buildings with full HVAC.

Global thermal comfort is based on the heat balance of the entire body and can thus be seen as an average for the body.

Six parameters influence global thermal comfort (Fanger 1970):

- Activity level
- Thermal resistance of clothing
- Air temperature
- Mean radiant temperature
- Relative air velocity
- Water vapour pressure in ambient air

The parameters are weighted in an equation that calculates the predicted mean vote (PMV) on the seven-point scale shown in Table 1.

Table 1 Seven-point thermal sensation scale

+3	Hot
+2	Warm
+1	Slightly warm
0	Neutral
-1	Slightly cool
-2	Cool
-3	Cold

Assuming that votes outside -1 and 1 can be regarded as persons being dissatisfied with the thermal environment, Fanger describes the relation between PMV and the predicted percentage dissatisfied, PPD, with Equation 1 (Fanger 1970). The relation is also shown in Figure 1.

Equation 1

$$PPD = 100 - 95 \cdot e^{-0.03353 \cdot PMV^4 - 0.2179 \cdot PMV^2}$$
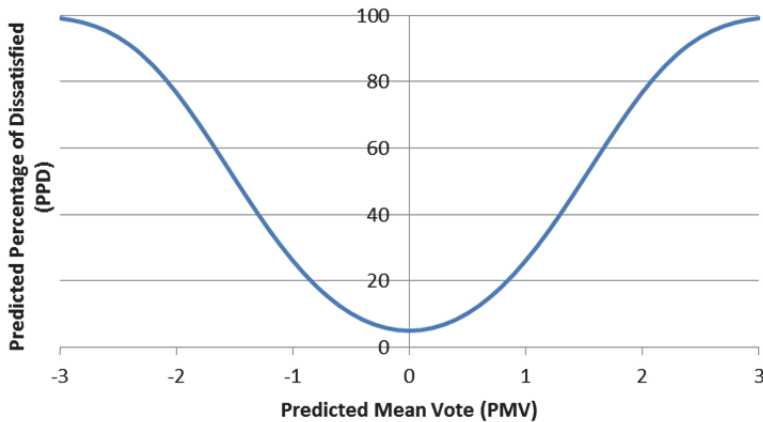

Figure 1 Predicted percentage dissatisfied, PPD, as a function of the predicted mean vote, PMV.

As can be seen from Figure 1, Fanger found that even with a PMV of zero, 5% would still be dissatisfied with the thermal environment, because thermal comfort is subjective.

In addition to global thermal comfort, Fanger found that local thermal discomfort can be caused by:

- Draught
- Radiant asymmetry
- Floor temperature
- Vertical air temperature gradient

These cause local thermal differences between body parts, which is perceived as uncomfortable, even if global thermal comfort is achieved. The percentages dissatisfied, due to each of the four causes were found through climate chamber experiments and correlation equations were developed.

ISO 7730 (CEN 2005) and EN 15 251 (CEN 2007)set up criteria for three thermal comfort categories in order to sum local and global thermal comfort. For each category, all criteria measured should be satisfied simultaneously. The criteria are listed in Table 2, were category D covers conditions outside the other ranges.

Table 2 Categories of thermal comfort.

Category	Global thermal comfort			Local thermal discomfort		
				PD caused by		
	PMV	PPD	DR	vertical air temperature difference	floor temperature	radiant asymmetry
		%	%	%	%	%
A	$-0.2 < PMV < 0.2$	< 6	< 10	< 3	< 10	< 5
B	$-0.5 < PMV < 0.5$	< 10	< 20	< 5	< 10	< 5
C	$-0.7 < PMV < 0.7$	< 15	< 30	< 10	< 15	< 10
D	$-0.7 \geq PMV \geq 0.7$	≥ 15	≥ 30	≥ 10	≥ 15	≥ 10

Fanger's methods are derived from climate chamber tests and only apply to buildings with HVAC. In order to make it applicable also to buildings with natural or hybrid ventilation, an expectation factor was added to the PMV calculations in 2002 (Fanger and Toftum 2002). The factor is multiplied to the calculated PMV and takes into account that occupants in non-air conditioned buildings have lower expectation to the thermal environment and therefor votes closer to neutral than would be the case in an air-conditioned building under the same thermal conditions. The expectation factor varies between 0.5, for regions with few air conditioned buildings, to 0.9 or 1.0, for buildings in regions where air conditioned buildings are common.

Assessment of method in relation to simultaneous optimisation of thermal comfort and energy efficiency

The method proposed by Fanger involves a number of parameters not calculated by a building energy simulation tool including air velocities and parameters related to occupants, which are factors with a great uncertainty and variation, both among people in a room and over time for a specific person or room.

The method requires iterations, because the skin temperature of the person depends on both activity level and conditions in the thermal environment, which will increase simulation time.

On the other hand, the methods by Fanger calculates one global thermal comfort parameter and four parameters for local thermal discomfort, making it possible to evaluate thermal comfort broadly, which in turn enhances the possibilities for optimising building design for better thermal comfort. The thorough and broad approach makes it possible to both pinpoint possible problems, mainly using the local thermal discomfort parameters, and make a compliance check of thermal comfort in a given building design.

ADAPTIVE THERMAL COMFORT

The adaptive approach to thermal comfort is based on field studies from around the world.

de Dear and Brager gathered measurements and questionnaires from 160 buildings in 9 different countries and compared the occupants' actual votes on the seven point scale in Table 1 with the calculated PMVs and PPDs using Fanger's equations (de Dear and Brager 1998). They found that for buildings with full HVAC systems, the calculated PPDs matched the actual votes, but for buildings with natural or hybrid ventilation Fanger's equations overestimated the percentage being dissatisfied under warm conditions. Further they found that occupants' actual votes in natural or hybrid ventilated buildings depended largely on the outdoor temperature.

Their findings led them to develop equations for calculating adaptive thermal comfort, where the human ability to adapt physiologically, psychologically and with its behaviour influences the perceived thermal comfort in buildings with natural or hybrid ventilation.

The adaptive thermal comfort model describes the optimum operative temperature inside the building as a function of the external temperatures for the previous days. In the ASHRAE-55 standard (ASHRAE 2010), the relation between external temperature and indoor comfort temperature is given as:

Equation 2

$$T_{comf} = 0.31 \cdot T_{mean,out} + 17.8°C$$

Where T_{comf} is the indoor comfort temperature and $T_{mean,out}$ is the mean outdoor temperature for a time period between 7 and 30 days back in time.

Centred on the indoor comfort temperature, a band of 5°C describes 90% acceptability among users and a band of 7°C describes 80% acceptability.

In the European standard on indoor environmental inputs, EN 15 251 (CEN 2007), adaptive thermal comfort is included for naturally ventilated buildings. Based on measures in European buildings, the indoor comfort temperature can be calculated as:

Equation 3

$$T_{comf} = 0.33 \cdot T_{mean,out} + 18.8°C$$

The bands in the European standard are 4°C for thermal comfort in category I, 6°C for thermal comfort in category II and 8°C for thermal comfort in category III.

In Figure 2, the limits for comfort temperatures are shown depending on the mean outdoor temperature according to the European standard, EN 15 251 (CEN 2007).
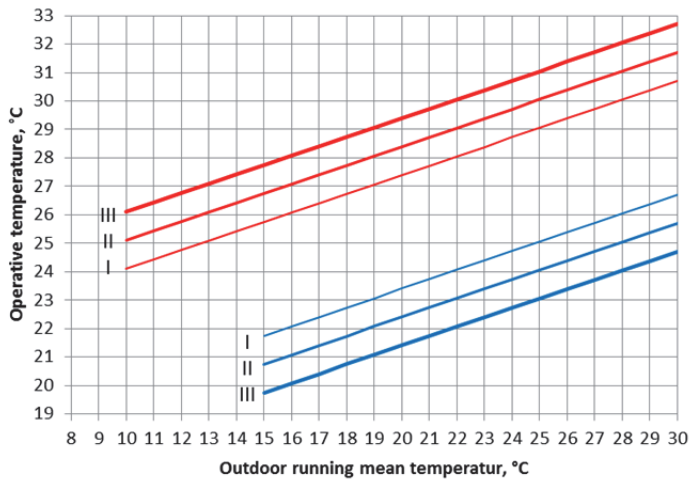

Figure 2 Design limits for operative temperature indoor, depending on weighted running mean outdoor temperature when working with adaptive thermal comfort in buildings without mechanical cooling.

Assessment of method in relation to simultaneous optimisation of thermal comfort and energy efficiency

The adaptive method is simple to calculate, because it assumes that people will adapt to the thermal climate in the building, by regulating their clothing, adjusting window openings etc., which on the other hand limits the method to buildings where occupants have these opportunities for adjustments. Furthermore the method only applies to offices.

The equations for adaptive thermal comfort needs no information on activity level and clothing, which are factors with a great uncertainty and variation, both among people in a room and over time for a specific person or room.

For optimisation of thermal comfort, the adaptive method is only valid in buildings with natural or hybrid ventilation, which excludes HVAC buildings. Compared with Fanger's method, the calculations are much simpler and all inputs are known from building energy simulation tools, but adaptive thermal comfort is also a black box calculation. The method is based on measures in several office buildings, where some probably worked better than others.

The method is well suited for a general compliance check of a building's thermal comfort, especially if combined with Fanger's measures for local thermal discomfort.

In an optimisation process, poor design might not be caught if the mean air temperature in the room is acceptable and the method is therefore weak in the design phase.

THERMAL ENVIRONMENT AND PRODUCTIVITY

Fanger's method and the adaptive method of evaluating thermal comfort are both focused on how occupants perceive the thermal environment. Another approach is to connect thermal conditions with workers productivity.

Most recent studies in this field focus on office work in call centres, schools and laboratories. In 2006 Seppänen et al. (Seppänen, Fisk, and Lei 2006) compiled data from several field studies to find the most reliable correlation between thermal environment and productivity:

Equation 4

$$P = 0{,}1647524 \cdot t_{in} - 0{,}0058274 \cdot t_{in}^2 + 0{,}0000623 \cdot t_{in}^3 - 0{,}4685328$$

Where P is the productivity relative to maximum value and t_{in} is the indoor room temperature in °C.

The equation is subject to high uncertainty as the performance measured varied greatly from study to study. All buildings in the studies had full HVAC and the tasks measured were routine in nature.

Jensen (Jensen 2008) bases his correlation on climate chamber tests and describes the relation between productivity and thermal sensation vote, as:

Equation 5

$$P = -0,0029 \cdot tsv^2 - 0,0034 \cdot tsv + 0,999$$

Where P is the productivity relative to the maximum value and tsv is the thermal sensation vote on the scale from -3 to 3 in Table 1.

The relationships between thermal environment and productivity by both Seppänen (Seppänen et al. 2006) et al. and Jensen (Jensen 2008) are plotted in Figure 3. In order to compare the correlations, the horizontal axes are chosen to cover approximately the same range.
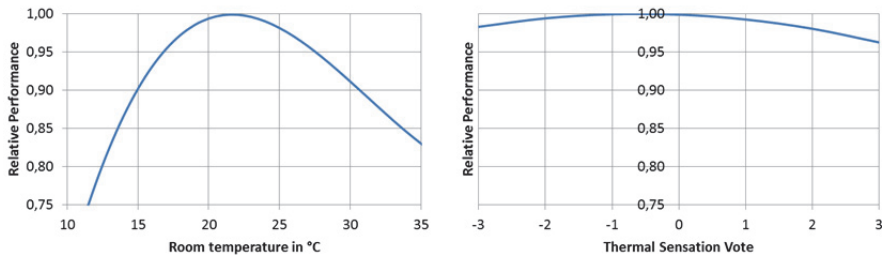
Figure 3 Relative performance as a function of thermal environment. To the left the relation found by Seppänen et al. (Seppänen et al. 2006) from field studies and to the right the relation found by Jensen (Jensen 2008) from climate chamber tests.

Both correlations describe the highest performance at a slightly cool environment. But were performance is found to be highly dependent on room temperature in the studies by Seppänen et al. (Seppänen et al. 2006), Jensen (Jensen 2008) finds that performance only varies slightly with the thermal environment.

According to Leyten et al. (Leyten, Kurvers, and Raue 2013), the differences between the two studies can both be due to the uncertainties that lie within these types of studies, but also because the one by Jensen (Jensen 2008) is based on studies in a climate chamber, with relatively short time periods and the studies gathered by Seppänen et al. (Seppänen et al. 2006) are from field studies. Leyten et al. (Leyten et al. 2013) find that the productivity varies more with the thermal environment in field test than in climate chamber tests, presumably due to less motivation in the performed tasks in the climate chambers, and because in the

climate chamber the tests persons performed mental/creative work instead of simpler routine office work, which is the fundament of the field studies.

Assessment of method in relation to simultaneous optimisation of thermal comfort and energy efficiency

The relation between thermal environment and productivity is easy to calculate if either the indoor temperature or the thermal sensation vote is known. Calculation of the thermal sensation vote requires the use of Fanger's method and thereby knowledge on the six parameters affecting thermal comfort.

In an optimisation process, the method has the same disadvantages as the adaptive thermal comfort method, because it is not possible to identify causes of thermal comfort problems.

SELECTION OF METHOD FOR THERMAL COMFORT EVALUATION

Of the three methods described for evaluating thermal comfort, the method by Fanger is selected for further exploration on improving the simulation of thermal comfort.

Fanger's method is selected because it gives the best possibilities to point out causes for thermal discomfort, which is fundamental in the optimisation process of a building. Only by knowing if draught is a problem, is it possible to change the layout of inlet openings in a way to avoid it, or to take action when a large glassed façade generates radiant asymmetries in cold or warm parts of the year.

Fanger's method is the most complex of the methods and to be able to calculate both global thermal comfort and local thermal discomfort, the following input parameters are required:

Global thermal comfort:

- air temperature
- mean radiant temperature
- relative humidity
- relative air velocity
- clothing level
- activity level

Local thermal discomfort, draught:

- air temperature

- air velocity
- turbulence intensity

Local thermal discomfort, vertical air temperature difference:

- vertical air temperature difference between head and feet

Local thermal discomfort, warm and cool floors:

- floor temperature

Local thermal discomfort, radiant asymmetry:

- difference in thermal radiation side-to-side for a horizontal plate
- difference in thermal radiation side-to-side for a vertical plate

The air temperature, relative humidity and surface temperatures are normally known from building energy simulations. The rest of the needed parameters must be calculated to evaluate thermal comfort.

Of the input parameters, it is chosen to focus the further exploration on radiation, air velocities and the human factors: activity level and clothing level. These are chosen because they have the greatest influence on thermal comfort.

Thermal radiation affects both mean radiant temperature and radiant asymmetry. Mean radiant temperature affects global thermal comfort nearly as much as the air temperature. Mean radiant temperature is calculated from surface temperatures, emissivities of surfaces and view factors between surfaces and person. View factors describe how much each surface affects the person and do not vary with time for the same position and orientation. To take into consideration that we do not know where a person is situated at a given time, view factors must be calculated for several positions and orientations in the room, but they only need to be calculated once, in order to improve the calculations of thermal comfort in all time steps of a simulation.

Air velocities are chosen because draught is one of the main causes of complaints of thermal environments (Fanger et al. 1988) and air velocities also play an important role in global thermal comfort. Air velocities are chosen even though there is a contradiction between building energy simulation tools and the calculation of air velocities, as one of the pillars in building energy simulation tools is the assumption of full mixture of the air in the room.

Clothing is interesting because it is a quick way for occupants to influence their thermal comfort. According to Fanger's equation, a change in clothing from trousers and t-shirt (0.6 clo) to a light business suit (0.9 clo) can change PMV from -1.2 to -0.5, which corresponds to PPDs of 35.2% and 10.2%. Fanger found that under the same conditions, including same clothing insulation, there will always be at least 5% dissatisfied with the thermal environment. In a real building, people can vary their clothing to optimise their thermal comfort and in order to make realistic simulations, it is vital to take this effect into consideration, as it may potentially lead to more realistic evaluations of thermal comfort.

Activity level is also a means for occupants to influence their own thermal environment by e.g. standing up or sitting down. A change in activity level from seated relaxed (0.8 met) to standing (1.2 met) can change PMV from -2.2 to -0.3, resulting in a change in PPD from 84.9% to 6.9%. Occupants' thermal adjustment through activity level is extremely interesting to be able to simulate.

UNCERTAINTY AND VARIATIONS

The nature of the parameters required for simulating thermal comfort using the equations by Fanger differ very much. Some are related to the building, others are related to the occupants. Some vary greatly over time, others are more stable. Some we can calculate very precisely, others are highly uncertain predictions regardless of how much effort we put into it.

To do justice to the research of Fanger and the future decisions made based on the calculated results, it is important to somehow take into account, the effect of uncertainty and variations of the input parameters. This is seen as very important, because calculations like this can quickly be branded as useless because some parameters have both high uncertainty and high impact on the results. If instead it is possible to show the range of the results in the sample space, decisions can be made on an informed basis.

The objectives for the rest of this paper are therefor to explore possibilities for:

- Simulation of thermal comfort in current building energy simulation tools
- Calculating the input parameters: mean radiant temperature, air velocity, clothing and activity level, in a setup where optimisation of thermal comfort is based on building energy simulations
- Handling uncertainties and variations on input parameters in the final results.

BUILDING ENERGY SIMULATION TOOLS AND THERMAL COMFORT

Four building energy simulation tools were explored; all of them have made an effort to give a better estimate of thermal comfort than an operative temperature based on area weighted mean radiant temperature and air temperature.

In TRNSYS (Klein and et al. 2010) the simulation of predicted mean vote (PMV) and predicted percentage dissatisfied (PPD) was built in by Solaini et al. (Solaini et al. 1996) in 1996. Mean radiant temperature is calculated by a sphere representing the human body, while the user should provide information on: air velocity, humidity, clothing and activity level.

EnergyPlus (Crawley et al. 2000) can simulate global thermal comfort measured by PMV and PPD, and additionally it is possible to simulate adaptive thermal comfort. The simulation of global thermal comfort is based on inputs given by the user on activity level, air velocity and clothing level. Mean radiant temperature can be calculated in three different ways: as an area-weighted mean of surface temperatures, as a so called "surface-weighted mean" and by using angle factors. The "surface-weighted mean" is used to simulate a person situated close to a surface and is calculated as the average between the surface temperature in question and the area-weighted mean of all surfaces in the room. The angle factor mean radiant temperature is found by weighting the surface temperatures according to the angle factors or view factors, which have to be given by the user.

ESP-r (Hand 2012) and IDA ICE (EQUA Simulation AB n.d.) also provide possibilities of calculating global thermal comfort when the user provides information on air velocity, activity level and clothing level, while the tools can calculate simplified mean radiant temperatures.

None of the four building simulation programs were able to calculate the thermal radiant impact on a person in multiple points in a room, to calculate thermal comfort with only minimum of extra input from the user or to calculate any of the measures for local thermal discomfort. The next sections will explore whether it is possible to make these calculations, since it hasn't been implemented yet.

RADIANT IMPACT

Thermal comfort is influenced by radiation in two ways: heat loss to the surroundings by thermal radiation and asymmetry in thermal radiation. Radiation affects both global thermal comfort and local thermal discomfort.

Thermal radiation can be divided into short-wave radiation and long-wave radiation. Short-wave radiation is the type of radiation received from the sun or a radiant

heater, and long-wave radiation describes the radiation between surfaces or objects by emission due to temperature differences. Short-wave radiation transports most energy and is directed, while long-wave radiation can be treated as diffuse.

Thermal comfort in building energy simulations is typically evaluated by the operative temperature, which is the average of the air temperature and the mean radiant temperature in the room. In most programs, only a single operative temperature is found for a room and it is calculated as the surface area mean, even though the mean radiant temperature can vary greatly e.g. if the room has large glassed areas.

The impact of thermal radiation depends on surface temperatures, the emissivities of surfaces and how big a part that the given surface covers of a person's radiant field, which is measured by a factor named either the view factor (Cannistraro et al. 1992) or the angle factor (Steinman, Kalisperis, and Summers 1988). Knowledge about the view factor between a person and the surfaces surrounding him is one of the things needed for a better calculation of the radiant impact and thereby better calculations of thermal comfort.

A person exchanges radiation with the surroundings through his effective radiation area. The effective radiation area is smaller than the total skin area because parts of the body exchange radiation with the body itself, e.g. between fingers or between the legs. James D. Hardy and Eugene F. DuBois (Hardy and DuBois 1938) measured the effective radiation area in 1938 by means of a wrapping method. A person was wrapped in paper like an Egyptian mummy, and the surface area was measured by rubber-coating the paper – a technique similar to the one used for measuring the total area of the human skin also known as the DuBois area.

Later on, several studies used photographs to find the effective radiation area, the projected area and the projected area factor of the human body. Guibert and Taylor (Guibert and Taylor 1952) had people lying down in four different postures from erect to crouching. The study involved three persons, and 32 photographs were taken of each person. The photographs were taken in a half sphere, taking advantage of the bilateral symmetry of the human body. The distance between the person and the camera was 10.7 m - 12.2 m. A large distance is desirable to be able to assume that the measured projected area equals the spherical projection. The radiation area was found dependent of posture and independent of body type. Photos were taken of both nude and clothed persons, where the effective radiation area of the clothed body was a factor 1.14 higher than for the nude body. The effective radiation area factor was found to be 0.77 for a standing person and 0.70 for a seated person. Projected area factors were given as diagrams for the four postures.

Geometrical shapes as simplifications of the human body were suggested for easier calculation of projected area factor and view factor. Taylor (Taylor 1956) suggests

the use of a sphere to represent the seated person and a cylinder for the standing person. Underwood and Ward (Underwood and Ward 1966) suggest an oval cylinder as a good fit for their results for standing persons. Underwood and Ward's results were obtained by a photographic method, with photos taken of 25 male and 25 female test persons. The photos were taken at a distance of 4.57 m and with irregular steps of altitude angles due to their test fixture. The small distance between subject and camera required them to make corrections of the measurements to compensate for the parts of the body close to the camera being bigger than the parts furthest from the camera. To avoid these compensations, they found that pictures should have been taken from a distance of a least 20 m.

Fanger et al. (Fanger, Angelius, and Kjerulf-Jensen 1970) adopted the test set-up by Underwood and Ward with some modifications. Mirrors were used in the fixture to "double" the distance between subject and camera to 7 m and to make the switches between altitude angles quicker, because the camera itself was not moved; only the mirrors were adjusted. 78 pictures were taken of each of the 10 male and 10 female subjects with angle steps of 15° for both altitude and azimuth in 1/8 of a sphere. The results were given as diagrams for projected area factors for seated and standing persons. The projected area factors were used for making diagrams of view factors from a person to walls, ceilings and floors in an orthogonal room, because in contrast to the earlier studies mentioned, this study was aimed at thermal comfort in a room. To read the view factors from the diagrams, each surface must be divided as shown in Figure 4 and the distances a, b and c used as input to read the diagrams.
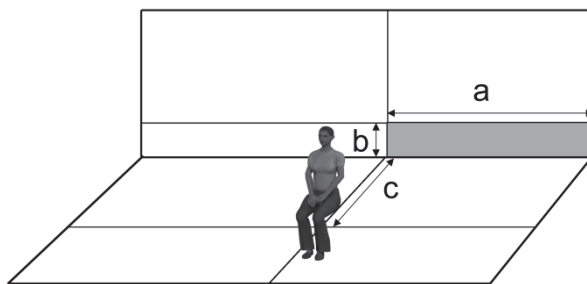
Figure 4 To read the view factor of a surface from Fanger's diagrams, the surface needs to be divided according to the centre of the person and the distances a, b and c known.

The results for view factors between man and surrounding surfaces were used when planning the studies on radiant asymmetry (Fanger et al. 1980, 1985). In the 1980 article, Fanger et al. introduced the term 'radiant temperature asymmetry' as being the difference between the plane radiant temperatures of two opposite sides of a plate. Discussions on how this definition reflects the sensation by a person has not been found.

In 1988 Steinman et al. (Steinman et al. 1988) developed view factor diagrams for inclined surfaces by using computers and cubic spline to connect the results obtained by Fanger. With the new diagrams, view factors are no longer limited to orthogonal rooms. The principle of dividing the surfaces according to the person's centre, as shown in Figure 4, is also used in the new diagrams, supplemented with angles for the inclination.

Researchers using the photographic method to determine projected area factors make an effort to approach the results as if pictures are taken from an infinite distance. Horokoshi et al. (Horikoshi et al. 1990) question this approach as applicable in the calculation of view factors between a person and the surfaces in a room, especially concerning the floor. They argue that a more realistic measure of how a surface affects a person is found by means of an orthographic projection camera method, especially for surfaces close to the person, as the findings of Fanger are only valid if the distance to a surface is at least 7 m. In their own study, photographs were taken from a number of points on a surface instead of on a sphere. The method better takes into consideration that the human body is not plane, and parts of the body closest to a surface therefor appear larger.

With the new decade, the 1990s, diagrams were substituted with algorithms that can be used in computers to calculate both projected area factors and view factors. Rizzo et al. (Rizzo, Franzitta, and Cannistraro 1991) and Cannistrato et al. (Cannistraro et al. 1992) transformed Fanger's diagrams into polynomial algorithms. The algorithms calculate the projected area factor for a standing or a seated person from input on azimuth angle and altitude angle, and view factors are calculated from inputs on the position of the surface in correlation with the person, using the method shown in Figure 4. In 2000, algorithms for inclined surfaces were added (Nucara, Pietrafesa, and Rizzo 2000), making it possible to calculate view factors for any plane surface.

New studies have been made using digital photographs and computer technology for measuring the projected area of a number of Italian subjects (Calvino et al. 2005, 2009; La Gennusa et al. 2008), and these measures are used in a tool for calculating view factors to any plane surface, though still dividing the surface according to the centre of the person, as shown in Figure 4.

A comparison between studies of projected area factors shows that nationality only has a slight influence when comparing data for subjects from Australia, Italy, China, Japan, Germany and the US (Nucara et al. 2012).

Instead of using a camera and real persons, Tanabe et al.(Tanabe et al. 2000) use numerical computing to calculate projected area factors. The shape of a person used is obtained by commercially available software, and the shape is chosen to be close to the measures for Fanger's test persons. Tanabe et al.(Tanabe et al. 2000) found

agreement within 10% accuracy of Fanger's results when converting the results into diagrams for reading view factors to surfaces. Thereby, they showed that numerical simulations can be used in studies of projected areas and view factors.

The use of numerical simulations and thermal manikins provide a basis for more detailed studies on the radiant impact of specific body parts (Kubaha et al. 2003, 2004) and has been used for finding projected area factors of standing and walking persons and for comparisons between people with different weight and gender (Park and Tuller 2011).

In conclusion it is found that the area of radiation to the human body has been researched for decades, though none of the developed calculations have been built into simulation tools. Based on the research it looks promising to develop a method for calculation of view factors suitable for thermal comfort simulations and thereby improve simulation of mean radiant temperature and thermal radiant asymmetry in building energy simulation tools. An advantage in this connection is that view factors do not change over time, calculation of view factors therefore only needs to be performed once for the room, while still improving calculations in all time steps.

AIR VELOCITIES

Air velocities affect both global thermal comfort and the sensation of draught.

Exact calculations of future airflows are almost impossible because airflows are so easily affected by obstacles or differences in temperature. The most precise calculations can be made by computational fluid dynamics (CFD), though the calculation time is a major drawback in connection with long-term simulations.

A premise of this literature review is the ability to make long-term, whole room simulations of thermal comfort in connection with building energy simulations. The review has, therefore, covered not only CFD but also zonal models and flow elements.

CFD AND BUILDING ENERGY SIMULATIONS

Building energy simulations and CFD complement each other in the simulation of thermal comfort. The needed boundary conditions to CFD are outputs from building energy simulations, and CFD is able to make detailed calculations of the airflows, which enhances the calculations of building energy simulations.

The fundamentals of CFD are the solutions of Navier Stokes equations e.g. by using the finite volume method. Navier Stokes equations are differential equations and the finite volume method solves them by means of discretisation, where a balance

equation is set up for each small volume in the room as described by Patankar (Patankar 1983).

In 1988, Chen (Chen 1988) combined CFD and building energy simulation to optimise the simulations of energy consumption and CFD is used to improve the calculations of heat transfer caused by differences in air temperatures in the room.

Beausoleil-Morrison (Beausoleil-Morrison 2000) researches and describes in his thesis how a coupling between CFD and the building simulation program ESP-r should be done in order best to model indoor airflow and internal surface convection. He develops an adaptive controller that monitors the evolving thermal conditions and airflow conditions in the room, and this information is used to select suitable boundary condition for each surface to be used in the CFD simulations. The integration between CFD and ESP-r makes it possible to make better calculations of internal airflows and heat flows between rooms. The objective of the study was not long-term evaluations of thermal comfort, but better calculations for shorter periods of time, where the combination between the tools makes simulations for evolutions of flows better and easier.

By coupling CFD and building energy simulations, it is possible to make CFD simulation for longer periods by assuming stationary conditions for each calculation instead of calculating the evolution of the flows in the room. Zhai et al. (Zhai et al. 2002) describe a number of strategies for coupling between the programs. One strategy can be to make CFD simulations for specific hours of each day, e.g. 8:00 am. Each time, in which CFD simulations are used, it can be chosen to make iterations between the programs until the results converge or it can be chosen to simply move on to the next time step without iterations.

Zhai et al. (Zhai and Chen 2006) give an overview of different strategies for the coupling between building energy simulations and CFD and lists some fundamental rules based on sensitivity analysis and cost-benefit of when to choose a coupling strategy and which coupling strategy to choose. For instance, it is recommended to use simple energy simulations in the early design phase, while a method coupling energy simulations with CFD is recommended if the indoor air environment is heavily dependent on thermal boundary conditions. The type and frequencies of coupling depend on the size of fluctuations and influences from the outdoor environment on air movements and how precise the results need to be.

All articles found are focused on short-term simulations of e.g. one day, when more accurate simulations were made. Long-term simulations are not feasible with CFD due to the long calculation time.

ZONAL MODELS

 "A zonal model is an intermediate method between representing a space by a single homogenous node and that offered by the CFD techniques" (Megri, Snyder, and Musy 2005)

Zonal models make it possible to make simulations of indoor air fields with lower calculation times than CFD. The models use a coarser grid supplemented with models for airflow. Zonal models are easier for a user to define than CFD models and are, therefore, more applicable as a tool in the early design phase of buildings.

In 2001, Haghihat et al. (Haghighat, Li, and Megri 2001) developed a zonal model that can be integrated into building energy simulation tools and can calculate global thermal comfort in a room. Jet characteristic equations are used to model mechanical ventilation, and good agreements were found between the results of the zonal model, the CFD model and the experimental data. They find that the model can be used to study the impact of e.g. room layout and air inlet diffuser types on thermal comfort, and they conclude that their model is a feasible approach for thermal simulation of naturally and mechanically ventilated rooms from an engineering view point.

A method quite similar to a zonal model is the nodal model. Rees and Haves (Rees and Haves 2001) developed a nodal model for rooms with displacement ventilation and chilled ceilings. The room is divided into a number of vertical zones, and calculation nodes are placed in each zone and at the boundaries between zones. The method separates the air movement in the plumes from the rest of the room in the calculations and is able to reasonably reproduce measured air balances and room temperatures.

FLOW ELEMENTS

Flow elements are based on a principle of dividing the flow in the room into areas that can be treated independently of surrounding flows. Flow element theory is based on a combination of theoretical fluid dynamics and empirical experiments and observations.

Flow elements describe the flow pattern from e.g. an inlet based on input on initial air speed, air inlet area and a diffuser constant, K. The diffuser constant is found experimentally for each inlet device. In case of non-isothermal flows, the temperature difference affects the flow and the effect is expressed by the Archimedes number and a constant taking the distribution of heat sources in the room into account.

According to P.V. Nielsen (Nielsen 1994), flows occurring in ventilated rooms can be divided into four categories with a total of 14 flow types, as shown in Figure 5.
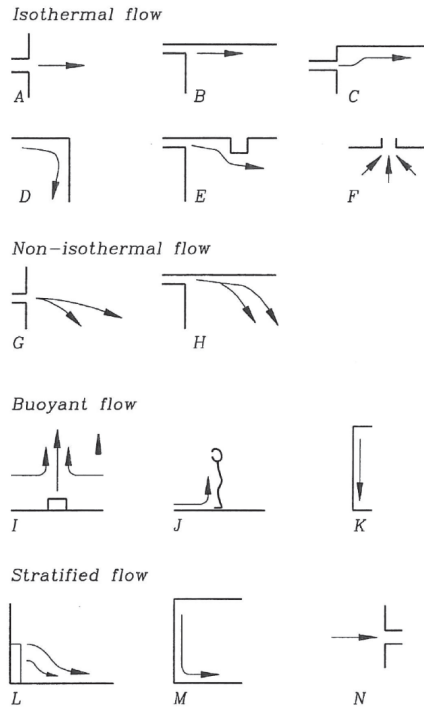

Figure 5 Flow elements occurring in ventilated rooms. The flow elements are divided into four categories (Nielsen 1994).

Some of the first descriptions on flows in a room – that are still in use – are from the 1950s when Koestel described the velocity decay (Koestel 1954) and trajectory (Koestel 1955) of a horizontal free jet.

Flow elements are typically based on experiments in empty rooms with a simple box geometry while the buildings in real life would be filled with furniture and occupants. J.R. Nielsen (Nielsen 1998) tests the influence of furniture on the air movements in the upper part of a room with mixing ventilation and the maximum velocity in the occupied zone. The study is made in order to determine if flow elements derived for empty rooms are fully valid in furnished rooms. Air velocities are measured in a test room that could have three different lengths, and the velocities are measured both with and without furniture in the half of the room opposite the wall mounted inlet. It was found that the velocity in the occupied zone is lower in the furnished room than in the empty room. Thus designing according to an empty room is on the safe side in relation to avoiding draught.

In the paper "Analysis and Design of Room Air Distribution Systems" (Nielsen 2007), flow elements, CFD and full-scale experiments are discussed as complementary methods for designing room air distribution systems. Nielsen argues that flow elements are well suited when ventilation is either based on mixing or displacement strategies. However, some air distribution systems cannot be adequately described by flow elements, for example a textile ceiling diffusor inlet or vertical air distribution systems where draught is mainly generated by the heat load in the room and not by the air supply. In these situations, CFD or full-scale experiments are preferable.

Flow elements have been implemented in the Swedish software for indoor and climate simulation tool IDA ICE (Eriksson et al. 2012) . This tool assumes that when two flow elements collide, the one with the highest velocity will "survive".

Flow elements are also used in the flow program DIMcomfort, developed by the ventilation company Lindab. The airflows from their diffusers are shown with the ability to regulate airflow and temperatures to see how this influences the flow pattern in the room. Lindab's tool has been developed through measurements in an air laboratory and is specific for Lindab's diffusers, and this shows the possibilities of using flow elements for fast simulation and comprehensive visualisation of airflows in rooms.

The description of flow elements is continuously growing, covering more flows and interactions. Cao et al. (Cao, Ruponen, and Kurnitski 2010) have recently contributed to the description of flow elements describing the velocity distribution when a plane jet collides with a corner.

Of the three methods described here, flow elements and zonal models are the most promising in connection with simulations of thermal comfort based on building energy simulations.

THE PERSONAL FACTORS: CLOTHING AND ACTIVITY LEVEL

Two of the six parameters affecting global thermal comfort are related to the occupants and are outside the range of the engineer's optimisation. These are the clothing and activity levels.

In building simulations, occupants are often assumed to have one of two fixed clothing levels: one for summer conditions and one for winter conditions, typically 0.5 clo and 1.0 clo.

To investigate how variation in clothing affects the building's energy demand, G.R. Newsman (Newsham 1997) performed building energy simulations with varying flexibility in the clothing adjustment and found that significant energy savings can

be obtained through optimal adjustments of clothing without compromising thermal comfort. G.R. Newsman used a simplified version of Fanger's thermal comfort equation in a finite difference model. G.R. Newsman concludes that it is vital to consider occupants' behaviour when modelling buildings' energy demand and thermal comfort.

Through a literature review of field experiments, G.S. Brager and R.J. de Dear (Brager and de Dear 1998) find a distinction between thermal comfort in air-conditioned vs. naturally ventilated buildings and conclude that the difference is caused by adaptation. Through adaptation of i.e. clothing, better thermal comfort is experienced in naturally ventilated buildings under the same circumstances as in air-conditioned buildings.

Several studies have investigated how people vary their clothing. A study in Sydney by C. Morgan and R.J. de Dear (Morgan and de Dear 2003) showed that people vary their clothing according to outdoor temperature when a strict dress code is not employed. During the warm summer of 2006 in Switzerland, Haldi and Robinson (Haldi and Robinson 2008) found that people mainly opened windows and adjustments of solar shading to improve their thermal comfort. Clothing was seldom varied during the day but the level of clothing was found to be correlated to the outside temperature at 6 a.m. Also, de Cali et al. (De Carli et al. 2007) found a correlation between clothing level and the outside temperatures the same morning and the previous days. In the same study, they found that the clothing level is independent of gender.

None of the studies investigating the effect of adjusting clothing led to people being more satisfied with the thermal environment, but several studies show a better estimation of clothing level based on outdoor temperatures, than the two steady assumptions often used.

Activity level is a way of influencing a person's thermal environment; unfortunately the uncertainty of the activity level is high, both because it is difficult to measure and estimate for a given situation, and because the metabolic rate for the same activity varies among people. Uncertainty on the metabolic rate is typically around 50% but can be as high as 100% according to Parsons and Hamley (Parsons and Hamley 1989).

As the measure of thermal comfort, PMV is greatly influenced by both activity level and clothing. Havenith et al. (Havenith, Holmér, and Parsons 2002) question the use of PMV as a measure, because both activity level and clothing level are subject to high uncertainty. To determine the activity level, they list six methods ranging from measurements to classification according to the kind of activity in a table. The most accurate method has an accuracy of 15%, and Havenith et al. find that a difference in activity level of 15% can easily lead to a difference in the calculated PMV of 0.3.

The comfort categories suggested in ISO 7730 (CEN 2005) are, therefore, questionable.

In conclusion only few studies were found on activity level in connection with thermal comfort and they show that the activity level is hard to estimate. To improve simulation of thermal comfort, more research in this area would be beneficial, e.g. starting with a thorough literature review focused solely on activity level and including physiologic journals and researchers.

DEALING WITH UNCERTAINTIES

Simulations of thermal comfort and building simulations in general are subject to uncertainty, especially due to occupant behaviour. This means that the results of the simulations are only valid if we have correctly assumed how people will act, which is nearly impossible in real life.

For a known set of indoor climate conditions, the predicted mean vote (PMV) can be calculated from the equations in ISO 7730 (CEN 2005). Taking into consideration that not all votes are equal to the mean, Jensen et al. (Jensen, Toftum, and Friis-Hansen 2009) made a Bayesian network between the thermal conditions in a room, gender, age and thermal vote based on the ASHRAE RP-884 database (de Dear 1998). The Bayesian network gives the probability of each thermal comfort vote when thermal conditions, gender and age are known. By using the Bayesian network, the uncertainties associated with human behaviour are included in the simulations.

Hoes et al. (Hoes et al. 2009) evaluated the effect of user behaviour on building performance with the aim of creating a tool to help make buildings that are more robust to the influence of user behaviour. The background of the study is that the more energy-efficient buildings become, the higher the impact of users gets on the buildings'energy consumption. User behaviour is modelled using a Monte Carlo approach together with the building simulation tool ESP-r, and they find from simulations of five test cases that improved modelling of user behaviour can optimise the overall building performance.

These two examples show that the handling of uncertainties in building energy simulation tools is definitely possible, whether it is using a Bayesian network or the simpler Monte Carlo approach.

CONCLUSION

For optimisation of thermal comfort in parallel with building energy optimisation, the methods described by Fanger were found to be most adequate. The methods make it possible to spot causes of thermal comfort problems, but are also the most

complicated and uncertain to calculate as several of the input parameters are not direct outputs from building energy simulations.

A closer look into four building energy simulation tools, which claim to be able to calculate PMV and PPD, showed that inputs were needed by the user on e.g. view factors, air velocities, clothing and activity level.

Based on the review, it looks promising to develop methods for automatic calculations of view factors, air velocities and clothing level from output parameters from building energy simulations. The activity level was found to be highly uncertain and to vary among people. In the investigated literature, there no studies were found on the variation in activity level in a way that could be used for building simulations.

Several studies on dealing with uncertainties in building simulation because of uncertain occupant behaviour were found and the methods also apply to simulation of thermal comfort.

It is therefore recommended to expand building simulation tools with calculation of thermal comfort based on the work by Fanger to assist designers in optimising buildings with regards to energy and thermal comfort simultaneously.

The second article presents the research on clothing level, how it varies with time and among people. The article also explores the possibilies of taking into account thermal adaptation through adjustment of clothing, when calculating thermal comfort.

Second article:
DOES VARIATION IN CLOTHING MAKE US MORE THERMALLY COMFORTABLE?

Mette H VORRE[1,*], Rasmus L JENSEN[2]

[1]Energy and Environment, Danish Building Research Institute, Aalborg University, Copenhagen, Denmark
[2]Department of Civil Engineering, Aalborg University, Aalborg, Denmark

*Corresponding email: mhv@sbi.aau.dk

SUMMARY

In the same room, people will wear different amounts of clothes if there is no strict dress code. Ideally everybody would put on just the right amount to feel thermally comfortable, but that is not always the case. To improve simulations of thermal comfort, an estimate of clothing insulation is needed. This includes the distribution within a group of people and if this causes more or less people to be dissatisfied. From the research data, the relation between temperature and clothing insulation was found and the distribution among people was studied. It was found that the variation in clothing among people is higher at low temperatures than at high temperatures, and that people do choose their clothing according to thermal preference, but that the distribution of thermal comfort votes is the same.

INTRODUCTION

Improving comfort is one of the main reasons for the development of both buildings and clothing. Basic needs were fulfilled centuries ago, and refinements are no longer made just to improve comfort, but also to promote an image by making eye catching buildings and fashionable clothing. At the same time, we still expect to be thermally comfortable in buildings. To ensure thermal comfort in future buildings, prior simulation of thermal conditions gives an opportunity to compare different layouts of the buildings in order to optimise both thermal comfort and energy consumption. To get the most reliable simulations of thermal comfort, the variation and

distribution of clothing insulation of the occupants is essential, as it has a great influence on the perceived thermal comfort. If we can understand how clothing insulation varies over time, with the factors already known from the building energy simulation tools, the simulation results would come closer to reality. But also the distribution in clothing insulation within a group of people is interesting, and a hypothesis tested in this paper is that "when people choose their clothing, they will (to some extent) do it in relation to their thermal preferences, and that will result in less people being dissatisfied with the thermal climate, than can be calculated by the relation between Predicted Mean Vote (PMV) and Predicted Percentage of Dissatisfied (PPD) as found by P.O. Fanger (Fanger 1970)".

The calculation methods developed by P.O. Fanger (Fanger 1970) are based on climate chamber observations where subjects were exposed to the same thermal climate with the same amount of clothing and activity level. From the studies, variations in thermal preference was found, and these are the reason for PPD being equal to 5% at optimum thermal conditions, PMV = 0. In the adaptive thermal comfort model (de Dear and Brager 1998) both activity level and clothing insulation is taken out of the equation, which is much more simple than Fanger's model. The adaptive model is based on data from real buildings and not climate chambers, and it is part of these data that were used in the study together with some of Fanger's data. By finding the variation of clothing insulation over time, this part of the adaptation should be possible also to simulate by using PMV and PPD, giving a more reliable result compared with using a standard clothing level of e.g. 1.0 in winter and 0.5 clo in summer.

The variation in clothing insulation was earlier found to be independent of sex (De Carli et al. 2007) and more dependent on the outside temperature in the morning and the previous days.

In the current study, the relation between clothing insulation and both indoor and outdoor temperatures is studied. The relation to the current indoor temperature is relevant if assuming that users know their buildings and choose their clothing according to their expectations and adjust according to the climate they perceive. The study also covers whether the distribution in clothing depends on thermal preference and whether this leads to less people being dissatisfied.

METHODOLOGIES

The database from the RP884-project (de Dear 1998) was used. Only class 1 projects contain information on clothing insulation. The class 1 data in the RP884 project come from 15 projects including 62 buildings in Canada, Australia and USA, in both summer and winter conditions. The buildings are used for office, court, police and jail with activity levels between 1 and 1.8 met.

Data were deleted where information on clothing level, activity level or vote of the thermal climate were missing, and also where clothing was set at 0 clo (naked).

The data were divided on buildings with and without mechanical cooling. In turn, these data were divided by different parameters: operative temperature, outside morning temperature, insulation level of clothing, etc. One or two parameters were used to divide the data each time, to see how the variation was relative to the parameters. In each subgroup, mean and standard deviation was calculated. This gives a picture where each temperature step is weighted equally even though they did not contain the same amount of data. Subgroups containing less than 10 data points were not taken into consideration.

Example: To investigate the influence of operative temperature on the level of clothing insulation (including chair), the data was divided according to the operative temperature inside the building with steps of 1°C, and within each step a mean value of the insulation was calculated together with the standard deviation. The data point 23°C includes incidences where the operative temperature had been ≥22.5°C and <23.5°C.

The distribution of the amount of data within each temperature step of the operative temperature is shown in Figure 6, together with the distribution on the outside temperature at 6AM.
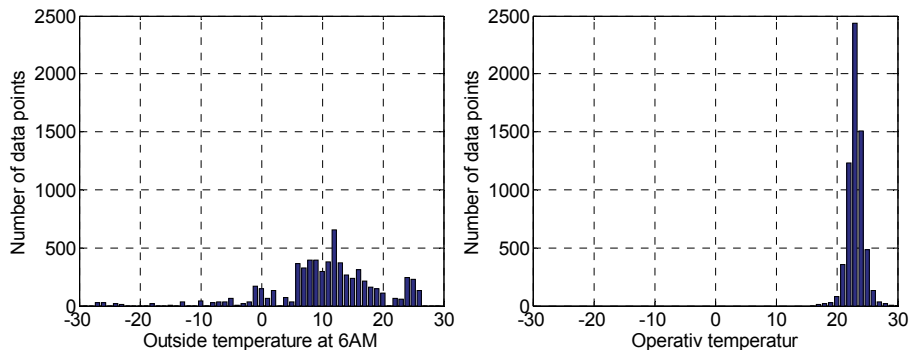

Figure 6 Amount of data within each temperature interval

Histograms showed that most data were collected at the operative temperatures of 22°C and 23°C. More variation was seen in relation to the outside temperature, where most data were found between 5°C and 18°C.

The first investigation aimed to find a relation between clothing insulation and a parameter known or calculated in a building simulation program, in order to be able to make better predictions of the thermal comfort in future buildings.

Secondly the distribution of clothing insulation among the subjects was investigated, to see whether it reflected a wish to improve thermal comfort, and whether taking the distribution into consideration it would give less standard deviation on subjects vote on the ASHRAE scale, that ranges from -3 (cold) to 3 (hot).

RESULTS AND DISCUSSION

CLOTHING INSULATION VARIATION WITH TEMPERATURE

When a person decides how much clothing to put on, this depends on a lot of factors where both fashion and thermal comfort are surely some of them. While it is hard to simulate how fashion influences the clothing level, it is easier to evaluate the influence of the wish to gain thermal comfort.

As it is often in the morning that an outfit is chosen, the temperature at that time of day could very well influence how much clothing is put on. This parameter has earlier been found to be a good indicator of the amount of clothing (De Carli et al. 2007). In Figure 7, the insulation of clothing and chair is illustrated in relation to the outside temperature at 6AM for buildings with and without mechanical cooling.

For both types of buildings, there is a clear relation between the outside temperature at 6AM and the mean of the chosen clothing insulation. There was no clear difference between the building types. The standard deviation from the mean of clothing insulation were greatest for low temperatures, while at high temperatures each value was closer to the mean, which might be due to a lower limit of acceptable clothing at work places.

The relation between the mean insulation (all buildings) and outside morning temperature can be described by:

Equation 6

$$clo_{mean} = -0,012 \cdot t_{out6AM} + 0.9144 \qquad\qquad R^2 = 0.83$$

Where clo_{mean} is the mean clothing insulation (including chair) and t_{out6AM} is the outside temperature at 6AM.
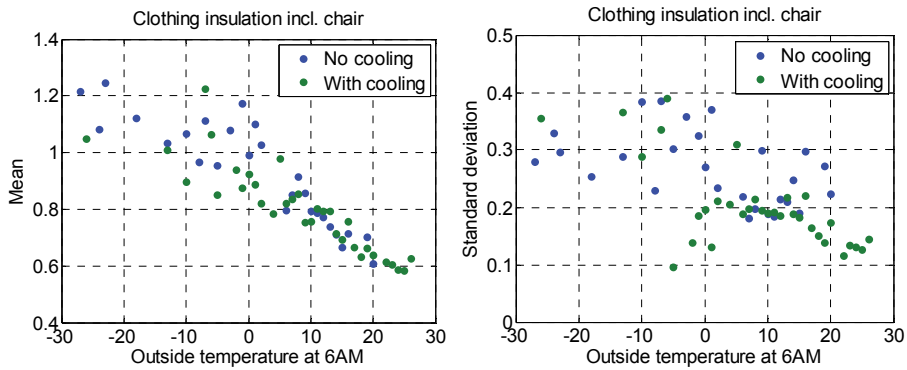
Figure 7 Insulation of clothing and chair in relation to the outside temperature at 6AM. To the left, the mean within each temperature step is shown and to the right the standard deviation to the mean is shown for each temperature step.

Another parameter that intuitively affects the chosen level of clothing insulation is the current temperature inside, the operative temperature. The relation between operative temperature and clothing insulation (including chair) is shown in Figure 8.
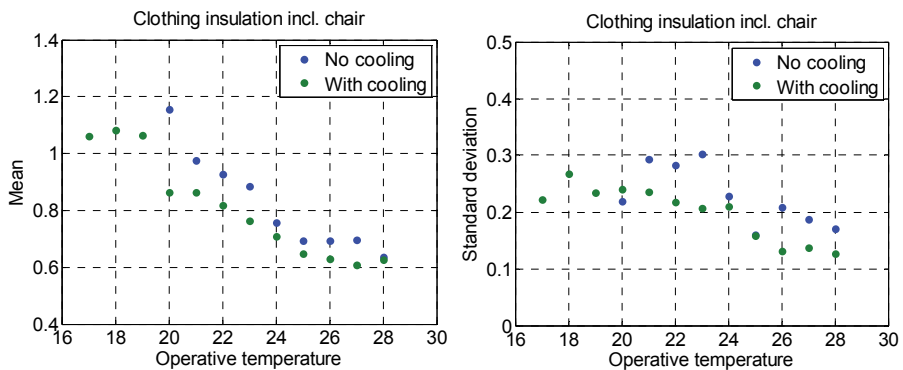

Figure 8 Insulation of clothing and chair in relation to the current operative temperature. To the left, the mean within each temperature step is shown and to the right the standard deviation from the mean is shown for each temperature step.

The clothing insulation related to the operative temperature inside shows a distinction between buildings with and without mechanical cooling, where people in buildings without cooling (which include buildings with natural and mixing ventilation) put on more clothing, than people in buildings with cooling (AC). Both building types show a linear relation under 25°C and a constant level above 25°C. The standard deviation to the mean (right figure) showed that there was more variation in clothing at low temperatures than at high temperatures and it also looked as if the variation was higher in buildings without cooling. Compared with the standard deviations seen in Figure 7, the standard deviations here are lower.

Equations for the calculation of clothing insulation related to the operative temperature were divided into buildings with and without cooling and below / above 25°C.

With cooling:

Equation 7

$$clo_{mean} = \begin{cases} -0.0552 \cdot t_{op} + 2.486 & \text{for} \quad t_{op} < 25°C \quad (R^2 = 0.95) \\ 0.65 & \text{for} \quad t_{op} > 25°C \end{cases}$$

Without cooling:

Equation 8

$$clo_{mean} = \begin{cases} -0.0858 \cdot t_{op} + 2.8294 & \text{for} \quad t_{op} < 25°C \quad (R^2 = 0.96) \\ 0.69 & \text{for} \quad t_{op} > 25°C \end{cases}$$

The equations calculating the relation between clothing insulation and operative temperature have a square error closer to 1 than the one found in relation to the morning temperature. The standard deviations from the mean values (right hand side in Figure 8) in each temperature step were also smaller. These are indicators that the operative temperature is a better predictor for clothing insulation.

These equations can be used when estimating the clothing insulation for calculating PMV in for example building energy simulation tools instead of using a single or a few different values during the year.

Clothing insulation distribution among people

Even though equations were found that could calculate the mean clothing insulation within each temperature step, there is still the distribution of clothing insulation within a group of people. To illustrate how PMV and PPD vary with clothing insulation, an example was calculated with average values from the whole data set:

$M = 1.2$ met $C = 0.78$ clo $t_{air} = 23.0°C$ $t_{rm} = 23.2°C$ $u = 0.14$ m/s $rh = 0.45$

where M is the metabolic activity, C is the clothing insulation, t_{air} is the air temperature, t_{rm} is the mean radiant temperature, u is the air velocity and rh is the relative humidity.

With the given values, PMV is -0.09 and PPD is 5%, a more or less perfect situation. If we then vary the clothing insulation by 0.25 which is close to the average standard

deviation in Figure 8, PMV ranges from -0.6 to 0.3, giving a PPD's of 12% and 7% respectively. If varying by the standard deviation in Figure 7, which is approximately 0.35, PMV ranges from -0.8 to 0.4 and PPD at 19% and 8%.

The distribution of clothing insulation between subjects might be due to their thermal preference, and then there would actually be less dissatisfied people. To evaluate whether this is the case, we can start by looking at the differences in clothing insulation between people in cooled buildings and non-cooled buildings. Looking at the calculated PMV in each temperature step, as well as the subjects' actual votes within each temperature step, the mean values are shown in Figure 9.
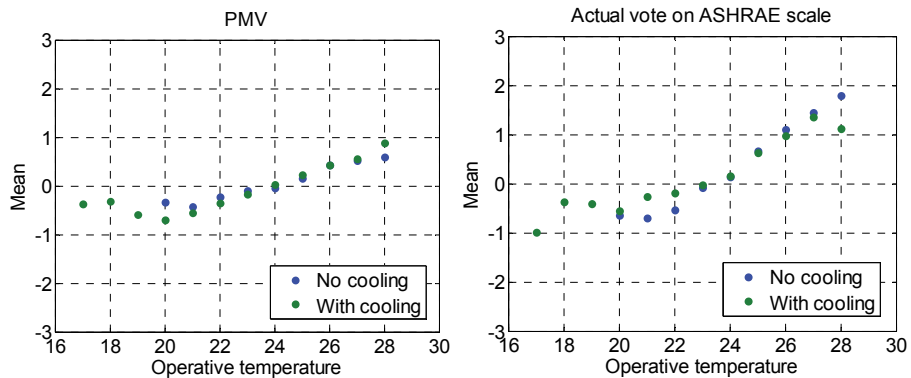

Figure 9 Relation between the mean calculated PMV and the operative temperature, as well as the mean actual vote by the subjects and the operative temperature.

The difference in clothing insulation level between building types cannot be found in the thermal sensation. Both the calculated PMV and the actual votes showed no distinction between building types. Combined with the earlier findings shown in Figure 8, this indicates that the thermal climate in the buildings without cooling is a bit chillier and more clothing is necessary.

To get a closer look at the influence of clothing on the perceived thermal comfort, data were divided according to clothing level. Here there was no distinction between the building types, as the data in each subgroup would then be too small.

The relation between operative temperature, clothing insulation and PMV is seen to the left in Figure 10, and the relation to the actual vote to the right in the figure.
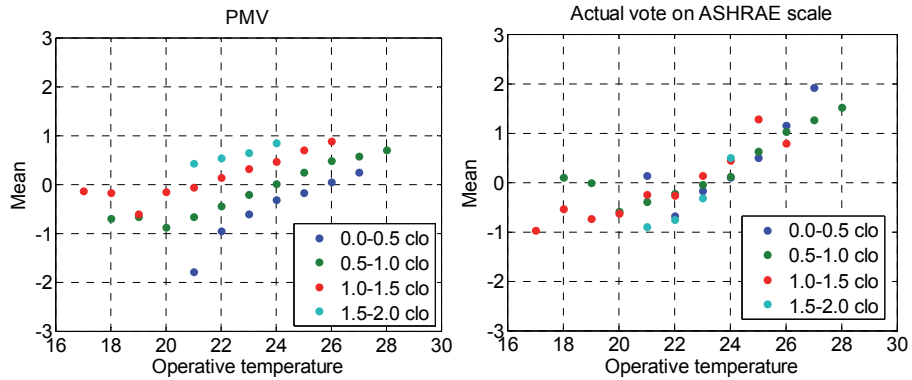
Figure 10 Relation between operative temperature, clothing insulation and PMV to the left and the relation to the actual vote to the right.

As opposed to the relation between building types in Figure 9, there is a clear distinction in the calculated PMV in Figure 10 between the different levels of clothing insulation, the less insulation the lower the calculated PMV. This means that the differences in clothing level is not just to compensate for differences in the thermal comfort, because the result is a clear distinction in PMV and a clear relation between the insulation level and the PMV.

The relation to the actual votes is interesting in order to see whether (some of) the variation was due to optimising the perceived thermal comfort. To the right in Figure 10 it is seen that there is no clear distinction between the levels of insulation. So independent of their clothing insulation, people have more or less the same mean value of votes on the ASHRAE scale, which indicates that people (at least to some extent) vary their clothes in relation to their thermal preference. But as can be seen in Figure 11, the division into clothing levels does not lower the standard deviation on the thermal votes by the subjects. On the right in the figure, standard deviation when dividing into building type can be seen for comparison.
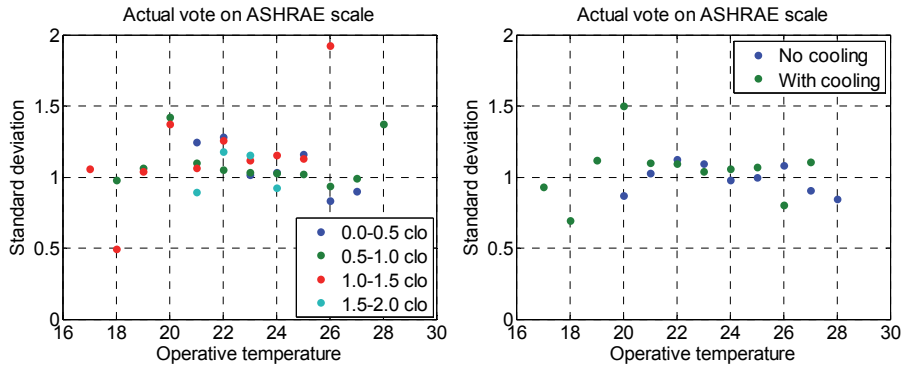
Figure 11 Standard deviations to mean values in each temperature step for the actual votes of subjects, divided by clothing insulation to the left and building type to the right.

A division according to clothing level does not give a lower standard deviation in the thermal votes. To quantify the standard deviation in Figure 11 the standard deviation on the data used to make the calculations for PPD (Fanger 1970) are shown in Figure 12 along with the mean votes according to ambient temperature.
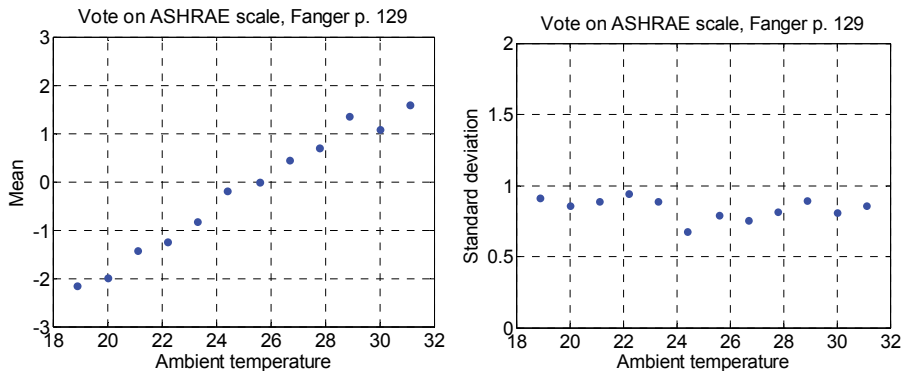

Figure 12 Plots of the data used by Fanger for PPD calculation from PMV.

At the same clothing and activity level in a laboratory, the standard deviation on the thermal votes was less than 1, while it was a bit higher in the plots in Figure 11. So even when taking insulation of clothing into consideration, we must still expect (at least) the same level of dissatisfied as was found from laboratory studies under a clothing insulation dictated by the test setup.

CONCLUSIONS

A study of the RP884 database showed that the clothing level of the people in a building has a linear correlation with both the temperature outside at 6AM and the

operative temperature inside. The correlation is better for the operative temperature, where a minimum clothing level is achieved at 25°C.

People in buildings without air conditioning (including naturally ventilated buildings) put on more clothing than people in air-conditioned buildings. This does not lead to higher PMV though, so the higher insulation must be to compensate for higher air velocities.

In general, looking at all buildings together, there is a variation in clothing which is higher when it is cold and a bit lower when it is warm. The variation gives a variation in the calculated PMV, higher PMV for high clo-values, but when looking at the actual votes, there is no correlation with the insulation; people perceive the thermal comfort the same way. This indicates that the distribution in clothing is due to people's different thermal preferences.

In the hypothesis, it was established that by taking the distribution in clothing among people into consideration a better estimate of thermal comfort would be achieved. However even when looking at the thermal votes, divided on clothing insulation, the same standard deviation was found, as when taking them all together. This means that even though we can see that people vary their clothing to get better comfort, the variation in thermal votes is not just dependent on this. The variation in clothing is still big, because there are also other reasons, like fashion, for varying the insulation.

To obtain a better understanding of the variations in thermal votes, more studies need to be carried out. Until then the variation of clothing insulation with operative temperature can be used for calculation of PMV in building energy simulation tools and other places, with the same expected percentage of dissatisfied as described by Fanger.

The next article researches the simulation of air velocities for use in thermal comfort evaluations.

Third article:
DRAUGHT RISK INDEX TOOL FOR BUILDING ENERGY SIMULATIONS

Mette H VORRE[1,*], Rasmus L JENSEN[2], Peter V NIELSEN[2]

[1]Department of Energy and Environment, Danish Building Research Institute, Aalborg University, Copenhagen, Denmark
[2]Department of Civil Engineering, Aalborg University, Aalborg, Denmark

*Corresponding email: mhv@sbi.aau.dk

ABSTRACT

Flow elements combined with a building energy simulation tool can be used to indicate areas and periods when there is a risk of draught in a room. The study tests this concept by making a tool for post-processing of data from building energy simulations. The objective is to show indications of draught risk during a whole year, giving building designers a tool for the design stage of a building.

The tool uses simple one-at-a-time calculations of flow elements and assesses the uncertainty of the result by counting the number of overlapping flow elements. The calculation time is low, making it usable in the early design stage to optimise the building layout. The tool provides an overview of the general draught pattern over a period, e.g. a whole year, and of how often there is a draught risk.

INTRODUCTION

Draught is one of the main causes of complaints about the indoor environment in buildings (Fanger et al. 1988). When people perceive draught, they take action to avoid it. This may lead to higher energy consumption, e.g. by turning up the heat to compensate. By predicting the draught risk in the early design stage, the building design can be optimised for both low energy use and low draught risk. In naturally ventilated buildings, this is especially important, as the ventilation is integrated in the building envelope and is closely linked to the current outdoor climate.

Draught risk can be simulated by CFD, but this is time consuming and therefore not used. On the other hand, building energy simulation tools are available that are faster but lack information on airflows. The two tools have been linked (Beausoleil-Morrison 2002) to supplement each other for thermal comfort simulation, but the CFD is slowing the process down.

Another way of estimating draught risk is to use flow elements. Flow elements describe the airflow in a room by equations for velocity distribution and flow patterns. Flow elements are derived for a number of standard situations and can be divided into categories depending on e.g. isothermal / nonisothermal, 2D plane flow / 3D flow, flow close to a wall or ceiling / free flow. Flow elements also describe flow by a cold down draught from a cold wall like a fully glassed wall (Nielsen 1994, 1995).

By using flow elements, velocities can be calculated in any affected point in the room and the accuracy in each point is not dependent on a grid or grid density. Using flow elements combined with building energy simulation tools, the draught in the room can be estimated for a whole year for each time step. This makes it possible to evaluate not only worst-case scenarios, but also any other situation, giving an overview of the draught risk and a picture of how robust the chosen building design is against draught e.g. under different weather conditions.

FLOW ELEMENTS FOR INLETS

Equations for calculating air velocity decays and flow patterns by flow elements constituted the basis of the method. Inputs were needed on room geometry, air temperature, and furthermore the inlet geometry, location, air velocity, air temperature outside and/or surface temperature (depending on the type of flow) were needed for each flow to be evaluated. These data are typically available from building energy simulation tools.

For some typical inlets, the velocity in the centre of a jet at a given distance x can be calculated by:

	3D jet	Plane flow (2D)
Free jet	*Equation 9* $u_x = \dfrac{K_a}{\sqrt{2}} \cdot \dfrac{\sqrt{a_0}}{x + x_0} \cdot u_0$	*Equation 10* $u_x = \dfrac{K_p}{\sqrt{2}} \cdot \sqrt{\dfrac{h_0}{x + x_0}} \cdot u_0$
Wall jet	*Equation 11* $u_x = K_a \cdot \dfrac{\sqrt{a_0}}{x + x_0} \cdot u_0$	*Equation 12* $u_x = K_p \cdot \sqrt{\dfrac{h_0}{x + x_0}} \cdot u_0$

Where u_x is the velocity in the center of the jet, a_0 is the area and h_0 is the height of the opening, x_0 is the distance to the virtual origin of the flow at the opening; K_a and K_p are constants depending on the inlet opening.

The velocities outside the centre of the jet are calculated from the universal velocity profiles shown in Figure 13.
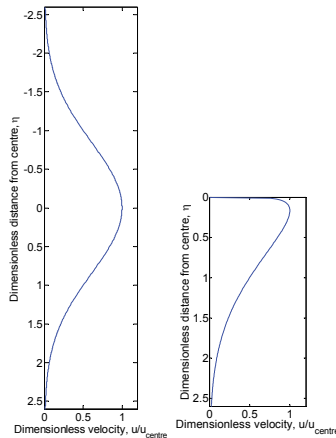

Figure 13 Universal velocity profiles for a free jet and a wall jet, the latter found by Verhoff (Verhoff 1963) .

The flow pattern of a jet mainly depends on the Archimedes number and the location of the inlet. The air will be accelerated downward by gravitational forces if the supply air is cool. Koestel (Koestel 1955) found that a free horizontal jet follows a trajectory given by:

Equation 13

$$y = 0.6 \cdot \frac{Ar}{K_a} \cdot \left(\frac{x}{\sqrt{a_0}} \right)^3 \cdot \sqrt{a_0}$$

Where y is the vertical displacement of the flow at distance x, Ar is the Archimedes number.

If the inlet is close to the ceiling (wall jet), the coanda effect will prevent the air jet from following the trajectory in Equation 13. Instead the jet will be attracted to the nearby ceiling until gravitational forces become greater than the pressure forces from the coanda effect. The distance from the inlet to this point is called the penetration length and (Grimitlin 1970; Nielsen and Möller 1987, 1988) derived the equations for the calculation of the penetration lenght:

3D jet:

Equation 14

$$x_s = 0.19 \cdot K_{sa} \cdot K_a^2 \cdot Ar^{-0.5} \cdot \sqrt{a_0} - x_0$$

Plane flow (2D):

Equation 15

$$x_s = 0.1 \cdot K_{sp} \cdot K_p^2 \cdot Ar^{-0.7} \cdot h_0 - x_0$$

Where x_s is the penetration length, K_{sa} and K_{sp} are constants depending on the room and heating distribution.

When the jet detaches from the ceiling, it will not follow the trajectory given for a free jet (Equation 13). The results in (Jacobsen et al. 2002) show that the flow can be approximated with a straight line at an angle of 45° to the ceiling. However, the air will fall directly down if the inlet temperature is so low that the jet is not attracted to the ceiling.

The four trajectories that a wall jet can follow depending on the penetration length are shown in Figure 14.
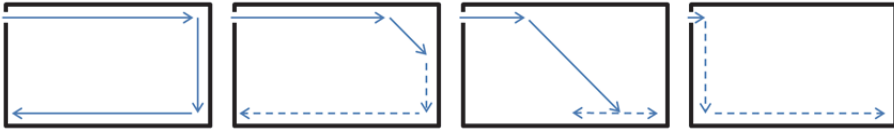
Figure 14 A wall jet comming into a room is assumed to follow one of four trajectories, depending on the penetration length. The dashed lines represent the parts of the flow that still need to be implemented in the draught risk index tool.

FLOW ELEMENTS FOR A GLASSED WALL

A fully glassed wall can induce a cold down draught that will continue at the floor similar to displacement ventilation. The velocity at the floor depends on the distance to the wall and the height of the wall (Heiselberg 1994):

Equation 16

$$u_x = \begin{cases} 0.055 \cdot \sqrt{H \cdot (t_{air,oc} - t_{window})} & \text{for } x < 0.4 \text{ m} \\ 0.095 \cdot \dfrac{\sqrt{H \cdot (t_{air,oc} - t_{window})}}{x + 1.32} & \text{for } 0.4 \text{ m} \le x \le 2 \text{ m} \\ 0.028 \cdot \sqrt{H \cdot (t_{air,oc} - t_{window})} & \text{for } 2 \text{ m} < x \end{cases}$$

Where H is the height of the cold wall, $t_{air,oc}$ is the air temperature in the occupied zone, t_{window} is the inside surface temperature of the window and x is the distance to the wall.

DRAUGHT RISK INDEX TOOL

A tool for calculating the draught risk was made for post-proccesing of data from a building simulation tool.

By using flow elements, velocities can be calculated in any affected point in the room and the accuracy in each point is not dependent on a grid or grid density. To get a picture of the velocity distribution in the room, a grid was used and velocities were calculated in each node.

If more flow elements were present in the room, each flow was calculated individually, not taking into consideration the effect of the other flows in the room. The velocities in each node were compared and the highest used to estimate the draught risk. In each node, the number of flow elements was counted, if the velocities were above a certain threshold limit. This was used as a measure of the uncertainty of the calculations.

PRESENTATION OF THE RESULTS

For each time step, the results can be visualised as a plot on the floor plan. At each node on the floor, the maximum velocity was found in the column from the floor to the top of the occupied zone; the principle is shown in Figure 15. Depending on the maximum velocity, the draught risk in each area was ranked as no (white), low (green), medium (yellow) or high (red).
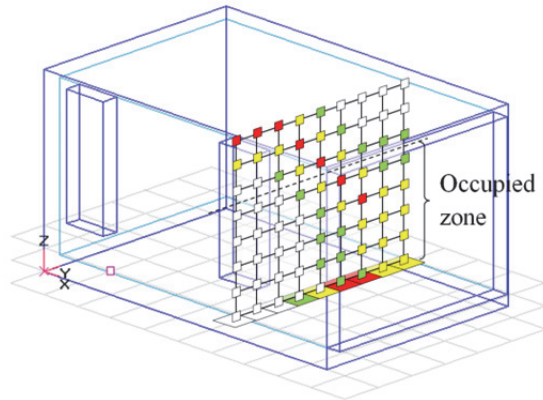

Figure 15 Draught risk is estimated in the nodes of a grid structure and the highest value in each column is plotted on the floor plan.

The same was done for the number of flow elements meeting where the maximum number of flow elements in a node was shown on a floor plot. The more flows that meet, the more uncertain both the calculated risk of draught and the areas in the room, where the flows causes risk of draught.

For longer periods, the results were summed showing the draught risk index and number of meeting flow elements as percentages of the floor area. These plots can be used to point out periods of interest.

EXAMPLE: OFFICE WITH NATURAL VENTILATION

An office with natural ventilation was modelled in the building energy simulation tool BSim (Wittchen, Johnsen, and Grau 2013) using a Danish weather datafile. The room is shown in Figure 16 together with a brief description.
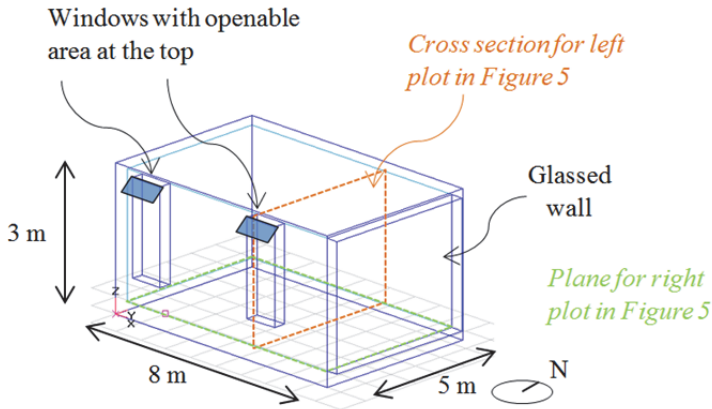
Figure 16 The room as simulated in BSim. Inside dimensions of room: height 3 m, length 8 m, width 5 m. There are two openable windows, each with a controlled opening area at the top of up to 0.33 m2. The end wall is fully glassed.

From BSim, data were extracted for the draught-risk index tool. These were: indoor and outdoor air temperatures, interior window surface temperatures, airflow velocities through the window openings and opening area of the windows, all extracted for each time step. For the openanble windows K_a was set to 5 (Equation 11, Equation 13 and Equation 14) corresponding to a poor inlet device for mixing ventilation. K_{sa} was set to 1.5 (Equation 14), which corresponds to heat release in the floor area. The height of the occupied zone is set to 1.8 m.

For an hour in May the following parameters were found by BSim: $t_{in} = 21.4°C$, $t_{out} = 11.8°C$, $u_0 = 0.28$ m/s, $a_0 = 0.073$ m^2, $t_{window} = 19.7°C$.

The velocity distribution generated by each of the openable windows was calculated by the flow element of a 3D wall jet. In Figure 17 velocities in a vertical cross-section through a window are shown together with the maximum velocity in the occupied zone projected onto the floor plane. Velocities below 0.05 m/s are plotted with white colour (no risk), velocities of 0.05 – 0.1 m/s are shown in green (low risk), velocities of 0.1 – 0.2 m/s are shown in yellow (medium risk) and velocities above 0.2 m/s are shown in red (high risk). The flow from the other openable window is identical.
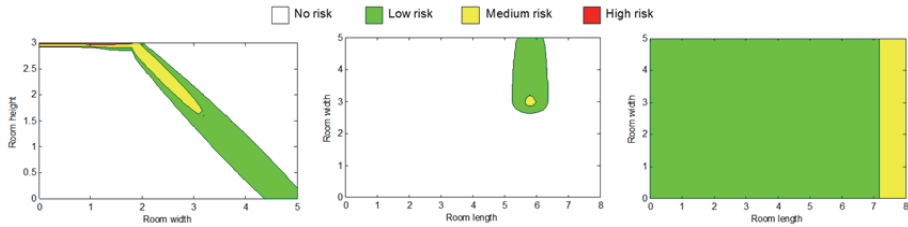
Figure 17 The left figure shows the velocity distribution calculated in the central plane of one of the openable windows. The flow enters in the top corner of the room and attaches to the ceiling for approximately 2 meters before it drops into the occupied zone. The middle figure shows the room seen from above with a marking of maximum velocities in the occupied zone of the flow element from one of the openable windows. The right figure shows the velocity distribution in the room created by down draught from the glassed wall, projected down onto the floor plan.

The incoming airflows from the windows create velocities in the occupied zone resulting in medium risk of draught in two small areas of the room and low risk in areas that are slightly larger.

In Figure 17 on the right, the draught risk created by the cold glassed wall is shown. The glassed wall creates a down draught due to temperature difference, and the flow continues at floor level, with the highest velocities closest to the wall.
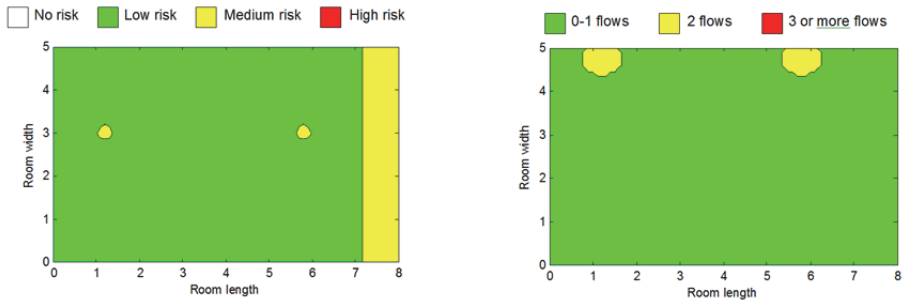
Figure 18 The left shows the maximum velocities in the occupied zone from all of the three flow elements, projected down onto the floor plan. The right shows the number of flow elements meeting in each area.

The results for all three flows were given in one plot, Figure 18 left. This plot shows the maximum risk of draught in each area, as calculated by flow elements one at a time. There is a low risk in most of the room and a medium risk close to the glassed wall and in two areas inside the room caused by airflows from the windows.

The estimated uncertainty of the flow element calculations was evaluated by counting the number of velocities above a threshhold of 0.05 m/s in each node, and

for each column the maximum number is projected down onto the floor, Figure 18 right.

In the two small areas of the room, shown in yellow in the right plot of Figure 18, both the openable windows and the glassed wall generates risk of draught in the same nodes. This is because the flow from the windows reaches the floor in these areas. Actually the areas could be bigger, as the tool at the moment does not handle how the flow from the windows continues after it reaches the floor.

As a summary of the draught risk over a longer period, the areas of the risk intervals (Figure 18 left) were found for each time step and can be shown, e.g. over a week in May as seen in Figure 19. The same is done for the uncertainties as seen in the right part of Figure 19.
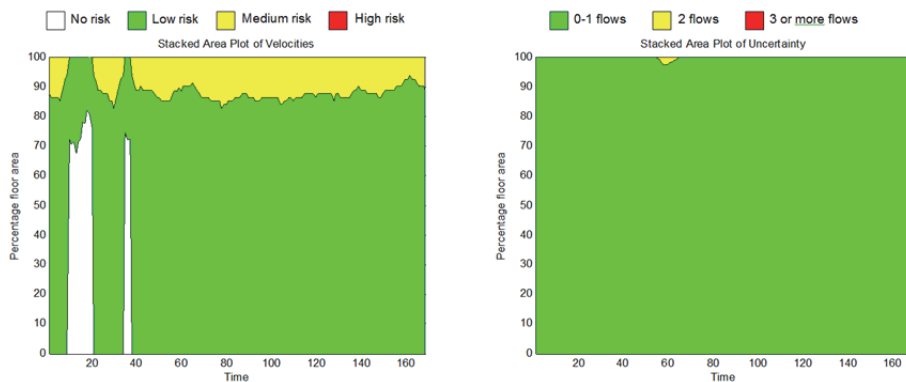
Figure 19 Summary of the draught risk over a longer period of the velocity distribution (left) and meeting flow elements (right) in the room. The room areas divided into risk intervals in each time step, here one hour.

During this week in May, most of the time there was a low risk of draught in about 90% of the room area and medium risk in the remaining area of the simulated room. Only in a short period do more flow elements meet.

DISCUSSION AND CONCLUSION

The developed tool uses inputs generated by building energy simulation software to give an overview of how often and where there is a risk of draught in a room. The tool is simple in the sense that it handles one flow element at a time and when flow elements meet, the one generating the highest velocity is used to estimate the draught risk.

Flow elements are developed for simple geometries and when using them on more complex inlets and room geometries, the calculated velocities and flow patterns will only be estimates, even with just one element present. If flow elements are oppositely directed or have co-flow, there is no description of what occurs and the uncertainty is therefore higher. In the tool, this is handled by plotting the number of meeting flow elements, so that the user can realise that the calculations are uncertain. The idea of the tool is not to make highly precise estimates for any time step, but to give an overview of when and where draught may be a problem.

From the plots produced by the tool, it should be possible to conclude one of three: (Green) There is a low risk of draught and the uncertainty is low – the design is acceptable, (Red) There is a high risk of draught – the design should be changed, or (Yellow) There is a risk of draught or the uncertainty is high – either change the design or make further investigation e.g. by CFD.

Further work needs to be put into the tool to cover more flow elements and for calculating the parts of the flow market with dashed lines in Figure 14.

The next article researches the calculation of thermal radiation, which is the last of the parameters chosen for further research. Thermal radiation affects both global thermal comfort and local thermal discomfort due to radiant asymmetry. The article researches how thermal radiation to a person in a room can be calculated and describes a method for the calculation of view factors to the surfaces in a room.

RADIATION EXCHANGE BETWEEN PERSONS AND SURFACES FOR BUILDING ENERGY SIMULATIONS

Mette Havgaard VORRE[1,*], Rasmus Lund JENSEN[2], Jérôme Le DRÉAU[2]

[1]Energy and Environment, Danish Building Research Institute, Aalborg University, Copenhagen, Denmark
[2]Department of Civil Engineering, Aalborg University, Aalborg, Denmark

[*] *Corresponding author: Mette Havgaard Vorre*

ABSTRACT

The inclusion of thermal radiation within buildings is a significant component of thermal comfort. Typically the methods applied for calculating view factors between a person and its building surfaces requires great computational time. This research is about developing a view factor calculation method suitable for building energy simulations. The method developed calculates view factors by numerical integration of projected area factor.

Over time the projected area factor of a person has been simplified by geometrical shapes. These shapes were compared with more complex equations on both precision and calculation time. The same was done for the resulting view factors, where the results were compared with view factors found by ray tracing. While geometrical simplifications of the human body gave the fastest calculations, the complex equations gave the most accurate results.

Non-rectangular surfaces and obstacles are treated by comparing intersection points with the edges of the surface, making the method applicable to rooms with complex geometry. The method for calculating view factors is robust and applicable to building energy simulation tools. Calculation time can be long depending on the complexity of geometry, grid-size and the choice of method for the projected area factor, but view factor calculations has to be done only once for a for a whole year simulation.

INTRODUCTION

Thermal radiation accounts for a substantial part of thermal comfort, and knowledge on radiation is therefore vital when simulating thermal comfort in buildings. To comply with legislation, architects and engineers work to optimise the building design in order to obtain lower energy consumption. Thermal comfort is often ensured by constraining variations in operative temperature in the energy optimisation process; but better measures would be predicted mean vote, PMV, or predicted percentage dissatisfied, PPD, and percentage dissatisfied, PD, calculated in a grid, to cover differences in the room. The overall goal is to be able to optimise the thermal comfort of the occupants in parallel with the buildings' energy consumption and the major objective is to describe a method for calculating view factors between persons and surfaces in a room for use in calculations of mean radiant temperature and radiant asymmetry.

By improving the calculation of thermal comfort in building energy simulation programs, it is possible to see the consequences on the thermal comfort when changing the building design, not just as an average in a room but on a number of different points, taking more aspects into consideration than the operative temperature. It is especially important in buildings with a complex geometry, where mean radiant temperature and radiant asymmetry varies in the room and an area-weighted mean of surface temperatures is far from accurate.

Global thermal comfort is calculated as the energy balance of the whole body, affected by 6 parameters: air temperature, mean radiant temperature, air velocity, relative humidity, clothing level and activity level (Fanger 1970). Local thermal discomfort can be caused by draught, temperature gradients, asymmetric thermal radiation and cool/warm floors (Fanger et al. 1985; Olesen et al. 1973).

Previous work by the authors describe ways to improve the simulation of clothing level (Vorre and Jensen 2014) and air velocity and draught risk (Vorre, Jensen, and Nielsen 2014) for use in building energy simulation tools.

The objective of this paper was to present a methodology for calculating thermal radiant impact on a person for better simulation of thermal comfort in building energy simulation tools. The method calculates view factors by integration of the projected area factor over the surfaces and can be used for any plane surface, taking account of obstructions in the room. The method also applies for view factors for calculating radiant asymmetry. The same basic method is used for calculations between surfaces and between surfaces and a person.

For view factors involving a person, different methods and simplifications for calculating the projected area factor are compared, and the calculated view factors

are compared with other methods. The comparison is made on both results and calculation time.

THEORY

For the calculation of thermal comfort by using PMV or PPD and PD caused by radiant asymmetry, knowledge of the mean radiant temperature and radiant asymmetry are needed (Fanger 1970; Fanger et al. 1985). Mean radiant temperature is defined as that uniform temperature of a black enclosure which would result in the same heat loss by radiation as the actual enclosure under study. The definition covers both short wave radiation from the sun or a high-intensity radiant heater and long-wave radiation by emission from surfaces. This paper is focused on the latter while the impact on thermal comfort from short-wave radiation is treated by e.g. Karlsen (Karlsen et al. 2014). Radiant asymmetry is defined as the difference in mean radiant temperature for each side of a small horizontal or vertical plate at the person's position in the room (Fanger et al. 1980).

For comparing scenarios, the mean radiant temperature is an expression that is easier to relate to than a number of different temperatures of the surfaces.

The mean radiant temperature at a specific location is found by calculating the heat transfer through radiation in the actual enclosure. The radiant energy exchange between a person and a surrounding surface is calculated as between any two objects:

Equation 17

$$q_{1 \to 2} = \varepsilon \cdot \sigma_s \cdot F_{1 \to 2} \cdot A_{1, \, eff} \cdot (T_1^4 - T_2^4) = -q_{2 \to 1}$$

Where $q_{1 \to 2}$ is the heat flow by radiation from object 1 to object 2 in W, ε is the multiple of the emissivities of the objects, $\sigma_s = 5.67 \cdot 10^{-8}$ W/m^{2}K^4 is the Stefan-Boltzmann constant, $F_{1 \to 2}$ is the radiation view factor or angle factor from object 1 to object 2 (how big an area does object 2 cover compared with the whole area that object 1 radiates to), $A_{1, \, eff}$ is the effective radiation area of object 1 in m^2, T_1 is the surface temperature of object 1 in K, T_2 is the surface temperature of object 2 in K, $q_{2 \to 1}$ is the heat flow by radiation from object 2 to object 1 in W.

Equation 17 is only valid if reflection can be disregarded; which is only a reasonable assumption when the emission of the surfaces is close to the emission of a black body, where all radiation is absorbed and none is transmitted nor reflected. This is the case for many building materials and items of clothing, though glass is an exception as its emissivity can be very low, also for long-wave radiation.

To calculate the radiant exchange to a person, we need to know the surface temperature of the person and the surrounding surfaces, their areas, emissivities and the view factors between them.

The highest view factor is found when a surface surrounds a person, as the view factor of the surface is then equal to 1, as is the case for a sphere. The view factor is calculated from the projected area factor, and the projected area factor describes how much of an object is illuminated from a given point, as illustrated by the single light bulb in Figure 20.
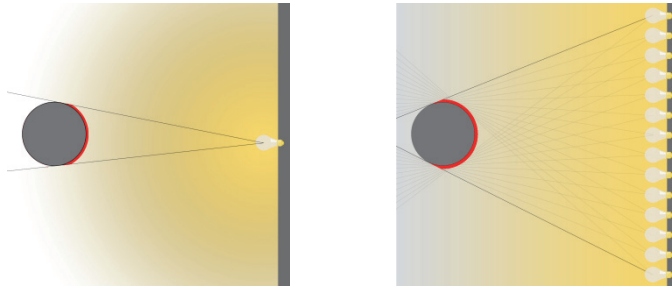

Figure 20 To the left the projected area factor illustrated by the part of the body illuminated by a single light bulb. To the right the view factor to a wall illustrated by the part of the body illuminated by a wall of light bulbs.

The view factor describes how much of the object is illuminated from a whole wall of light bulbs and can be found by integrating the projected area factor for each light bulb over the entire wall as illustrated to the right in Figure 20.

For a person in a room, the sum of view factors to all surfaces equals 1.

The projected area of a person can be illustrated by his silhouette and depends on the view point to the person. The view point is described by the azimuth angle, α, and the altitude, β, as illustrated in Figure 21.

The effective radiation area of a person is the area that emits and receives radiation from the surroundings. This area is smaller than the total skin area of the body, as parts of the body do not exchange radiation with the surroundings, e.g. between the toes or under the arms.
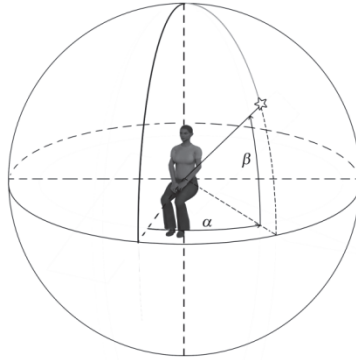
Figure 21 The azimuth angle α and the altitude β.

A HISTORICAL VIEW OF VIEW FACTORS INVOLVING PERSONS

Interest in the view factors between a person and surrounding surfaces arose in the late 1960s with HVAC systems and Fanger's studies on thermal comfort (Fanger 1970). Before then, studies on thermal radiation to persons were mostly done to calculate the impact on persons from direct solar radiation, because the military needed knowledge about the effect of the sun on soldiers (Breckenridge 1961). The first studies in the field were therefore not with the aim of describing view factors but merely the projected area factor of a person from different angles.

In the 1930s, James D. Hardy and Eugene F. DuBois used a wrapping method to determine the effective radiation area of a person. A person was wrapped in paper like an Egyptian mummy, and the surface area was measured by rubber-coating the paper, a technique similar to the one used to measure the total area of the human skin also known as the DuBois area. The effective radiation area was found to be 78.3% and 78.4% of the total skin area for the two persons they measured. (Hardy and DuBois 1938)

In 1952, Guibert and Taylor used photographs to determine projected areas and the total effective radiation area. Photos were taken in a half sphere, with the person in a standing and a sitting position. The pictures were taken from a distance of 12 m and treated as though taken from an infinite distance, as would be the case with radiation from the sun. (Guibert and Taylor 1952)

For calculating the projected area factor, a sphere represented a seated person and a cylinder represented a standing person. The relation between height and radius of the cylinder was found from observations. (Taylor 1956)

As the sun was the challenge, the sun was also used in the research, and the solar angles and shadows cast were measured for a standing person facing the sun and with the person turned sideways to the sun. (Chrenko and Pugh 1961)

In 1966, the photographic method was used by Underwood and Ward on standing men and women. The pictures were taken from different azimuth and altitude, though with irregular steps due to their test fixture. The photos of 25 men and 25 women were taken from a distance of 4.57 m. Underwood and Ward suggested an oval cylinder to represent a standing person in the calculations of projected area factors. (Underwood and Ward 1966)

The photographic method and test setup of Underwood and Ward were adopted by Fanger, who in his doctoral thesis described experiments involving 10 male and 10 female test persons from northern Europe. All subjects were photographed from 78 different angles with steps of 15 degrees. Photos were taken for both a standing and a seated position. Fanger presented his results for the projected area factor as diagrams in order to get closer to the actual geometry of the human body. He supplemented with diagrams for the view factor between person and surfaces in an orthogonal room. (Fanger et al. 1970) (Fanger 1970)

Discomfort caused by asymmetric thermal radiation was investigated in a climate chamber where the surface temperatures could be regulated independently for the two half-parts of the room, for a suspended ceiling or other part surfaces. In the experiments view factors between surfaces and persons were found by use of Fanger's diagrams and in 1980 the term radiant temperature asymmetry is introduced. Radiant temperature asymmetry is defined as the difference in plane radiant temperature for a small plane element and is probably introduced in order to be able to make a direct measurement. (Fanger et al. 1980, 1985; Olesen et al. 1973)

Diagrams for reading view factors to inclined surfaces were made in 1988 by use of cubic spline on Fanger's results for the projected area factor. (Steinman et al. 1988)

In 1990, Horikoshi et al. made similar experiments as Fanger, but using an orthographic projection camera, where the parts of the person close to the camera are bigger than those further from the camera. This is in contrast to the earlier work, where an effort was put into measuring the projected area as seen from infinity. As surfaces and especially the floor are not infinitely far away, they argue that this method is more accurate especially when considering the heat exchange to floors with heating and in relatively small rooms. The results of Horikoshi et al. are presented as diagrams for reading view factors. (Horikoshi et al. 1990)

In the beginning of the 1990s, the computer era affected the world of thermal radiation calculation and Fanger's diagrams for reading both the projected area factor and the view factor in orthogonal rooms are put into algorithms. Just like with

the principle in Fanger's diagrams for view factors, it is still necessary to divide all surfaces according to the centre of the person and categorise the divisions in front or behind, above or below the centre, on the side, vertical or horizontal. (Cannistraro et al. 1992; Rizzo et al. 1991)

In 2000, algorithms for view factors to inclined surfaces were added (Nucara et al. 2000).

In the beginning of the new millennium, a study similar to Fanger's was made in Italy on Italian subjects. The study involved more subjects and smaller angle steps, since digital photos and computer software measure the projected area of the persons in the photos much quicker than the manual measures taken 40 years earlier. The results showed fair agreements with the projected area factors for standing persons found by Fanger, but for seated persons the differences where significant. (La Gennusa et al. 2008)

Apart from these methods, CFD programs and computer games use ray tracing for calculating radiation very precisely. Ray tracing has a longer calculation time and demands more input than the other methods.

This paper suggests using numerical integration for calculation of view factors. The method was chosen because it is applicable for both person-to-surface calculations and surface-to-surface calculations. The method implies knowledge of the projected area factor of a person, or surface, as a function of the angle that the person is viewed from.

The method can also be used to compute radiant temperature asymmetry, by calculating view factors for each side of a small horizontal and a small vertical plate. The correlations between radiant asymmetry and thermal comfort are described for the small plates, though during the studies the actual view factors to the heated or cooled surfaces were also calculated. By calculating view factors for a person, while keeping track of azimuth and altitude angles, it is possible to also compute thermal radiant asymmetry for an actual person, and the results were compared to the results using small plates.

PROJECTED AREA FACTOR OF A PERSON – COMPARISON OF CALCULATION METHODS

Over time the projected area of a person was simplified to geometrical shapes for easier use in calculations, e.g. spheres and cylinders. In this study, numerical integration is suggested for calculating view factors, and it is therefore interesting to compare the geometrical simplifications for calculation of the projected area factor to more complex algorithms on both precision and calculation time.

Comparisons were made for both standing and seated persons. The projected area factor of a seated person was calculated assuming a sphere, a cube and a box. A standing person was simplified to a cylinder and an oval cylinder. As more complex equations, the results by Rizzo et al. were used (Rizzo et al. 1991). Their equations are derived from original data provided by Fanger. Unfortunately, it was not possible to obtain access to the data found in the Italian experiments (La Gennusa et al. 2008), and the calculated values are therefore only compared with the data points from Fanger's experiments.

Only the results for standing persons are shown here. The equations for seated persons are used in the later comparison of calculated view factors.

The simplest suggestion of a standing person is a cylinder. In Figure 22, the cylinder is compared with the results by Fanger. On the left, the cylinder is 1.65 m high and has a radius of 0.23 m as found by Taylor (Taylor 1956) and on the right, the cylinder was optimised by the least square error compared with Fanger's data, height 1.11 m and radius 0.26 m.
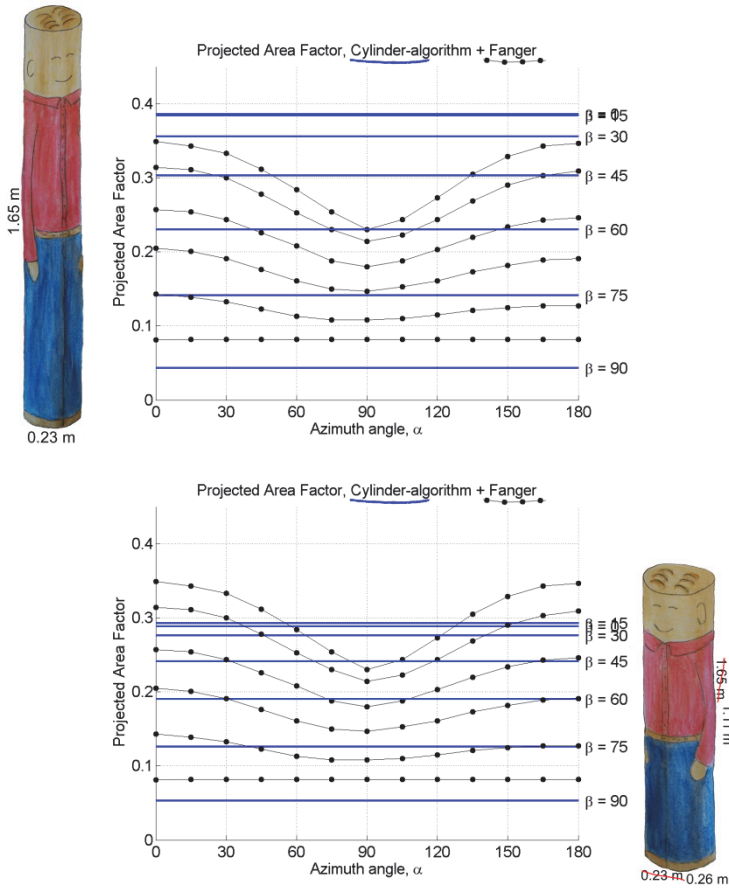
Figure 22 Projected area factors of a standing person, calculated by using a cylinder as suggested by Taylor (Taylor 1956) and optimised according to Fanger's results (thick/blue line) compared with the results of Fanger's measurements indicated by the thin line with dots.

A cylinder is axisymmetric and the projected area does therefore not vary with the azimuth angle; on the other hand it does have quite an identical behaviour for the altitude.

An oval cylinder of 1.5 m in height, a large radius of 0.29 m and a small radius of 0.19 m was suggested by Underwood and Ward (Underwood and Ward 1966). In Figure 23, the projected area factor of the original oval cylinder is compared with data points from Fanger on the left and on the right an optimised cylinder is compared, height 1.1 m, large radius 0.32 m and small radius 0.21 m.
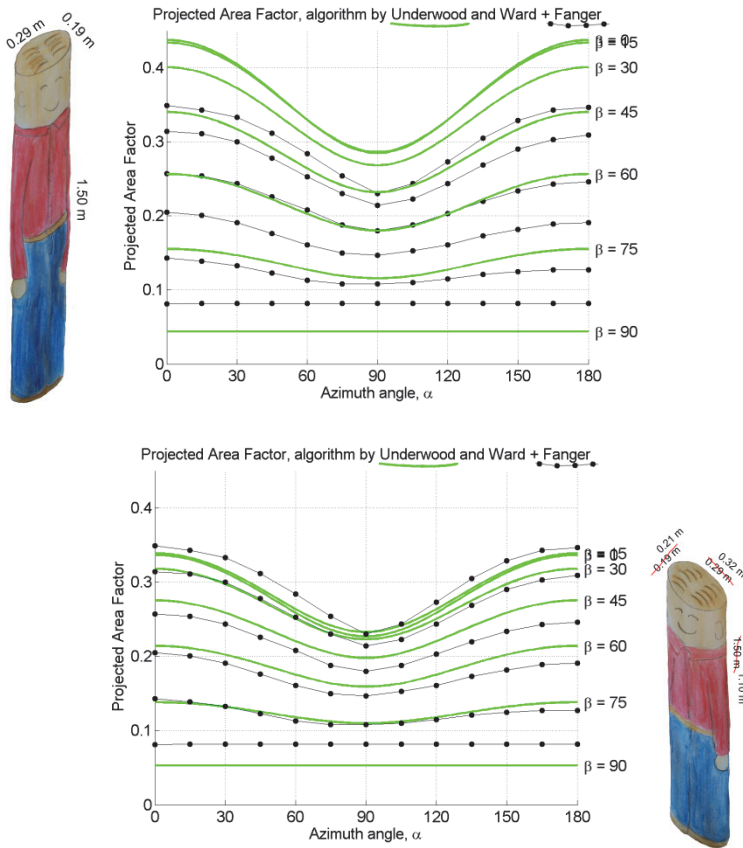
Figure 23 Projected area factors of a standing person, calculated by using an oval cylinder as suggested by Underwood and Ward (Underwood and Ward 1966) and an optimised oval cylinder (thick / green line) compared with the results of Fanger's measurements indicated by the thin line with dots.

The oval cylinder has many similarities with Fanger's results and depicts both the variations in azimuth and altitude.

The last method for calculating the projected area factor in the comparison is the algorithm derived by Rizzo et al. (Rizzo et al. 1991) on the basis of Fanger's results. The algorithm is a double variable polynomial where the azimuth angle is of degree 4 and altitude is of degree 3. The algorithm is only valid for azimuth angles between 0° and 180° and for the altitude between 0° and 90°. In Figure 24 the algorithm is compared to the results by Fanger.
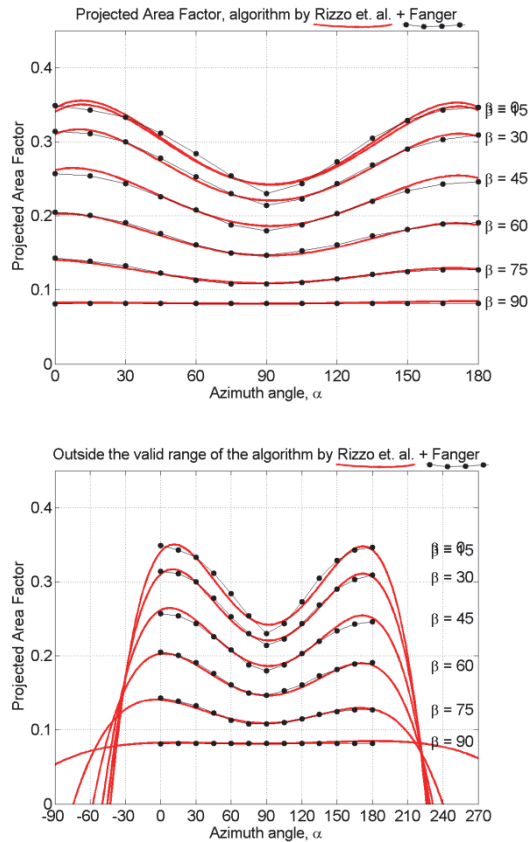
Figure 24 Comparison of the projected area factor for a standing person as measured by Fanger (thin line with dots)and calculated using of the algorithm found by Rizzo et al.(Rizzo et al. 1991) (thick / red line). To the right is shown the behaviour of the algorithm outside the valid range.

Of the three calculation methods (cylinder, oval cylinder and algorithm) the best fit is found by using the algorithm derived from Fanger's data, as shown in Figure 24, though the algorithm shows less similarities at the front and back of the person (azimuth angle close to 0° and 180°) especially at low altitudes. The differences close to the limits of the valid range is due to the nature of the developed polynomial, as can be seen when plotting values outside the valid ranges, shown on the right side in Figure 24.

The calculation time is the cost of achieving the higher precision by using the algorithm. While the oval cylinder is only a little slower than the simple cylinder, the algorithm's calculation time is approximately 4 times that of the cylinders. For the calculation of view factors where a high number of calculations are needed when using the integration method. The calculation time may end up being an issue,

though for building energy simulation tools the calculation of angle factors are only done once for every position of the person, not at every time step.

FROM PROJECTED AREA FACTOR TO VIEW FACTOR FOR A PERSON

In this section, a methodology is described for calculating the view factor between a person and a plane surface of any geometry, the method can also be used between two surfaces and when other surfaces obstruct the radiation.

A person receives and emits heat by radiation. If a person is placed in a sphere, all radiation from that person will hit the sphere, while not all of the radiation from the sphere will hit the person, as most of it will instead hit the sphere itself.

If the radiation is diffuse, then:

Equation 18

$$A_{Person} \cdot F_{Person-Sphere} = A_{Sphere} \cdot F_{Sphere-Person}$$

Where A_{person} is the effective radiation area of a person in m², $F_{Person-Sphere}$ is the view factor from the person to the sphere (how much of the radiation leaving the person reaches the sphere), $A_{Sphere} = 4 \cdot \pi \cdot r^2$ is the surface area of the sphere in m², $F_{Sphere-Person}$ is the view factor from the sphere to the person (how much of the radiation leaving the sphere reaches the person), r is the radius of the sphere in m.

As all radiation leaving the persons effective radiation area reaches the sphere, the view factor from the person to the sphere is known: $F_{Person-Sphere} = 1$, and Equation 18 can then be written as:

Equation 19

$$A_{Person} = A_{Sphere} \cdot F_{Sphere-Person}$$

The view factor from the sphere to the person cannot be calculated directly. It has to be integrated over the surface of the sphere.
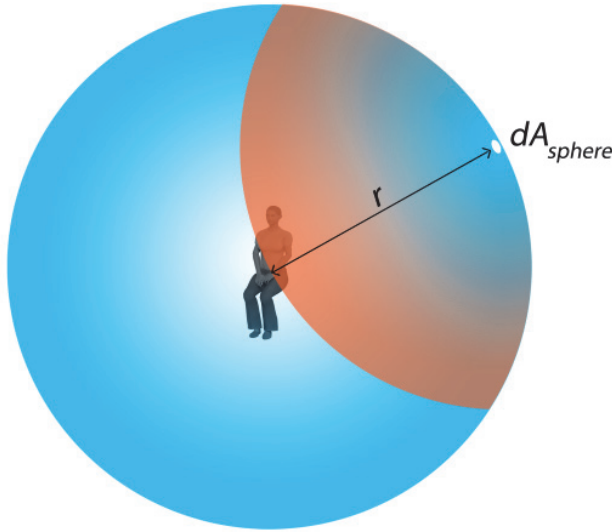
Figure 25 A person in the middle of a sphere. The small area dA$_{sphere}$ radiates diffusely in a sphere that is cut off by the sphere surrounding the person.

If looking at the radiation from the small area dA_{sphere} to the person, then dA_{sphere} radiates diffusely in a sphere. This radiation-sphere reaches the person at a distance equivalent to the radius, r, of the sphere, as illustrated in Figure 25. The view factor from dA_{sphere} to the person is therefore the projected area of the person, $A_{projected}$, as seen from dA_{sphere} compared with the total area of the radiation-sphere with the radius r cut off by the sphere surrounding the person, which also has the radius r. The surface area of a sphere cut off by another sphere with equal radius is ¼ of the total surface area of the sphere. The view factor is then given by:

Equation 20

$$F_{dA_{sphere}-Person} = \frac{A_{projected}}{\frac{1}{4} \cdot 4 \cdot \pi \cdot r^2} = \frac{A_{projected}}{\pi \cdot r^2}$$

Where $F_{dA_{Sphere}-Person}$ is the view factor from the small area dA_{sphere} to the person, $A_{projected}$ is the person's projected area as seen from dA_{sphere} in m², r is the radius of the sphere in m.

Most surfaces surrounding us are not spheres. If instead of looking at a sphere, we look at a plane rectangular surface with the area *A*, as shown in Figure 26, then this area can be divided into areas so small that it is reasonable to assume that the whole area *dA* has the same distance to the person, and it is possible to calculate it like for the sphere.
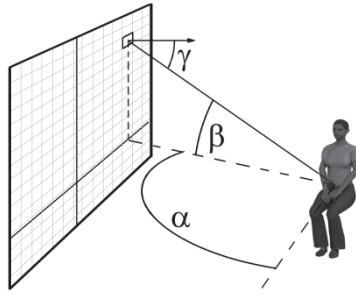
Figure 26 Person seated beside a plane rectangular surface. The surface is divided into small areas, dA, for which the projected areas of the person are calculated.

For the small area dA, Equation 18 can be written as:

Equation 21

$$A_{eff} \cdot dF_{Person-dA} = dA \cdot F_{dA-Person}$$

Because the person sees the small area dA under the angle γ, the area that the person sees is $dA \cdot \cos(\gamma)$, which means that the view factor from the small area dA to the person is

Equation 22

$$F_{dA-Person} = \frac{A_{projected}}{\pi \cdot r^2} \cdot \cos(\gamma)$$

$dF_{Person-dA}$ can then be calculated as:

Equation23

$$dF_{Person-dA} = \frac{dA \cdot F_{dA-Person}}{A_{eff}} = \frac{dA \cdot A_{projected}}{A_{eff} \cdot \pi \cdot r^2} \cdot \cos(\gamma)$$
$$= \frac{A_{projected}}{A_{eff}} \cdot \frac{1}{\pi \cdot r^2} \cdot \cos(\gamma) \cdot dA = \frac{f_{projected}}{\pi \cdot r^2} \cdot \cos(\gamma) \cdot dA$$

Where $f_{projected}$ is the projected area factor of the person, which relates the projected area of a person to the effective radiation area of the person. Like the projected area, it depends on the azimuth and altitude from where the person is viewed.

By integrating Equation23 over the surface, the view factor from the surface to the person can be found:

Equation 24

$$F_{Person-A} = \frac{1}{\pi} \int_A \frac{f_{projected}(\alpha,\beta)}{r^2} \cdot \cos(\gamma) \cdot dA$$

Where r is the radius of the sphere with the person in the centre and reaching dA or simply the distance between the person and dA, γ is the angle between the line person–dA and the normal of the surface, α is the azimuth angle measured from the persons sight direction to dA, β is the altitude to dA from the person's centre, $f_{projected}$ is the projected area factor.

To calculate the view factor to the entire surface, the integral in Equation 24 must be solved, which cannot be done analytically. Instead it is solved numerically:

Equation 25

$$F_{Person-A} = \frac{1}{\pi} \int_A \frac{f_{projected}(\alpha,\beta)}{r^2} \cdot \cos(\gamma) \cdot dA$$

$$\approx \frac{1}{\pi} \sum_A \cdot \frac{f_{projected}(\alpha,\beta)}{r^2} \cdot \cos(\gamma) \cdot \Delta A$$

$$= \frac{1}{\pi} \sum_y \left(\sum_x \cdot \frac{f_{projected}(\alpha,\beta)}{r^2} \cdot \cos(\gamma) \cdot \Delta x \right) \cdot \Delta y$$

The Simpson method is used for the numerical integration of Equation 25 and the procedure is described in the appendix.

View factors for calculation of radiant asymmetry are found by setting the projected area factor to zero, when the azimuth angle is to the left/right of the person or the altitude angle is above/below zero.

COMPLEX GEOMETRIES

The described method of integration over the surface is only applicable if the surface is rectangular. If it is not, the method should be supplemented with extra calculations.

For a non-rectangular surface, a rectangular surface is made that includes the whole surface, as shown in Figure 27. The rectangular surface is then divided by a grid for

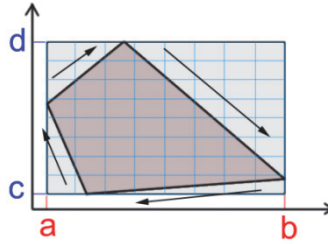the numerical integration and for each node it is checked, whether or not it is a part of the real surface.

Figure 27 Example of a non-rectangular surface with the vectors constituting the edges of the surface.

The position of all nodes is compared with the edge vectors of the real surface. If the node lays to the right of all edge vectors, it is within the surface. If the node lies to the left of just one edge, it is outside the real surface. The method is only valid for surfaces where all corner angles are less than 180°. If this is not the case, the surface needs to be divided into smaller surfaces where all angles are smaller than 180°.

The process is quite slow, so to reduce calculation time the check for a node against edge vectors is stopped if the node is found to lie to the left of an edge, as there is then no reason to check against other edges. Furthermore, it is seen that when going perpendicularly through the rectangular grid, if one node is inside the real surface and the next is outside, then all the following nodes in that row or column will also be outside.

If it is found that the node is outside the real surface, the projected area factor in Equation 25 of the subsurface is set to zero, otherwise the actual projected area factor is determined.

In the case of a room with one or more surfaces that in reality have corner angles more than 180°, it is important to realise that the person can actually be positioned "behind" some of the surfaces in the room. In Figure 28, the person has a view factor of zero to surface *d*, because the person is positioned behind the surface.
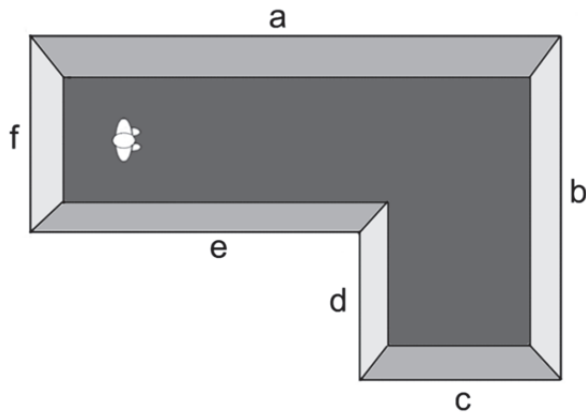
Figure 28 L-shaped room seen from above with a person. View factor between person and wall d equals zero. The view factor to wall c is also zero, as radiation between the surface and the person is blocked by surfaces d and e.

OBSTRUCTIONS BETWEEN SURFACE AND PERSON

The method of comparing a point to the edges of the surface is also used to determine whether other surfaces are obstructing the view between a subsurface and the person.

When calculating view factors between the person and surface *b* in Figure 28, the vectors between the person and each node on the surface are found. For each vector, it is checked whether the vector is blocked by another surface. If the intersection point of the vector on another surface is within the edges of the other surface, then the radiation is blocked, though only if the intersection point is between the person and the node. In Figure 28, radiation from surface *b* is partly blocked by both surface *d* and surface *e*, but as soon as it is found that the vector is blocked by one surface, there is no need to check intersection points with any other surfaces.

The vector between a node on surface *b* and the person can intersect with surface *f*, but the intersection point lies outside the range of the vector and is therefore irrelevant.

This is potentially a very slow process because all surfaces have to be checked, and consequently it is possible to simply disregard this step, if the room geometry yields that surfaces cannot block one another e.g. all corner angles are smaller than 180°.

Secondly, before the calculations of view factors are started, the potentiel obstructing surfaces are found for each surface and only these surfaces are checked. In an L-shaped room as shown in Figure 28, walls "*d*" and "*e*" are the only walls

that can block radiation. The rest of the walls will never block radiation between a person and a surface, regardless of where in the room the person is positioned.

VIEW FACTORS BETWEEN SURFACES

Surface temperatures in a room depend on the exchange of thermal radiation between surfaces. Consequently, view factors between surfaces are also necessary for improving the calculation of the radiant part of an occupant's thermal comfort. It is chosen not to take the obstruction by persons into consideration.

Before the use of computers, diagrams were used to find view factors between two surfaces for a number of standard situations and even though they were indeed useful, it was also a puzzle when the building under study did not fit into these standard geometries. As radiant energy exchange is a challenge also in other industries, several geometries can be handled by use of geometric equations, but for use in building energy simulation it is difficult to make a general solution with the minimum of user interaction and knowledge in the specific field.

Georg Walton tests different integration methods on both calculation time and precision, and further describes the method of integrating along the edges of the surfaces. His method integrates over any surface with corner angles of less than 180°. Obstructions between surfaces are handled by dividing the surfaces into smaller parts based on shadow cast by the obstruction. (Walton 2002)

In this paper it is chosen to use the same integration method for determination of view factors between surfaces as used for determination of view factors to persons. Because of the high irregularity of the human body, the method of integrating along the edges of the surfaces is not applicable when persons are involved. In order to determine the view factor between two surfaces, area integration of both surfaces is necessary and the Simpson method is therefore used twice.

For geometries other than rectangular surfaces, an orthogonal grid is still used and a check is made to determine whether a given point is part of the actual surface. The same method is used when other surfaces or objects obstructs parts of the radiation between two surfaces.

For radiation between any two objects the following interaction applies:

Equation 26

$$F_{1 \to 2} \cdot A_1 = F_{2 \to 1} \cdot A_2$$

Where $F_{1 \to 2}$ is the view factor from object 1 to object 2 (how much of the radiation leaving object 1 that reaches object 2), A_1 is the area of object 1, $F_{2 \to 1}$ is the view factor from object 2 to object 1, and A_2 is the area of object 2. The view factor states

how much of the total radiation from one object that reaches the other object and is therefore a factor between 0 and 1.

For two surfaces the view factor from surface 1 to surface 2 can be calculated as:

Equation 27

$$F_{1\to2} = \frac{1}{A_1 \cdot \pi \cdot} \cdot \int_{A_1} \int_{A_2} \frac{\cos\gamma_1 \cdot \cos\gamma_2}{r^2} \cdot dA_1 \cdot dA_2$$

Where A_1 is the area of surface 1, A_2 is the area of surface 2, r is the distance between dA_1 and dA_2, γ_1 is the angle between the normal to surface 1 and the line between dA_1 and dA_2, and γ_2 is the angle between the normal of to surface 2 and the line between dA_2 and dA_1.

The integral is solved numerically:

Equation 28

$$F_{1\to2} = \frac{1}{A_1 \cdot \pi} \cdot \int_{A_1} \int_{A_2} \frac{\cos\gamma_1 \cdot \cos\gamma_2}{d^2} \cdot dA_2 \cdot dA_1$$

$$\approx \frac{1}{A_1 \cdot \pi} \cdot \sum_{A_1} \left(\sum_{A_2} \frac{\cos\gamma_1 \cdot \cos\gamma_2}{d^2} \cdot \Delta A_2 \right) \cdot \Delta A_1$$

The numerical solution is found by using the Simpson method twice and is further described in the appendix.

CALCULATION EXAMPLE AND COMPARISON OF METHODS

The described method was used for the calculation of view factors between a person and the surrounding surfaces in a room by using four different assumptions for calculating the projected area factor. The results were compared with the algorithm for direct calculation of view factors by Cannistraro et al. (Cannistraro et al. 1992) and results by using ray tracing in the CFD software ANSYS CFX.

The calculations were made for a rectangular room with a seated person. The room geometry was chosen in order to be able to calculate view factors by the algorithm of Cannistraro et al. and the seated position chosen in order to compare results with a ray tracing model of a person modelled by a 3D laser scan of a thermal mannequin.

The room is 3.60 m long, 2.76 m wide and 2.75 m high. The person is seated 1.2 m from the end wall and 1.38 m from the side walls, facing a side wall.
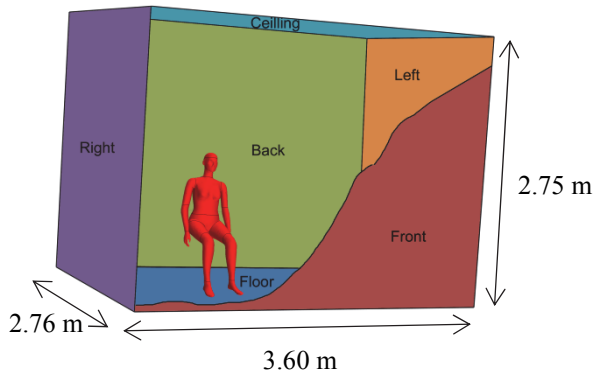
Figure 29 Sketch of the room used in the example with colour code for surfaces used in the diagrams.

In the CFD software, the view factors were found by giving all surfaces in the enclosure the same temperature and applying a higher temperature to the person. The amount of heat received by each surface was then used to calculate the view factors.

For each surface the view factor was found by numerical integration using four different methods for the calculation of the projected area factor of a seated person: the algorithm by Rizzo et al. based on Fanger's results (Rizzo et al. 1991), a sphere, a cube and a box. The dimensions of the box were optimised for the best fit with Fanger's data.

The view factors were adjusted to sum up to 1 by dividing each calculated view factor with the sum of the view factors for the whole room. The calculated view factors are shown in Figure 30 and when comparing to ray tracing, the difference is shown in Figure 31.
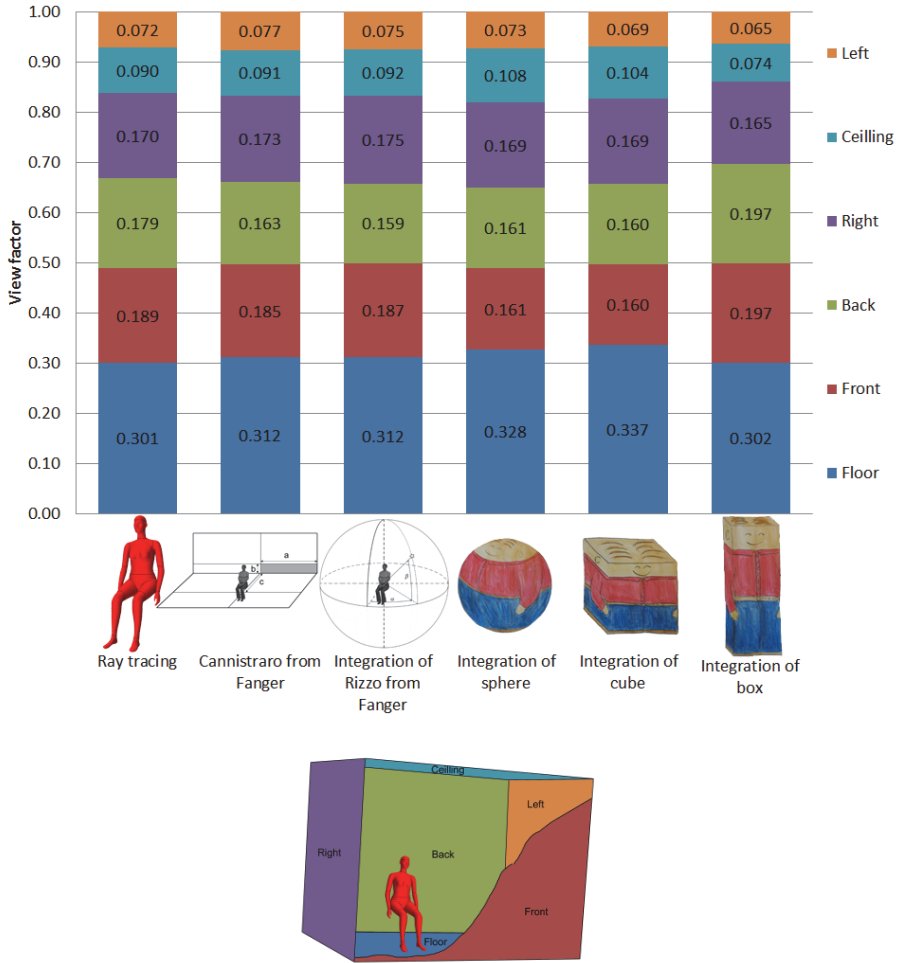
Figure 30 View factors calculated by using six different methods.
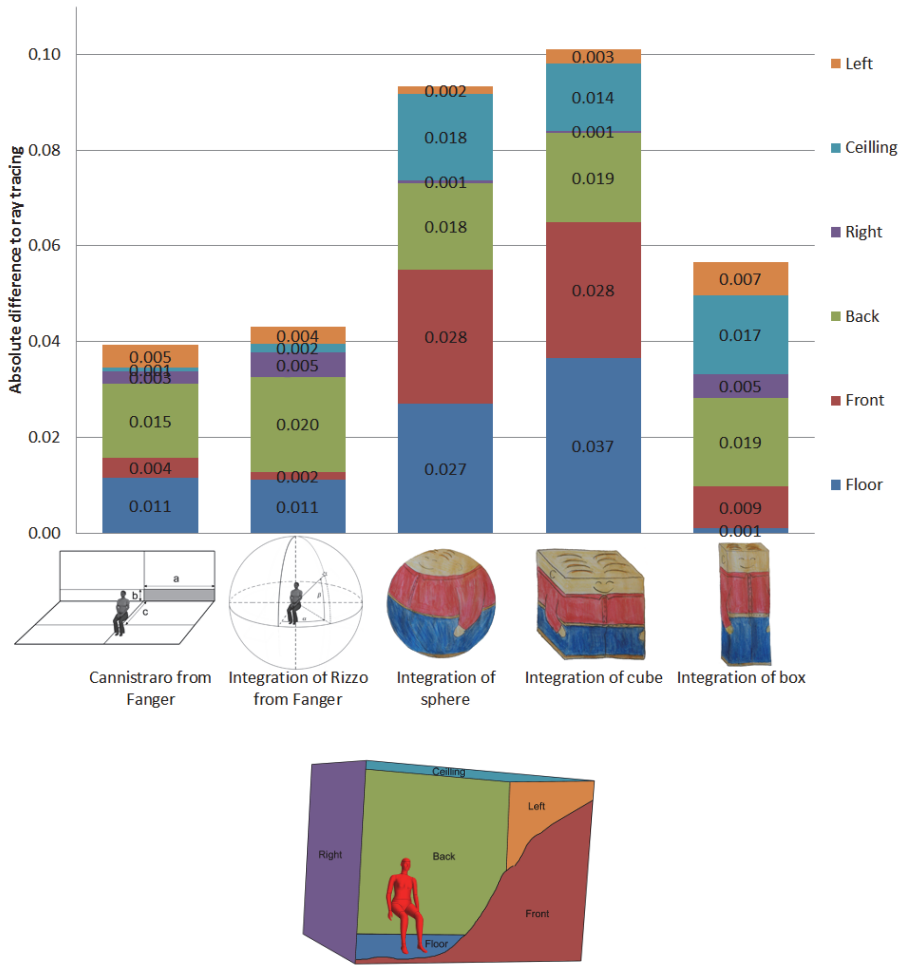
Figure 31. Difference between view factors calculated by ray tracing and five other methods.

The view factors in the calculation methods based on Fanger's work were the ones getting closest to the view factors found by ray tracing. The two simplest models, the cube and the sphere, differ the most. Complete agreement is probably not possible as the precise position of the seated person in the CFD model and the subjects photographed by Fanger could very well be different.

Another significant difference between the methods is the calculation time. The calculations were made in MatLab with steps of 0.01 m for the integration methods. The longest calculation time was for the integration of the algorithm for the projected area factor derived by Rizzo from Fanger's data (Rizzo et al. 1991). Only 50% of that time was used if assuming a geometrical shape, and just 1% was used

for the method of direct calculation of view factors as developed by Cannistraro from Fanger's data for view factors (Cannistraro et al. 1992).

But the example given was a very simple room. There were no inclined surfaces, the person was looking directly at a surface and everything was orthogonal. All surfaces had points correlated to the centre of the person, so no special calculations were needed.

GRID SIZE

When using a numerical integration method, the chosen grid size influences both the result and the calculation time. In the above example, a grid spacing of 0.01 m was used. If instead a grid space of 0.1 m had been used, the calculation time would be reduced from 0.64 seconds to 0.02 seconds when calculating the projected area factor for the room shown in Figure 29 and calculating the projected area factor by the method of Rizzo et al. (Rizzo et al. 1991) . In Table 3, the results of using a different grid sizes are shown together with the time used for calculating view factors of all six surfaces.

Gridsize in m	View factors for surfaces						Calculation time in seconds
	Left	Front	Right	Back	Floor	Ceiling	
1,000	0,07	0,190	0,172	0,163	0,305	0,091	0,995
0,500	0,07	0,186	0,174	0,158	0,312	0,091	0,995
0,100	0,07	0,186	0,174	0,158	0,309	0,091	0,992
0,050	0,07	0,185	0,174	0,158	0,309	0,091	0,992
0,010	0,07	0,185	0,174	0,158	0,309	0,091	0,992
0,005	0,07	0,185	0,174	0,158	0,309	0,091	0,992
0,001	0,07	0,185	0,174	0,158	0,309	0,091	0,992

Table 3 Calculated view factors for different grid sizes. All view factors are calculated using the method by Rizzo et al. for calculating projected area factor. The right column shows the calculation time for the room in Figure 29. [The numbers here are corrected from the verion published in Energy and Buildings, where an error had occured]

For the room in shown in Figure 29 it is seen that calculation time increases rapidly when decreasing grid size and that only little difference is found in the calculated view factors, when the grid size gets minor than 0.05 m.

By accepting slightly more uncertainty in the results, it is possible to greatly reduce the calculation time, though it is important to bear in mind that the calculation of view factors only need to be done only once for a building simulation for a whole year.

EFFECT OF CALCULATION METHOD ON MEAN RADIANT TEMPERATURE AND PMV

Mean radiant temperature, PMV and PPD are affected by thermal radiation and are the measures used for assessing global thermal comfort. The investigation of methods for calculation of the projected area factor and proposal of a method for view factor calculation had the purpose of improving the accuracy in the calculation of mean radiant temperature and PMV, and it is therefore interesting to see the influence that the calculation methods has on these values.

If assuming the same emissivity for all surfaces and that reflections can be disregarded, then the mean radiant temperature can be calculated using Equation 29.

Equation 29

$$T_{mr}^4 = \sum_{i=0}^{n} \left(F_{person \to surface\ n} \cdot T_{surface\ n}^4 \right)$$

In the room shown in Figure 29 all surfaces are set to have the same temperature of 22°C, except for the wall in front of the person which is assumed to be a poorly insulated window with a surface temperature of 5°C. Air temperature is set to 22°C, air velocity to 0.01 m/s, clothing level to 1 clo, activity level to 1 met and relative humidity to 50%. The difference in mean radiant temperature (MRT), PMV and PPD by using the different methods are calculated and results are shown in Table 4.
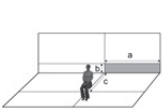
	Ray	Cannistraro	Rizzo	Sphere	Cube	Box
MRT	19.01°C	19.08°C	19.04°C	19.46°C	19.47°C	18.87°C
PMV	-0.66	-0.65	-0.66	-0.61	-0.60	-0.68
PPD	14.1	13.9	14.0	12.7	12.7	14.6

Table 4 Results for mean radiant temperature, PMV and PPD when using different methods for calculating view factors

In this example, integration over Rizzo is the most accurate, but it will vary depending on the error of view factors on the different surfaces. Depending on the calculation method, the mean radiant temperature is calculated to be as low as 18.87°C and up to 19.47°C, giving a variation in PMV ranging from -0.68 to -0.60 and PPD ranging from 14.6% to 12.7%.

If instead the wall to the right had been the window, see Figure 29, the two simplest methods (sphere and cube) would have been the most accurate. However, the objective was to illustrate the effect on the mean radiant temperature felt by the person.

RADIANT ASYMMETRY

Radiant asymmetry can cause discomfort, both for vertical and horizontal asymmetry. The relation between the percentage of people feeling discomfort and radiant asymmetry apply for the difference in thermal radiation side-to-side for a horizontal or a vertical plate (CEN 2005), though Fanger's diagrams were actually used in especially the first studies (Olesen et al. 1973).

With the method described earlier in this article it is possible to calculate the radiant asymmetry for both plates and a person represented by the algorithm of Rizzo et al by keeping track on when the azimuth angle is to the right or left of the person and when the altitude angle is above or below the persons centre.

For the room in Figure 29 the surfaces has one at a time been assumed to be a window with a surface temperature of 5°C while the rest where kept at 22°C. The results for radiant asymmetry at the point of the person are shown in Table 5 together with the calculated percentage of dissatisfied.

		Vertical plate		Horizontal plate		Rizzo	
		$\Delta T_{radiant}$	PD	$\Delta T_{radiant}$	PD	$\Delta T_{radiant}$	PD
Left / Right	Cold wall	1.2°C	0.2%			0.9°C	0.2%
Left / Right	Cold wall	8.8°C	2.7%			5.6°C	0.9%
Left / Right	Cold wall	4.2°C	0.6%			2.4°C	0.3%
Up / Down	Cold wall			-2.3°C	0.0%	-2.8°C	0.0%
Up / Down	Cold floor			14.7°C	37.6%	10.2°C	20.2%
Up / Down	Cold			-6.1°C	0.1%	-2.9°C	0.0%

Table 5 Radiant asymmetry calculated by the proposed method, using a plate and the algorithm for projected area factor by Rizzo et al, and the percentage dissatisfied caused by radiant asymmetry.

Radiant asymmetry calculated for a plate is higher than if calculating using more realistic human model. The difference between the methods is highest when the cold surface is parallel to the plate.

Using the more realistic human model in calculations of mean radiant temperatur will result in an underestimation of percentage dissatisfied.

DISCUSSION

The described method for calculation of view factors is a robust method and can be used to explore several positions and orientations of the person in a room. The calculation time is sensitive to the choice of method for determining the projected area factor and the grid size. Both also have an effect on the accuracy of the calculated view factors. In the example, the calculation time varied by a factor 2 depending on method, while the calculated mean radiant temperature varied by 0.6°C.

The objective of the paper was to develop a method for improving calculation of the radiant impact on occupants in building energy simulation tools. As the calculation of view factors only has to be performed once for a given room geometry, and not at every time step in a building simulation for a whole year, the higher calculation time can be justified in order to obtain more accurate results and the method is therefore clearly applicable for building energy simulation tools also in rooms with a complex geometry.

View factors involving persons are sensitive to the method for calculating the projected area factor of the person, both in calculation time and precision. Though even with the most complex model, it is still just a model, not taking into consideration the chair and the table where a person is normally seated. And it is relevant to consider whether the error when using a simplification of a person as a sphere compared with the complex model is actually larger than the difference between the complex model and reality, where e.g. the chair blocks a substantial part of the radiation to and from the person.

The calculation of radiant asymmetry using the algorithm by Rizzo, resulted in an underestimation of percentage dissatisfied, but the results come closer to how surfaces affect a real person. Further comparison between radiation asymmetry calculated for plates and the algorithm are suggested e.g. using the results of the original studies, in order to describe the relation between percentage dissatisfied and the more realistic radiant asymmetry. The current relation simplifies the problem to what is easily measured, whereas computers and thermal mannequins make it possible to improve both measurements and calculations to better reflect reality.

CONCLUSION

A method for calculating view factors between persons and surfaces by using Simpson integration was described and compared with ray tracing. Depending on the chosen way of calculating the projected area factor of the person, the results got

close to the ones found by ray tracing, though with a much lower calculation time and a simpler setup for a user.

The method is applicable for both simple and complex rooms.

ARTICLE APPENDIX

This appendix describes the calculation of angles used for determining projected area factors in the calculations of view factors and describes the basis in the Simpson method for numerical integration together with a quick way to build up the matrix used to weigh the results.

SURFACE TO PERSONS

For the calculation of the projected area factor, the angles α, β and γ, in Figure 26, must be known for each small area of the surface as well as the distance, r, between the person and the small area.

The normal vector of the surface, $\vec{n}$, is known as well as the position, P, and the orientation, $\vec{o}$, of the person in the room:

$$\vec{n} = \begin{bmatrix} x_n \\ y_n \\ z_n \end{bmatrix} \qquad P = \begin{bmatrix} x_P \\ y_P \\ z_P \end{bmatrix} \qquad \vec{o} = \begin{bmatrix} x_o \\ y_o \\ z_o \end{bmatrix}$$

For each small part of the surface, ΔA, we look at, the position of it's centre is known, and the vector, $\vec{r}$, from the person to ΔA is given by:

$$\vec{r} = \begin{bmatrix} x_P - x_{\Delta A} \\ y_P - y_{\Delta A} \\ z_P - z_{\Delta A} \end{bmatrix} = \begin{bmatrix} x_r \\ y_r \\ z_r \end{bmatrix}$$

Then the angle, γ, between the normal vector of the surface, $\vec{n}$, and the vector, $\vec{r}$, is:

Equation 30

$$\cos(\gamma) = \frac{\vec{n} \cdot \vec{r}}{|\vec{n}| \cdot |\vec{r}|} = \frac{\begin{bmatrix} x_n \\ y_n \\ z_n \end{bmatrix} \cdot \begin{bmatrix} x_r \\ y_r \\ z_r \end{bmatrix}}{\sqrt{x_n^2 + y_n^2 + z_n^2} \cdot \sqrt{x_r^2 + y_r^2 + z_r^2}}$$

The azimuth angle, α, is found in the same way, using the person's orientation, $\vec{o}$, and the vector. $\vec{r}$, though only calculated in the horizontal plane:

Equation 31

$$\cos(\alpha) = \frac{\overrightarrow{o_{xy}} \cdot \overrightarrow{r_{xy}}}{|\overrightarrow{o_{xy}}| \cdot |\overrightarrow{r_{xy}}|} = \frac{\begin{bmatrix} x_o \\ y_o \end{bmatrix} \cdot \begin{bmatrix} x_r \\ y_r \end{bmatrix}}{\sqrt{x_o^2 + y_o^2} \cdot \sqrt{x_r^2 + y_r^2}}$$

The altitude, β, is the angle between the vector, $\vec{d}$, and the projection of the vector, $\vec{d}$, onto the horizontal plane:

Equation 32

$$\cos(\beta) = \frac{\vec{r} \cdot \overrightarrow{r_{xy}}}{\left(|\vec{r}| \cdot |\overrightarrow{r_{xy}}| \right)} = \frac{\begin{bmatrix} x_r \\ y_r \\ z_r \end{bmatrix} \cdot \begin{bmatrix} x_r \\ y_r \\ 0 \end{bmatrix}}{\sqrt{x_r^2 + y_r^2 + z_r^2} \cdot \sqrt{x_r^2 + y_r^2}}$$

The Simpson method is used to optimise the calculation time when solving Equation 25. The Simpson method combines the centre method with the trapeze method, where the value of a small area is calculated at the centre of the area and as a mean of the values in the corners. The method requires the number of small areas to be an even number in both directions.

The principle can be written as:

$$\int_A f(x,y) \cdot dA = \int_a^b \int_c^d f(x,y) \cdot dy \cdot dx$$

$$\approx \begin{bmatrix} f(a,c) & f(a+k,c) & f(a+2k,c) & & f(b-2k,c) & f(b-k,c) & f(b,c) \\ f(a,c+h) & f(a+k,c+h) & f(a+2k,c+h) & \cdots & & f(b-k,c+h) & f(b,c+h) \\ f(a,c+2h) & f(a+k,c+2h) & f(a+2k,c+2h) & & & & f(b,c+2h) \\ & \vdots & & \ddots & & \vdots & \\ f(a,d-2h) & f(a+k,d-2h) & f(a+2k,d-2h) & & & & f(b,d-2h) \\ f(a,d-h) & f(a+k,d-h) & f(a+2k,d-h) & \cdots & & f(b-k,d-h) & f(b,d-h) \\ f(a,d) & f(a+k,d) & f(a+2k,d) & & f(b-2k,d) & f(b-k,d) & f(b,d) \end{bmatrix}$$

$$\cdot \begin{bmatrix} 1 & 4 & 2 & & 2 & 4 & 1 \\ 4 & 16 & 8 & \cdots & 8 & 16 & 4 \\ 2 & 8 & 4 & & 4 & 8 & 2 \\ & \vdots & & \ddots & & \vdots & \\ 2 & 8 & 4 & & 4 & 8 & 2 \\ 4 & 16 & 8 & \cdots & 8 & 16 & 4 \\ 1 & 4 & 2 & & 2 & 4 & 1 \end{bmatrix} \cdot \frac{1}{9} \cdot k \cdot h$$

Where k is the grid size in x-direction, h, is the grid size in the y-direction.

The matrix weighting the results can be made in 5 steps:

Step 1: Make a matrix of ones with N rows and M columns corresponding to the division of the surface, both N and M has to be even numbers.

Step 2: Row $2 \to (N-1)$ is multiplied by 2

Step 3: Column $2 \to (M-1)$ is multiplied by 2

Step 4: Row $2 \to (N-1)$ is multiplied by 2 in every 2nd row

Step 5: Column $2 \to (N-1)$ is multiplied by 2 in every 2nd column

$$
\begin{bmatrix}
1 & 1 & 1 & 1 & 1 & 1 & 1 \\
1 & 1 & 1 & 1 & 1 & 1 & 1 \\
1 & 1 & 1 & 1 & 1 & 1 & 1 \\
1 & 1 & 1 & 1 & 1 & 1 & 1 \\
1 & 1 & 1 & 1 & 1 & 1 & 1 \\
1 & 1 & 1 & 1 & 1 & 1 & 1 \\
1 & 1 & 1 & 1 & 1 & 1 & 1
\end{bmatrix}
\to
\begin{bmatrix}
1 & 1 & 1 & 1 & 1 & 1 & 1 \\
2 & 2 & 2 & 2 & 2 & 2 & 2 \\
2 & 2 & 2 & 2 & 2 & 2 & 2 \\
2 & 2 & 2 & 2 & 2 & 2 & 2 \\
2 & 2 & 2 & 2 & 2 & 2 & 2 \\
2 & 2 & 2 & 2 & 2 & 2 & 2 \\
1 & 1 & 1 & 1 & 1 & 1 & 1
\end{bmatrix}
\to
\begin{bmatrix}
1 & 2 & 2 & 2 & 2 & 2 & 1 \\
2 & 4 & 4 & 4 & 4 & 4 & 2 \\
2 & 4 & 4 & 4 & 4 & 4 & 2 \\
2 & 4 & 4 & 4 & 4 & 4 & 2 \\
2 & 4 & 4 & 4 & 4 & 4 & 2 \\
2 & 4 & 4 & 4 & 4 & 4 & 2 \\
1 & 2 & 2 & 2 & 2 & 2 & 1
\end{bmatrix}
$$

$$
\to
\begin{bmatrix}
1 & 2 & 2 & 2 & 2 & 2 & 1 \\
4 & 8 & 8 & 8 & 8 & 8 & 4 \\
2 & 4 & 4 & 4 & 4 & 4 & 2 \\
4 & 8 & 8 & 8 & 8 & 8 & 4 \\
2 & 4 & 4 & 4 & 4 & 4 & 2 \\
4 & 8 & 8 & 8 & 8 & 8 & 4 \\
1 & 2 & 2 & 2 & 2 & 2 & 1
\end{bmatrix}
\to
\begin{bmatrix}
1 & 4 & 2 & 4 & 2 & 4 & 1 \\
4 & 16 & 8 & 16 & 8 & 16 & 4 \\
2 & 8 & 4 & 8 & 4 & 8 & 2 \\
4 & 16 & 8 & 16 & 8 & 16 & 4 \\
2 & 8 & 4 & 8 & 4 & 8 & 2 \\
4 & 16 & 8 & 16 & 8 & 16 & 4 \\
1 & 4 & 2 & 4 & 2 & 4 & 1
\end{bmatrix}
$$

SURFACE TO SURFACE

In the calculations, the numerical solution is found by first looking at the small area ΔA_1 and calculating the view factor from this small area to object 2. When this has been done for all the small areas of object 1, then the total view factor can be found.

The normal vectors of the surfaces are given as:

$$
\overrightarrow{n_1} = \begin{bmatrix} x_{n_1} \\ y_{n_1} \\ z_{n_1} \end{bmatrix}
\qquad
\overrightarrow{n_2} = \begin{bmatrix} x_{n_2} \\ y_{n_2} \\ z_{n_2} \end{bmatrix}
$$

For each small are of the surfaces, ΔA_1 and ΔA_2, we look at the position of the centres and can thus calculate the vector, $\vec{r}$, between them:

$$
\vec{r} = \begin{bmatrix} x_{\Delta A_2} - x_{\Delta A_1} \\ y_{\Delta A_2} - y_{\Delta A_1} \\ z_{\Delta A_2} - z_{\Delta A_1} \end{bmatrix} = \begin{bmatrix} x_r \\ y_r \\ z_r \end{bmatrix}
$$

The length of $\vec{r}$ is: $\qquad r^2 = x_r^2 + y_r^2 + z_r^2$

The angle, γ_1, between the normal vector of surface 1, $\overrightarrow{n_1}$, and the vector, $\vec{r}$, is:

$$\cos(\gamma_1) = \frac{\overrightarrow{n_1} \cdot \vec{r}}{|\overrightarrow{n_1}| \cdot |\overrightarrow{r}|} = \frac{\begin{bmatrix} x_{n_1} \\ y_{n_1} \\ z_{n_1} \end{bmatrix} \cdot \begin{bmatrix} x_r \\ y_r \\ z_r \end{bmatrix}}{\sqrt{x_{n_1}^2 + y_{n_1}^2 + z_{n_1}^2} \cdot \sqrt{x_r^2 + y_r^2 + z_r^2}}$$

The angle, γ_2, between the normal vector of surface 2, $\overrightarrow{n_2}$, and the vector, $\vec{d}$, is:

$$\cos(\gamma_2) = \frac{\overrightarrow{n_2} \cdot (-\vec{r})}{|\overrightarrow{n_2}| \cdot |\overrightarrow{r}|} = \frac{\begin{bmatrix} x_{n_2} \\ y_{n_2} \\ z_{n_2} \end{bmatrix} \cdot \begin{bmatrix} -x_r \\ -y_r \\ -z_r \end{bmatrix}}{\sqrt{x_{n_2}^2 + y_{n_2}^2 + z_{n_2}^2} \cdot \sqrt{x_r^2 + y_r^2 + z_r^2}}$$

To optimise the calculation time when solving Equation 28 the Simpson method is used - twice.

The last article researches the handling of uncertainties and variation in the calculations and in the presentation of the results.

Fifth article:
USING BUILDING SIMULATION TO EVALUATE GLOBAL AND LOCAL THERMAL COMFORT ACCORDING TO ISO 7730

Mette Havgaard VORRE[1,*], Rasmus Lund JENSEN[2], Kim Trangbæk JØNSSON[2]

[1]Energy and Environment, Danish Building Research Institute, Aalborg University Copenhagen, A. C. Meyers Vaenge 15, 2450 Copenhagen SV, Denmark
[2]Department of Civil Engineering, Aalborg University, Sofiendalsvej 9-11, 9200 Aalborg SV, Denmark

[*]*Corresponding author: Mette Havgaard Vorre*

ABSTRACT

An application was developed for long-term evaluation of global and local thermal comfort based on building energy simulation tools. The application handles the whole room and facilitates assessment of uncertainty. Methods prescribed by ISO 7730 are used for calculating the predicted mean vote in a grid together with percentage dissatisfied by draught, radiant asymmetry and floor temperature, all based on research by Fanger.

This paper describes how the data from building simulations are processed to make evaluations of local and global thermal comfort. Air velocities were found by means of flow elements, clothing level was calculated by a correlation with operative temperature and thermal radiant impacts were found from calculations of view factors at all nodes in a grid and for different orientations.

Uncertainty and variations of input parameters and their effect on results are handled by making a number of calculations for each point while varying the input.

The results obtained by using the thermal comfort application are plots showing a summation of the obtained categories and a number of plots for deriving when, where and why thermal comfort in a room is categorised A, B, C or D respectively and how variations and uncertainty can affect the results.

INTRODUCTION

The objective of this study was to describe a method for the long-term evaluation of global and local thermal comfort based on the international standard for thermal environment ISO 7730 (CEN 2005) and building energy simulations. The method is applicable for optimisation and for classification of the thermal indoor environment of a building.

The most widely used measures for thermal comfort were derived by P.O. Fanger and consist of a comfort measure for the body as a whole, supplemented with measures for discomfort caused by draught or parts of the body being exposed to temperature differences (Fanger 1970, 1981; Fanger et al. 1985, 1988; Olesen et al. 1973). The first ISO 7730 standard on thermal comfort published in 1984 was based on Fanger's research. The standard describes how global thermal comfort can be assessed by calculating the predicted mean vote (PMV) or predicted percentage dissatisfied (PPD); and local thermal discomfort by calculating the draught rate (DR) and percentage dissatisfied (PD) caused by thermal radiant asymmetry, floor temperature and vertical air temperature gradient.

In 2006, the standard was revised for the second time and the categories A, B and C were added to assess thermal comfort across the measures for global thermal comfort and local thermal discomfort. Methods for long-term evaluation were also added in the revision, though the long-term methods apply only to global thermal comfort and neither for local discomfort nor the summation of global and local by the new categories.

For the last two decades, building energy simulation tools have been used for most buildings in the design or renovation phase to calculate and optimise their expected energy consumption. Thermal comfort is closely related to the energy consumption of buildings and it is therefore ideal to base an application for assessing long-term thermal comfort on building energy simulation tools. The consequences of energy optimisation on thermal comfort can thus quickly be assessed and any problems can be solved early in the design process.

This paper presents an application for long-term evaluation of global and local thermal comfort by applying ISO 7730 and describes how results from a building energy simulation tool are processed in the calculations of thermal comfort. Some of the parameters, for calculating thermal comfort, vary in the room and others vary with the orientation of the person. Some of the parameters are more uncertain than others. The application deals with all this and gives a precise and detailed picture of the thermal comfort in a room.

The application takes the evaluation a step further than ISO 7730 by including a long-term evaluation of the whole room for both global thermal comfort and local

thermal discomfort, and moreover it assesses the effects of uncertainty and variations on the results.

AN APPLICATION FOR LONG-TERM THERMAL COMFORT SIMULATION

A way to improve thermal comfort in buildings is to improve the simulation of thermal comfort. Better simulations make it possible to optimise buildings for thermal comfort, to predict and deal with problems before they occur in real life.

The ideal application for simulation of thermal comfort would calculate PMV, PPD, DR and PD caused by floor temperature, vertical air temperature gradient and radiant asymmetry, as described in ISO 7730. The ideal application would make it possible to both get an overview and to go deeper into the results.

The ideal application should summarise the results for easy comparison of different building designs and the application should deal with and visualise the uncertainty of the results caused by uncertainties and variations in the input.

For optimisation of a building design, the application should make it possible to find out: what causes problems with thermal comfort, when problems with thermal comfort occur and where in the room is there a risk of poor thermal comfort.

Last but not least, the application should have a calculation time comparable to building energy simulation tools, which will make it possible to run a number of simulations in an optimisation process of a building.

ISO 7730

ISO 7730 describes how thermal comfort can be assessed for a building by using the equations derived by P. O. Fanger for both global thermal comfort and local thermal discomfort.

Global thermal comfort is calculated for the body as a whole and is based on the body's heat balance: heat production vs. heat loss to the surroundings. The relation between people's thermal sensation and the heat balance is found through tests in a climate chamber and is expressed by PMV and PPD.

Local thermal discomfort can be caused by draught, floor temperature and temperature differences. Local thermal discomfort is expressed by the percentage of people being bothered or dissatisfied. Draught dissatisfaction is expressed by the draught rate, DR, while temperature dependent causes are expressed by percentage dissatisfied, PD.

Calculating both global and local thermal comfort gives five different measures in each point. The number of dissatisfied given by the five measures should not be summed, as the same persons are often sensitive to more impacts. Instead, the total evaluation is done by categorising the indoor climate through criteria for the five measures as shown in Table 6.

Table 6

Category	Global thermal comfort			Local thermal discomfort		
				PD caused by		
	PMV	PPD	DR	vertical air temperature difference	floor temperature	radiant asymmetry
		%	%	%	%	%
A	$-0.2 < PMV < 0.2$	< 6	< 10	< 3	< 10	< 5
B	$-0.5 < PMV < 0.5$	< 10	< 20	< 5	< 10	< 5
C	$-0.7 < PMV < 0.7$	< 15	< 30	< 10	< 15	< 10
D	$-0.7 \geq PMV \geq 0.7$	≥ 15	≥ 30	≥ 10	≥ 15	≥ 10

ISO 7730 prescribes the categories A, B and C. The authors supplemented these categories with a category D to cover situations outside the ranges of categories A, B and C. In other norms and standards, similar categories are used for categorising the indoor environment. EN 15251 (CEN 2007) covers the indoor environment more broadly by taking lighting and acoustics into consideration. EN 15251 names the categories I, II, III and IV, where category IV covers cases outside the limits of category III, as suggested by the authors for category D. EN 15251 has the same limits for global thermal comfort as ISO 7730, but the norm does not cover local thermal discomfort, though it states that local thermal discomfort should be taken into consideration referring to ISO 7730.

ISO 7730 gives five methods for long-term evaluation of the thermal comfort. Method A calculates the number or percentage of hours that the criteria for PMV or operative temperature are not met. Methods B and C weight the hours outside the chosen criteria by a weighting factor which is a function of how many degrees or PPD's, the range has been exceeded. Method D is the average of the PPD's during the occupied hours and method E sums the PPD's during the occupied hours.

Compared with the features described in the previous section for a thermal comfort application, the standard ISO 7730 prescribes methods and levels for assessing both global thermal comfort and local thermal discomfort, but it lacks methods for long-term evaluation of local thermal discomfort, distribution in the room and assessment of uncertainties and variation effect on the results.

THE THERMAL COMFORT APPLICATION

The calculation methods and functionalities of the developed application for thermal comfort evaluation are described by means of an example.

A building energy simulation was performed in BSim (Wittchen et al. 2013) for an office situated in Denmark. The office was placed at an intermediate floor and was ventilated by natural ventilation through two highly placed windows in the south wall. The east wall was fully glassed and would generate down draught when cold. A sketch of the room is shown in Figure 32.
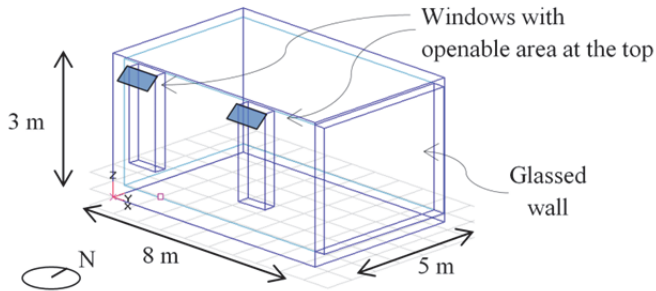

Figure 32 The room as simulated in BSim. Inside room dimensions: height 3 m, length 8 m, width 5 m. There were two openable windows, each with a controlled opening area at the top of up to 0.33 m². The east wall was fully glassed.

From the building energy simulation the following hourly results were used in the thermal comfort application:

- Inside and outside air temperatures
- Surface temperatures
- Inlet air velocities through the window openings
- Opening area of the windows
- Relative humidity

Besides these inputs, the application needs information on room geometry, including placement of the inlet openings.

The application calculates thermal comfort in a horizontal grid for a seated or a standing person. In this example, a grid size of 0.5 m was used and a seated person was assumed. The grid had nodes in the centre line of both openable windows. Calculations were made for eight different orientations of the person, to be able to assess how thermal comfort varies with the orientation.

All input parameters are subject to uncertainties or variations and in order to consider this when calculating thermal comfort, a number of calculations were performed with varying input parameters. For each time step a variation sample was generated, containing the chosen number of variations for each parameter. The same sample set was used for the whole room at a given time step. To cover the variation space optimally, the statistical method Latin hyper-cube was used for sampling sets of input parameters. The principle of Latin hyper-cube is explained in Figure 33. A sensitivity analysis on the number of variations was performed for the example and is presented later in the article.
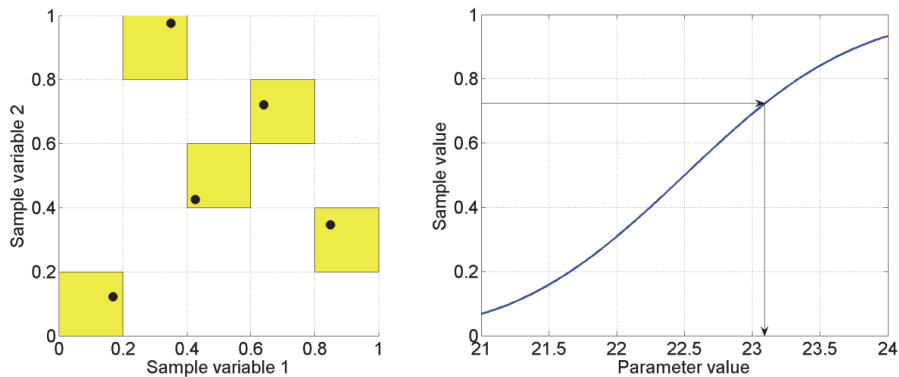

Figure 33 The principle of the Latin hyper-cube in a fictive case of two parameters and five samples. The samples are found as values between 0 and 1. For each parameter the sample space is divided into five intervals (the number of samples) and one random value is then picked randomly for each of the intervals. The five sample pairs are taken in a way that each interval is chosen only once for each parameter. The sample values are converted to a parameter value based on the distribution for each parameter, here it is a normal distribution with mean = 22.5, standard deviation = 1.5, minimum value = 21 and maximum value = 24.

CALCULATION OF PMV AND PPD

The global thermal comfort measures PMV and PPD are calculated from air temperature, air velocity, mean radiant temperature and relative humidity at the person's position as well as the person's clothing level and activity level.

In the following, it is explained how these parameters are found, treated and used in the application for thermal comfort.

Air temperature

Air temperature has a great influence on the thermal comfort in a room and it is therefore an important parameter in the application.

The inside air temperature is a core parameter in building energy simulations and full mixture of the air in the room is assumed in the simulations. In reality, air temperature can vary both horizontally and vertically depending on ventilation system, size and geometry of the room.

In the example, the air temperature was varied to depict the horizontal variation that might occur in the room. The following parameters were used for the variation of air temperature:

Distribution:	Normal
Standard deviation, σ:	1°C
Mean, μ:	Value from building simulation
Min:	$\mu - 1.5$°C
Max:	$\mu + 1.5$°C

Air velocity

Air velocity increases the heat transfer by convection and thereby influences thermal comfort of a person.

Air velocities are calculated by flow elements from the values of: velocities in inlet openings, opening area, surface temperatures, inside and outside air temperatures. A tool was developed by the authors for calculating air velocities on a long-term basis using flow elements(Vorre et al. 2014). Flow elements have the advantage compared with CFD that the calculation in a given point is independent of a grid and this makes it possible to calculate velocities only in points of interest, which lowers calculation time and makes long term simulations possible.

In the example, the chosen grid size for thermal comfort simulation was used in three dimension and air velocities were calculated in each node.

Each flow element was handled individually and if more flow elements affected the node, the highest of the calculated velocities in the node was used. The number of flow elements colliding in a point was used as a measure of the uncertainty of the results.

In each column from floor to the top of the occupied zone, the mean and the maximum velocities were found together with the highest number of colliding flow elements. The principle for maximum velocity is shown in Figure 34. As input for the calculations of air velocities were used the results from the building simulation and variation was applied afterwards.
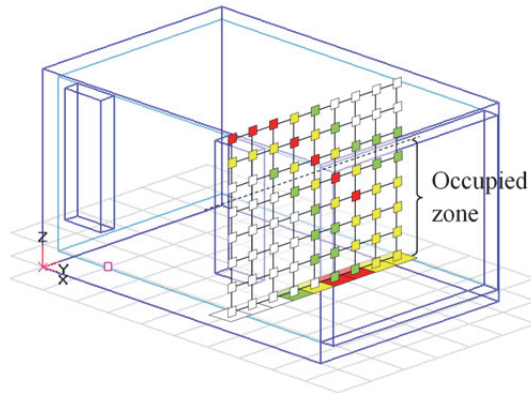
Figure 34 Air velocities are calculated in the nodes of a grid structure and the highest value in each column is found.

The calculated air velocities have a high uncertainty as several parameters can affect the flows in a room e.g. curtains, furniture or colliding airflows. To depict the varying uncertainty due to more flow elements in the same point, the number of colliding flow elements was used to set the standard deviation of the normal distribution.

The following parameters were used for the variation of air velocities, where "x" is the maximum number of colliding flows in the column:

Distribution:	Normal
Standard deviation, σ:	$0.01 \cdot x^2 + 0.01$ (x = 1→ 0.02, x = 2 → 0.05, x = 3 → 0.1)
Mean, μ:	Mean velocity for the column
Min:	0 m/s
Max:	Maximum velocity for the column

Mean radiant temperature

Mean radiant temperature is defined as that uniform temperature of a black enclosure which would result in the same heat loss by radiation from a person as the actual enclosure being studied.

Mean radiant temperature will vary in a room, both with the position and with the orientation of the person. Emissivity and reflections have been disregarded and mean radiant temperature calculated as:

Equation 33

$$T_{mr}^4 = \sum_{i=1}^{n} T_i^4 \cdot F_{person \rightarrow i}$$

Where T_{mr} is the mean radiant temperature in kelvin, T_i is the temperature of surface i in kelvin and $F_{person \rightarrow i}$ is the view factor between the person and surface i. View factors between the surfaces in the room and a person are calculated in each node in the grid for eight orientations of the person. View factors are calculated by numerical integration over each surface, where a person's projected area factor is modelled by the algorithm developed by Rizzo et al (Rizzo et al. 1991). The method is described in detail in an earlier work by the authors (Vorre, Jensen, and Le Dréau 2015). As view factors do not change over time, they only need to be calculated once for a room-geometry and not at every time step as the rest of the calculations.

Surface temperatures are calculated by building simulations and are considered relatively certain, though glass temperatures can be a problem depending on calculation methods of the simulation tools.

Variations in mean radiant temperature are simulated by varying surface temperatures to take variations over the surface into consideration.

Distribution:	Normal
Standard deviation, σ:	0.3°C
Mean, μ:	Surface temperatures found by building simulation
Min:	$\mu - 1$°C
Max:	$\mu + 1$°C

Relative humidity

Relative humidity only influences thermal comfort very little when looking at conditions likely to occur in offices, schools etc.

The humidity of the air in a room is calculated by building energy simulation tools and the results are considered as having high certainty. Full mixture of the air is assumed in the simulations, though in reality some variation can occur e.g. due to plumes of ventilation air.

In the example the relative humidity was varied to depict the horizontal variation that could occur in the room. The following parameters were used for the variation of relative humidity:

Distribution:	Normal
Standard deviation, σ:	5%

Mean, μ: Value from building simulation
Min: 20%
Max: 70%

Clothing level

Clothing is the heat insulation between a person's skin and the surroundings, and it has a high impact on thermal comfort. Clothing insulation is measured in in $\frac{m^2 \cdot K}{W}$ or clo, where 1 clo equals 0.165 in $\frac{m^2 \cdot K}{W}$.

In the experiments that P.O. Fanger used for developing the equations for PMV and PPD, the test persons have very strictly measured clothing insulation(Fanger 1970). From the experiments it was found that under the same thermal conditions and with the same clothing insulation the number of dissatisfied will not get below 5% even at optimum conditions, because people have different thermal preferences. If people had been asked to adjust their clothing in order to obtain thermal comfort, the number of dissatisfied would presumably be lower and maybe it would be possible to satisfy all.

Knowledge of clothing insulation in real life is needed for simulation of thermal comfort on a long-term basis. The ASHRAE RP-884 database(de Dear and Brager 1998) was used by the authors to find a relation between clothing insulation in real buildings and a thermal parameter that is known from building energy simulations (Vorre and Jensen 2014). The current operative temperature, t_{op}, was found to be the best parameter and the relations between operative temperature and mean clothing insulation for buildings with and without cooling are given in Equation 34 and Equation 35.

With cooling:

Equation 34

$$clo_{mean} = \begin{cases} -0.0552 \cdot t_{op} + 2.486 & \text{for} \quad t_{op} < 25°C \\ 0.65 & \text{for} \quad t_{op} > 25°C \end{cases}$$

Without cooling:

Equation 35

$$clo_{mean} = \begin{cases} -0.0858 \cdot t_{op} + 2.829 & \text{for} \quad t_{op} < 25°C \\ 0.69 & \text{for} \quad t_{op} > 25°C \end{cases}$$

For both building types, it was found that a minimum clothing level is reached at 25°C.

The data in the database RP-884 are from real working environments where people had some degree of freedom in their choice of clothing. From the above equations it is seen that people vary their clothing according to the operative temperature, but another interesting result from the study was, that even though people vary their clothing according to operative temperature and - on average - also according to their thermal preference, no relation was found between clothing level and thermal comfort vote when looking at a given operative temperature. Actually, the same standard deviation in thermal comfort votes was found as in Fanger's experiments in climate chambers with a strict dress code. This is probably because there are so many other reasons for the choice of clothing than just thermal comfort, e.g. fashion. It is concluded that the opportunity to adapt clothing according to thermal preference is being used by some, but an equal number of people choose clothing that does not get them closer to thermal comfort.

As variation in clothing at a given operative temperature did not affect the thermal comfort vote, it was chosen not to make variations in clothing in the application, because clothing varies when variations are done for the operative temperature.

In the example, clothing level was calculated using Equation 35.

Activity level

Activity level equals the heat production of the body minus effective mechanical work (W). The activity level has a high impact on thermal comfort. The activity level or metabolic rate (M) is measured in either W/m^2 or met where 1 met equals 58 W/m^2.

The effective mechanical work by a person (W) can be regarded as 0 for typical office work, sedentary tasks or low activity tasks.

ISO 7730 provides a table for estimation of metabolic rate depending on activity. For office work, it ranges between 1.0 met (seated, relaxed) and 1.2 met (sedentary activity e.g. office and school).

The uncertainty on metabolic rate is very high, both because it is difficult to measure and estimate for a given situation, but also because the metabolic rate for the same activity varies between people. Uncertainty on metabolic rate is typically around 50% but can be as high as 100% (Parsons and Hamley 1989). A difference of just 15% of metabolic rate can easily lead to a difference of 0.3 of the calculated PMV (Havenith et al. 2002).

In the example, the activity level was varied with the following distribution and parameters:

Distribution:	Normal
Standard deviation, σ:	0.05
Mean, μ:	1.2
Min:	1.0
Max:	1.4

DRAUGHT RATE

Draught is probably what causes most complaints about the indoor environment. Draught rate is a measure of the percentage dissatisfied by draught and is calculated from the air velocity, turbulence intensity and air temperature.

Air velocity

Air velocity has a high impact on the sensation of draught.

The air velocity for calculation of draught risk is found in the same way as for PMV. The following parameters were used for the variation of air velocities, where "x" is the maximum number of colliding flows in the column:

Distribution:	Normal
Standard deviation, σ:	$0.01 \cdot x^2 + 0.01$ (x = 1 → 0.02, x = 2 → 0.05, x = 3 → 0.1)
Mean:	Maximum velocity for the column
Min:	0 m/s
Max:	$2 \cdot \mu$

When doing the calculations, the same random value is used for calculating air velocities for both global thermal comfort and draught risk, only the mean values, standard deviation and min/max values are changed. This ensures correlation between calculated values for global thermal comfort and draught risk.

Turbulence intensity

Turbulence intensity affects the sensation of draught.

A turbulence intensity of 40% was used in the example.

Air temperature

Draught rate is affected by the air temperature.

The application uses the air temperature in the room for the calculations of draught rate and adopts the same variations.

VERTICAL AIR TEMPERATURE DIFFERENCE

The thermal comfort application does not cover percentage dissatisfied because of vertical air temperature difference. The foundation of building energy simulation tools is full mixture of the air and consequently it is impossible to simulate the vertical air temperature gradient.

FLOOR TEMPERATURE

Local thermal discomfort can be caused by both a too cold or too warm floor temperature. The calculation of dissatisfied due to floor temperature is only dependent on the floor temperature.

The floor temperature found by the variations of surface temperatures as explained in the section on mean radiant temperatures is used in the example.

RADIANT ASYMMETRY

Asymmetry in thermal radiation can cause thermal discomfort. Radiant asymmetry is defined as the difference in mean radiant temperature between two sides of small plate. For a vertical asymmetry, the highest discomfort occurs between left - right side, whereas front – back causes less discomfort.

Radiant asymmetry is found by calculating mean radiant temperature for each side of a small plate placed vertically or horizontally in the centre of the person. The same numerical method as used for mean radiant temperature of a person is used for calculation of view factors to each side of a small vertical and a small horizontal plate. A more detailed description of the calculations is given in an earlier article by the authors (Vorre et al. 2015), where radiant asymmetries calculated for the small plates are compared with calculations using the same model of a person as used for calculating mean radiant temperature. Radiant asymmetry calculated with a model of a person gives a better picture of the temperatures felt by the person than the plates, but it would require a new correlation with percentage dissatisfied, PD.

In the example, varying surface temperatures were used for calculating radiant asymmetry and the calculations were performed in all nodes in the room and for the eight orientations of the person.

OUTPUT AND RESULTS FROM THE THERMAL COMFORT APPLICATION

For each hour of the year, four measures of thermal comfort are calculated: PPD, DR, PD caused by floor temperature and PD caused by radiant asymmetry. For each measure, the resulting category, A, B, C or D, is found together with the aggregate category. The calculations are performed in a grid and for a number of orientations. Furthermore, all the calculations are performed a number of times with variations on input parameters to take uncertainty into consideration. The result is a probability distribution between the four categories in Table 6 for each node, each orientation and each hour. An example of distribution is given in Table 7.

Table 7

A	B	C	D
13%	19%	68%	0%

To get an overview, the mean values of orientation, the room or time were calculated depending on the focus. The mean values of all occupied hours of the whole year, the whole room and all orientations were used for a sensitivity analysis for the number of variations performed for the room in the example.

Whole year calculations were made with 10, 20, 30, 40, 50, 60, 70, 80, 90, 100, 200, 500 and 1000 variations in each point and for each orientation. The distributions between categories for each point and orientation were compared with the distributions found using 1000 variations. The results of the comparisons are shown in Figure 35 as a mean of the absolute differences for each calculation and as a mean of the difference in per cent for each calculation.
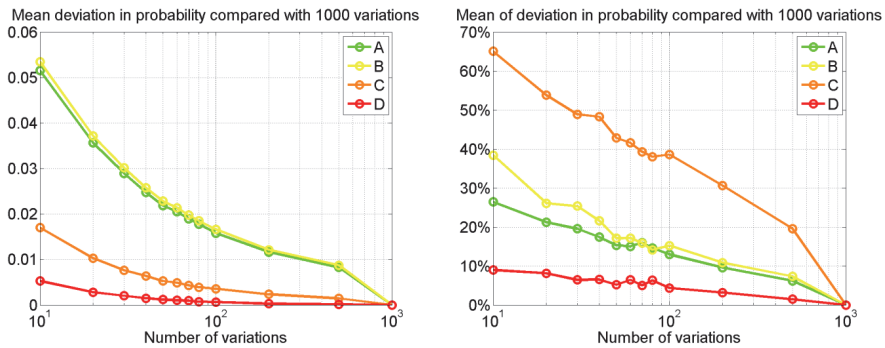
Figure 35 Sensitivity analysis of the number of variations made in the calculations. To the left, the absolute difference is shown and to the right, the difference is shown in percentage. All numbers are compared with results by 1000 variations.

The greatest effect of adding more variations is seen at the low number of variations, but as the number of variations affects the calculation time linearly, it is worth considering the gain in accuracy by using e.g. 200 instead of 100 variations.

The results presented in this paper are found from the calculations using 1000 variations.

OVERVIEW

To give an overview of the results, the distribution between categories was averaged for each hour. Position in the room and orientation of the person is thereby regarded as variations. For each hour, the category for respectively 5%, 25%, 50%, 75% and 95% quantiles of the calculations is found. In Table 8 the categories for the five quantiles are shown if assuming the distribution in Table 7.

Table 8

5%	25%	50%	75%	95%
A	B	C	C	C

By counting the number of hours in each quantile for each of the four categories, a summary for the whole year can be made as a bar plot for all hours or all occupied hours as seen for the example in Figure 36.
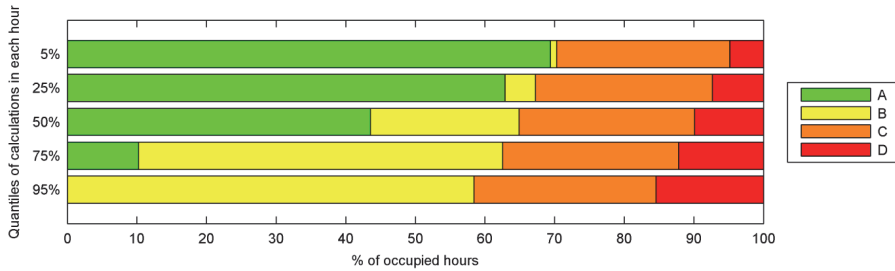
Figure 36 Percentage of hours in each category. The top bar shows the category in the best 5% of the calculations in each hour; the next bar shows the best 25%. The middle bar shows the 50% quantile or the median and represents approximately the mean of the calculations. The bottom bars shows the 75% and 95% quantiles in each hour.

Figure 36 gives an overview of the percentage of hours in each category and how much the results are affected by variations in the input. If the five bars are alike, the thermal comfort is robust to the variations; if they differ, the thermal comfort is sensitive to the variations.

The 50% quantile, or the median, approximately represents the mean of the results. For the example 43% of the occupied hours were in category A for the 50% quantile. Variations in inputs could cause the percentage to rise to more than 60% or fall to 10% or even 0%. Categories A and B were most sensitive to the variations.

FLOOR PLAN WITH PLOT OF THERMAL COMFORT

The distribution of thermal comfort in the room is shown as a floor plan with plot of the categories. The probability distributions for each category are averaged over time and orientation for each node in the room.

In Figure 37, categories are plotted for the whole year in the occupied hours. The big plot shows the median or 50% quantile of the results and smaller plots show quantiles of the results to assess the uncertainty.
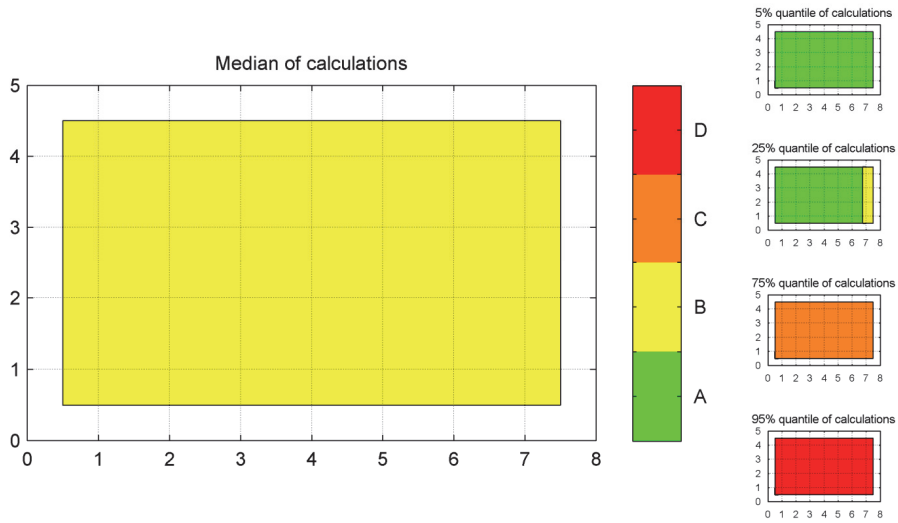
Figure 37 Floor plan of the room with plot of thermal comfort category for the median of the calculations for occupied hours of the whole year. To the right are plots for 5%, 25%, 75% and 95% quantiles.

The example showed that the entire room has thermal comfort of category B for the median of the results of all occupied hours. The small plots of quantiles show that the variations in input can cause thermal comfort to improve to category A or to drop to category C or even D in the entire room.

Time plot

The variation of thermal comfort over time is illustrated by calculating the hourly distribution between categories for shorter periods, months / weeks / days, using the same principles as for the bars in Figure 36. The results are shown as curves for the median of results, 25% and 75% quantiles. Figure 38 shows a plot of monthly values and Figure 39 shows a plot of weekly values.
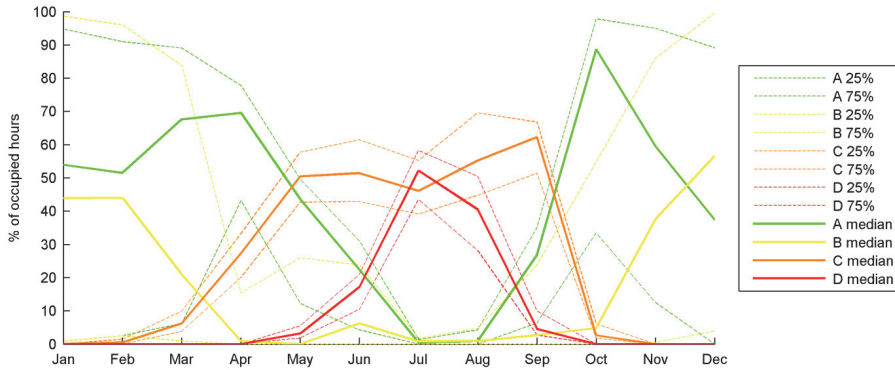
Figure 38 Graphs showing percentage of occupied hours in each category. Dashed lines represent 25% and 75% quantiles. Calculations are made for each month.

Figure 38 shows that thermal comfort is best in the spring and autumn months, and that there are problems in the summer months, where most hours are in either category C or D. The dashed lines representing 25% and 75% quantiles show that the uncertainty of categories are highest in winter, where category A and B are both able to go from nearly 0% to 100% of the occupied hours.
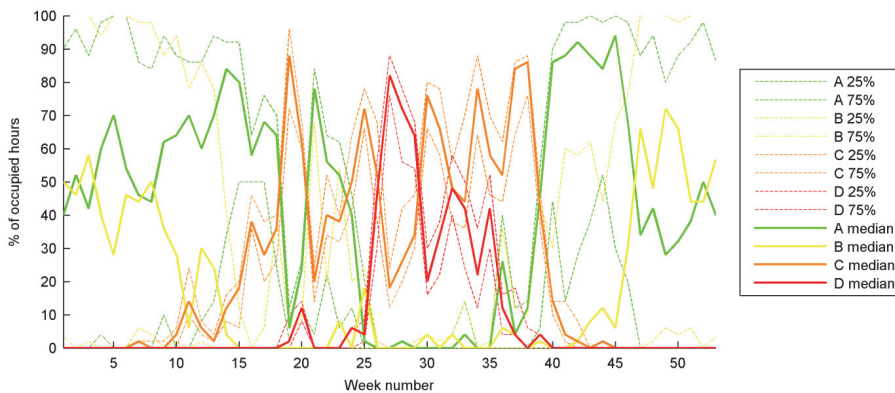

Figure 39 Graphs showing percentage of occupied hours in each category. Dashed lines represent 25% and 75% quantiles. Calculations are made for each week.

Figure 39 expresses the fluctuations between the weeks and gives a more detailed view than Figure 38. The room in the example mainly perceives poor thermal comfort in summer, but there is also a week in the late spring, when most hours are in catorgory C.

SEPARATION OF THERMAL COMFORT MEASURES

The categories shown in the above figures are found by taking the worst category of PPD, DR, PD caused by floor temperature and PD caused by radiant asymmetry in each calculation.

To be able to optimise a building design, it is vital to know the cause of a problem. Therefore it is possible to structure the results according to the four measures as shown in Figure 40.
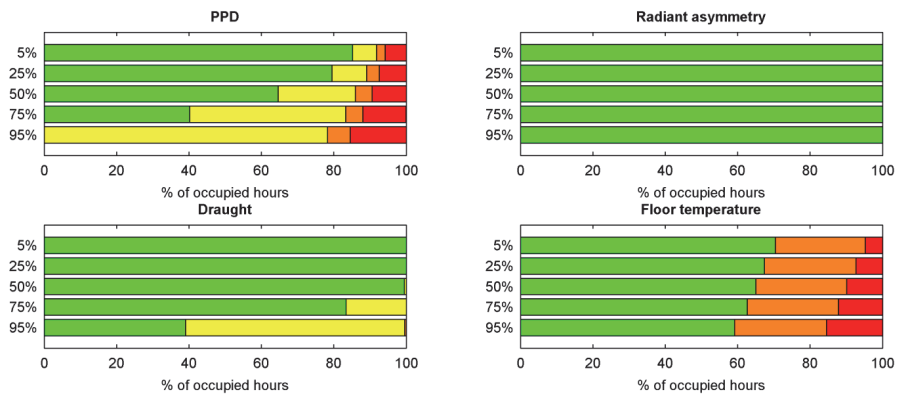

Figure 40 Distribution of hours in each category divided into the four criteria used in the tool.

It is clear from Figure 40 that in the example radiant asymmetry do not create problems and that the floor temperature is the main cause of comfort being in categories C and D. The uncertainty in inputs has the greatest effect on draught rate and PPD, while only little effect on the category caused by floor temperature. Direct radiation from the sun is not taken into consideration in the application at the moment, which is probably the cause of the good results for radiant asymmetry.

VARIATION IN THE ROOM OVER TIME

To get an overview of where in the room and when the different categories are achieved, plots of the floor can be made for each month, week, day or even each hour. Plots for every month are shown in Figure 41.
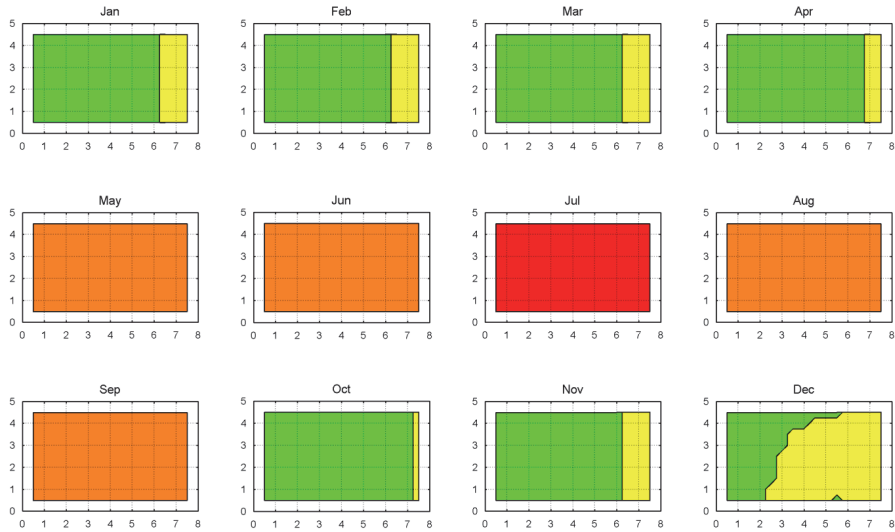
Figure 41 Plots of the floor plan with thermal comfort categories for each month.

From Figure 41 it is seen that from May to September the whole room is in category C, though D in July, while problems occur closest to the glassed façade during the remaining months.

VARIATIONS OF THE FOUR MEASURES OVER TIME

The four criteria for thermal comfort all vary during the year and to get an overview of when the different criteria cause problems, curves for percentage of time can be drawn individually. In Figure 42, the percentages of hours are calculated for each month.
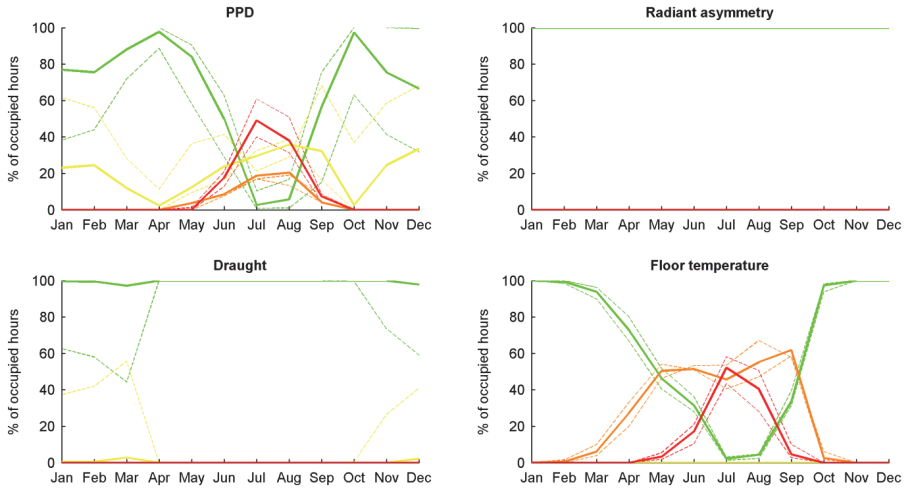
Figure 42 Curves showing the percentage of hours in each category. Dashed lines refer to 25% and 75% quantiles.

Figure 42 shows that PPD is poor in the summer, but also somewhat in winter. Floor temperature is only a problem in the warmer months and draught only occurres in winter. Radiant asymmetry is not a problem at all.

ORIENTATION

In the example, the calculations were made for eight different orientations of the person and the differences between them are shown in Figure 43.

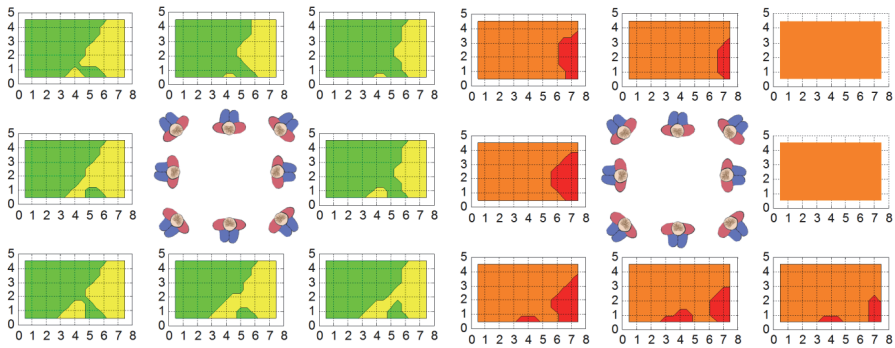*Figure 43 Plots of the floor plan for the eight orientations of the person. To the left is the total categories for week 8 and to the right the categories for PPD in week 26*

The plots show that thermal comfort varied with the orientation of the person, though the difference is small. For most weeks, the difference is close to non-existing.

The application makes it possible to zoom in on the results in all kinds of ways by combining the shown plots. All plots can be made for the resulting category or each measure individually, for a specific orientation or all together, for the whole year, each month or less. For all hours or only occupied hours, etc.

DISCUSSION

The application is based on the equations developed by Fanger. Other measures of the thermal environment are adaptive thermal comfort and productivity. Implementation of these could very well be the next step in the development of the application. The focus on thermal comfort through Fanger's perspective was chosen because it gives the most information that can be used in an optimisation process of a building, because the measures make it possible to see potential causes of poor thermal comfort.

Uncertainty is dealt with by making a number of variations in the input and showing the results including quantiles of results. This gives higher calculation times and might confuse an end user of a building; but it is considered very important that uncertainties can be communicated to end users because they need to be aware that these kinds of calculations are subject to uncertainties. The authors have endeavoured to optimise the presentation of the results so that they are comprehensible also to nontechnical persons.

The room temperature is used in the application for draught risk assessment, and the next step in the development could be to calculate the local temperature by means of the flow elements. This would give an even better estimation of the draught risk.

A shortcoming of the application is that it does not consider direct radiation from the sun. To do so, a method is needed to calculate how big a part of a person would be hit by the radiation at a specific point in the room.

CONCLUSION

The standard for thermal comfort was first issued in 1984 but the application presented in this article is the first tool to actually make it possible to simulate long-term thermal comfort for a room. This application gives an overview for comparison of different designs and makes it possible to structure the results in order to optimise a building.

CONCLUSION

The phd-study has demonstrated that it is possible to make fast calculations for thermal comfort evaluation. The possibilities for simulating parameters affecting thermal comfort were researched and three of them were chosen for further development of calculation and simulation methods.

For clothing level, a correlation was found between the indoor temperature and between whether the building has mechanical cooling or not. And it was found that even though people are free to vary their clothing, it does not mean that they obtain better thermal comfort, because clothing is so much more than thermal insulation.

Flow elements were found to be ideal for calculating air velocities, because the calculation time is low and each calculation is independent of its neightbours, making each calculation grid independent. A method was described for handling more than one flow element in a point and for overall presentation of results. The calculation method is fast and thereby applicable for calculations of several time time steps e.g. all hours of a month or a year.

Thermal radiation to persons was investigated and a method for calculating view factors applicable to even complex room geometries was described. The method can also be used for calculating radiant asymmetry and opens up for calculating radiant asymmetry using the human body instead of a plate as a measure.

The developed methodologies have been implemented in a working prototype for evaluation of thermal comfort on a long-term basis using output from building energy simulation tools for the calculations. The developed application deals with uncertainties and illustrates the consequences on the results, making it easy to communicate to non-technical people that such simulations are never accurate predictions of the future.

It is my hope that the methods will be implemented in one or more building energy simulation tools, and thereby lead to buildings with better thermal comfort.

LITERATURE LIST

ASHRAE. 2010. *ASHRAE Standard 55, Thermal Environmental Conditions for Human Occupancy*. 2010th ed. Atlanta: ASHRAE.

Beausoleil-Morrison, Ian. 2000. "The Adaptive Coupling of Heat and Air Flow Modelling within Dynamic Whole-Building Simulation." University of Strathclyde, Glasgow UK.

Beausoleil-Morrison, Ian. 2002. "The Adaptive Conflation of Computational Fluid Dynamics with Whole-Building Thermal Simulation." *Energy and Buildings* 34(9):857–71.

Brager, G. S., and Richard J. de Dear. 1998. "Thermal Adaptation in the Built Environment : A Literature Review." *Energy and Buildings* 27:83–96.

Breckenridge, John R. 1961. *Technical Report EP-175, Effective Area of Clothed Man for Solar Radiation*. Natick. Massachusetts.

Brunsgaard, C., P. Heiselberg, M. -a. Knudstrup, and Tine Steen Larsen. 2012. "Evaluation of the Indoor Environment of Comfort Houses: Qualitative and Quantitative Approaches." *Indoor and Built Environment* 21(3):432–51.

Calvino, Francesco, Maria La Gennusa, Antonino Nucara, Gianfranco Rizzo, and Gianluca Scaccianoce. 2005. "Evaluating Human Body Area Factors from Digital Images : A Measurement Tool for a Better Evaluation of the Ergonomics of Working Places." *Occupational Ergonomics* 5:173–85.

Calvino, Francesco, Maria La Gennusa, Gianfranco Rizzo, Gianluca Scaccianoce, and Angela Simone. 2009. "Measurements of Projected Areas of Seated and Standing People of Southern Italy Based on a Statistical Analysis." *Applied ergonomics*

Cannistraro, G., G. Franzitta, C. Giaconia, and G. Rizzo. 1992. "Algorithms for the Calculation of the View Factors between Human Body and Rectangular Surfaces in Parallelepiped Environments." *Energy and buildings* 19:51–60.

Cao, Guangyu, Mika Ruponen, and Jarek Kurnitski. 2010. "Experimental Investigation of the Velocity Distribution of the Attached Plane Jet after Impingement with the Corner in a High Room." *Energy and Buildings* 42(6)

De Carli, Michele, Bjarne W. Olesen, Angelo Zarrella, and Roberto Zecchin. 2007. "People's Clothing Behaviour according to External Weather and Indoor Environment." *Building and Environment* 42(12)

CEN. 2005. *EN ISO 7730:2005 Ergonomics of the Thermal Environment- Analytical Determination and Interpretation of Thermal Comfort Using Calculation of the PMV and PPD Indices and Local Thermal Comfort Criteria*. Brussels: EUROPEAN COMMTITEE FOR STANDARDIZATION.

CEN. 2007. *EN 15251:2007, Indoor Environmental Input Parameters for Design and Assessment of Energy Performance of Buildings Addressing Indoor Air Quality, Thermal Environment, Lighting and Acoustics*. Brussels: European Committee for standardization.

Chen, Q. 1988. "Indoor Airflow, Air Quality and Energy Consumption of Buildings." Delft University of Technology, the Netherlands.

Chrenko, F. A., and L. G. C. E. Pugh. 1961. "The Contribution of Solar Radiation to the Thermal Environment of Man in Antarctica." P. B155: 243–65 in *Proc. Roy. Soc.*

Crawley, DB, LK Lawrie, Crawley Pedersen, and FC Winkelmann. 2000. "EnergyPlus: Energy Simulation Program." *ASHRAE journal* 42(4):49–56.

De Dear, Richard J. 1998. "A Global Database of Thermal Comfort Field Experiments." *ASHRAE Transactions* 104(1B):1141–52.

De Dear, Richard J., and G. S. Brager. 1998. "Developing an Adaptive Model of Thermal Comfort and Preference." *ASHRAE Transactions* 104(1):145–67.

EQUA Simulation AB. n.d. "IDA Indoor Climate and Energy."

Eriksson, Lars et al. 2012. "CFD-FREE, EFFICIENT, MICRO INDOOR CLIMATE PREDICTION IN BUILDINGS." Pp. 149–56 in *BSO12 - First Building Simulation and Optimization Conference*.

Fanger, P. O. 1970. "Thermal comfort. Analysis and applications in environmental engineering." Lyngby, Denmark: Copenhagen: Danish Technical Press.

Fanger, P. O. 1981. "Prediction of Local Discomfort for Man." Pp. 221–27 in *Studies in environmental science*.

Fanger, P. O., O. Angelius, and P. Kjerulf-Jensen. 1970. "Radiation Data for the Human Body." *ASHRAE Transactions* (2168):338–73. Retrieved January 7, 2013

Fanger, P. O., L. Banhidi, Bjarne W. Olesen, and G. Langkilde. 1980. "Comfort Limits for Heated Ceilings." *ASHRAE Transactions* 86(2596):141–56.

Fanger, P. O., G. Langkilde, B. W. Olesen, N. K. Christensen, and S. Tanabe. 1985. "Comfort Limits for Asymmetric Thermal Radiation." *Energy and Buildings* 8(3):225–36.

Fanger, P. O., A. K. Melikov, H. Hanzawa, and J. Ring. 1988. "Air Turbulence and Sensation of Draught." *Energy and buildings* 12:21–39.

Fanger, P. O., and J. Toftum. 2002. "Extension of the PMV Model to Non-Air-Conditioned Buildings in Warm Climates." *Energy and Buildings* 34(6):533–36.

La Gennusa, Maria, A. Nucara, M. Pietrafesa, G. Rizzo, and G. Scaccianoce. 2008. "Angle Factors and Projected Area Factors for Comfort Analysis of Subjects in Complex Confined Enclosures: Analytical Relations and Experimental Results." *Indoor and Built Environment* 17(4):346–60.

Grimitlin, M. 1970. "Zuluftverteilung in Räumen." *Luft- und Kältetechnik* 5.

Guibert, A., and C. L. Taylor. 1952. "Radiation Area of the Human Body." *Journal of applied physiology* 5(1):24–37.

Haghighat, Fariborz, Yin Li, and Ahmed C. Megri. 2001. "Development and Validation of a Zonal Model — POMA." *Building and Environment* 36(9):1039–47.

Haldi, Frédéric, and Darren Robinson. 2008. "On the Behaviour and Adaptation of Office Occupants." *Building and Environment* 43(12):2163–77.

Hand, Jon W. 2006. *The ESP-R : Cookbook*. Glasgow: University of Strathclyde.

Hand, Jon W. 2012. *ESP-R Developers Guide*.

Hardy, JD, and EF DuBois. 1938. "The Technic of Measuring Radiation and Convection." *The Journal of Nutrition* 15(49):461–75.

Havenith, George, Ingvar Holmér, and Ken Parsons. 2002. "Personal Factors in Thermal Comfort Assessment : Clothing Properties and Metabolic Heat Production." *Energy and Buildings* 34:581–91.

Heiselberg, Per Kvols. 1994. "Draught Risk From Cold Vertical Surfaces." *Building and Environment* 29(3):297–301.

Hoes, P., J. L. M. Hensen, M. G. L. C. Loomans, B. de Vries, and D. Bourgeois. 2009. "User Behavior in Whole Building Simulation." *Energy and Buildings* 41(3):295–302.

Horikoshi, T. et al. 1990. "The Effective Radiation Area and Angle Factor between Man and a Rectangular Plane near Him." *ASHRAE Transactions* 96(1):60–66.

Jacobsen, Tine S., Elisabeth Mathiesen, P. V. Nielsen, Rikke Hansen, and C. Topp. 2002. "Thermal Comfort in a Mixing Ventilated Room with High Velocities Near the Occupied Zone." *ASHRAE Transaction* 108(2).

Jensen, Kasper Lynge. 2008. "Development of a Model to Calculate the Economic Implications of Improving the Indoor Climate." Technical University of Denmark.

Jensen, Kasper Lynge, Jørn Toftum, and Peter Friis-Hansen. 2009. "A Bayesian Network Approach to the Evaluation of Building Design and Its Consequences for Employee Performance and Operational Costs." *Building and Environment* 44(3):456–62.

Karlsen, Line, Grigori Grozman, Per Kvols Heiselberg, and Ida Bryn. 2014. "Operative Temperature and Thermal Comfort in the Sun – Implementation and Verification of a Model of IDA ICE." P. HP0681 in *Indoor Air 2014 (July 7-12, 2014, Hong Kong)*. Hong Kong.

Klein, S. A., and et al. 2010. "TRNSYS 17: A Transient System Simulation Program, Solar Energy Laboratory."

Koestel, Alfred. 1954. "Computing Temperatures and Velocities in Vertical Jets of Hot or Cold Air." *ASHVE Transactions* 60:385.

Koestel, Alfred. 1955. "Paths of Horizontally Projected Heated and Chilled Air Jets." *ASHVE Transactions*.

Kubaha, K., D. Fiala, KJ Lomas, and Scraptoft Campus. 2003. "Predicting Human Geometry-Related Factors for Detailed Radiation Analysis in Indoor Spaces." Pp. 681–88 in *Building Simulation 2003*.

Kubaha, K., D. Fiala, J. Toftum, and a H. Taki. 2004. "Human Projected Area Factors for Detailed Direct and Diffuse Solar Radiation Analysis." *International journal of biometeorology* 49(2):113–29.

Leyten, Joe L., Stanley R. Kurvers, and Arjen K. Raue. 2013. "Temperature, Thermal Sensation and Workers' Performance in Air-Conditioned and Free-Running Environments." *Architectural Science Review* 56(1):14–21.

Megri, Ahmed Chérif, Mark Snyder, and Marjorie Musy. 2005. "Building Zonal Thermal and Airflow Modelling – A Review." *International journal of ventilation* 4(2):177–88.

Morgan, Craig, and Richard J. de Dear. 2003. "Weather, Clothing and Thermal Adaptation to Indoor Climate." *Climate Research* 24:267–84.

Newsham, Guy R. 1997. "Clothing as a Thermal Comfort Moderator and the Effect on Energy Consumption." *Energy and Buildings* 26(3):283–91.

Nielsen, J. R. 1998. "The Influence of Office Furniture on the Air Movements in a Mixing Ventilated Room." Aalborg University.

Nielsen, P. V. 1994. "Air Distribution in Rooms - Research and Design Methods." in *The International Proceedings of ROOMVENT '94. Cracow, Poland.* Cracow, Poland.

Nielsen, P. V. 1995. *Luftströmung Und Luftverteilung in Räumen*. edited by H. (Hrsg.) Nowotny, S. : Feustel.

Nielsen, P. V. 2007. "Analysis and Design of Room Air Distribution Systems." *HVAC&R Research* 13(6):987–97.

Nielsen, P. V., and Å. T. A. Möller. 1987. "Measurements on Buoyant Wall Jet Flows in Air Conditioned Rooms." in *ROOMVENT '87, International Conference on Air Distribution in Ventilated Spaces*.

Nielsen, P. V., and Å. T. A. Möller. 1988. "Measurements on Buoyant Jet Flows from Ceiling-Mounted Slot Diffuser." in *Proc. of the 3rd Seminar on "Application of Fluid Mechanics in Environmental Protection - 88."*

Nucara, A., M. Pietrafesa, and G. Rizzo. 2000. "Computing View Factors between Human Body and Non Parallelepiped Enclosures." *Proceedings of Healthy Buildings* 2:611–16.

Nucara, Antonino, Matilde Pietrafesa, Gianfranco Rizzo, and Gianluca Scaccianoce. 2012. "Handbook of Anthropometry." Pp. 91–114 in *Handbook of Anthropometry*, edited by Victor R. Preedy. New York, NY: Springer New York.

Olesen, S., P. O. Fanger, PB Jensen, and OJ Nielsen. 1973. "Comfort Limits for Man Exposed to Asymmetric Thermal Radiation." Pp. 133–48 in *CIB Commision W45 (Human requirements) Symposium: Thermal Comfort and Moderate Heat Stress, September 1972*, vol. 45, edited by HMSO. London.

Park, Sookuk, and Stanton E. Tuller. 2011. "Human Body Area Factors for Radiation Exchange Analysis: Standing and Walking Postures." *International journal of biometeorology* 55(5):695–709.

Parsons, K. C., and E. J. Hamley. 1989. "Practical Methods for the Estimation of Human Metabolic Heat Production." *Thermal Physiology* 777–82.

Patankar, S. V. 1983. *Numerical Heat Transfer and Fluid Flow*. Hemisphere Publishing Corporation Washington.

Rees, S. J., and P. Haves. 2001. "A Nodal Model for Displacement Ventilation and Chilled Ceiling Systems in O Ce Spaces." 36:753–62.

Rizzo, G., G. Franzitta, and G. Cannistraro. 1991. "Algorithms for the Calculation of the Mean Projected Area Factors of Seated and Standing Persons." *Energy and Buildings* 17(3):221–30.

Seppänen, Olli, William J. Fisk, and Q. H. Lei. 2006. "EFFECT OF TEMPERATURE ON TASK PERFORMANCE IN OFFFICE ENVIRONMENT." in *5th international conference on cold climate hvac, Moscow*.

Solaini, G., G. Rossi, G. Dall'o, and P. Drago. 1996. "Energy and Comfort: A New Type for TRNSYS." *Renewable energy* 56–60a.

Steinman, M., LN Kalisperis, and LH Summers. 1988. "Angle Factor Determination from a Person to Inclined Surfaces." *ASHRAE Trans* 94(1):1809–23.

Tanabe, Shin-ichi, Chie Narita, Yoshiichi Ozeki, and Masaaki Konishi. 2000. "Effective Radiation Area of Human Body Calculated by a Numerical Simulation." *Energy and Buildings* 32(2):205–15.

Taylor, PF. 1956. *Middle East Trials: Meteorological Observations (July-August, 1955), Clothing and Stores Exper. Establ. Report No. 67*. Gt.Britain.

Underwood, C. R., and E. J. Ward. 1966. "The Solar Radiation Area of Man." *Ergonomics* 9(2):155–68.

Verhoff, A. 1963. *The Two-Dimensional, Turbulent Wall Jet with and without an External Free Stream*.

Vorre, Mette Havgaard, Rasmus L. Jensen, and Peter V Nielsen. 2014. "Draught Risk Index Tool for Building Energy Simulations." in *WSB2014 Barcelona*. Barcelona.

Vorre, Mette Havgaard, and Rasmus Lund Jensen. 2014. "Does Variation in Clothing Make Us More Thermally Comfortable?" in *Indoor Air 2014*. Hong Kong.

Vorre, Mette Havgaard, Rasmus Lund Jensen, and Jerome Jérôme Le Dréau. 2015. "Radiation Exchange between Persons and Surfaces for Building Energy Simulations." *Energy and Buildings* 101(15. august 2015):110–21.

Walton, GN. 2002. *Calculation of Obstructed View Factors by Adaptive Integration*. Gaithersburg, USA.

Wittchen, K. B., K. Johnsen, and K. Grau. 2013. *BSim User's Guide*. Copenhagen.

Zhai, Zhiqiang, Qingyan Chen, Philip Haves, and Joseph H. Klems. 2002. "On Approaches to Couple Energy Simulation and Computational Fluid Dynamics Programs." *Building and Environment* 37:857–64.

Zhai, Zhiqiang John, and Qingyan Yan Chen. 2006. "Sensitivity Analysis and Application Guides for Integrated Building Energy and CFD Simulation." *Energy and Buildings* 38:1060–68.